creative commons
COMMONS DEED

저작자표시-비영리-변경금지 2.0 대한민국

이용자는 아래의 조건을 따르는 경우에 한하여 자유롭게

- 이 저작물을 복제, 배포, 전송, 전시, 공연 및 방송할 수 있습니다.

다음과 같은 조건을 따라야 합니다:

저작자표시. 귀하는 원저작자를 표시하여야 합니다.

비영리. 귀하는 이 저작물을 영리 목적으로 이용할 수 없습니다.

변경금지. 귀하는 이 저작물을 개작, 변형 또는 가공할 수 없습니다.

- 귀하는, 이 저작물의 재이용이나 배포의 경우, 이 저작물에 적용된 이용허락조건을 명확하게 나타내어야 합니다.
- 저작권자로부터 별도의 허가를 받으면 이러한 조건들은 적용되지 않습니다.

저작권법에 따른 이용자의 권리는 위의 내용에 의하여 영향을 받지 않습니다.

이것은 이용허락규약(Legal Code)을 이해하기 쉽게 요약한 것입니다.

Disclaimer

dCollection

ULSAN NATIONAL INSTITUTE OF SCIENCE AND TECHNOLOGY

Doctoral Thesis

Study on the Multiphysics Modeling of Molten Salt Reactor Using Adjoint-based Sensitivity Analysis Method

Yeong Shin Jeong

Department of Nuclear Engineering

Graduate School of UNIST

2019

ULSAN NATIONAL INSTITUTE OF
SCIENCE AND TECHNOLOGY

Study on the Multiphysics Modeling of Molten Salt Reactor Using Adjoint-based Sensitivity Analysis Method

Yeong Shin Jeong

Department of Nuclear Engineering

Graduate School of UNIST

ULSAN NATIONAL INSTITUTE OF
SCIENCE AND TECHNOLOGY

Study on the Multiphysics Modeling of Molten Salt Reactor Using Adjoint-based Sensitivity Analysis Method

A dissertation
submitted to the Graduate School of UNIST
in partial fulfillment of the
requirements for the degree of
Doctor of Philosophy

Yeong Shin Jeong

12. 19. 2018

Approved by

Bang, In Cheol

Advisor

In Cheol Bang

ULSAN NATIONAL INSTITUTE OF SCIENCE AND TECHNOLOGY

Study on the Multiphysics Modeling of Molten Salt Reactor Using Adjoint-based Sensitivity Analysis Method

Yeong Shin Jeong

This certifies that the dissertation of Yeong Shin Jeong is approved.

12. 19. 2018

signature

Advisor: In Cheol Bang

signature

Ji Hyun Kim

signature

Seung Jun Lee

signature

Hisashi Ninokata

signature

Antonio Cammi

ULSAN NATIONAL INSTITUTE OF
SCIENCE AND TECHNOLOGY

Abstract

To pursue the nuclear energy as future energy resources, several reactor types of the nuclear power plant has been developed to achieve the advances in sustainability, reduction of nuclear waste, safety and reliability, proliferation resistance and competitive economies in the framework of the Generation IV International Forum (GIF). Among them, Molten Salt Reactor (MSR) is the only reactor that adopts liquid fuel serving as a coolant as well, which is not a new concept in retrospect of the history of the nuclear reactor. Fermi's water boiler, the first nuclear reactor fueled with uranium-235 enriched uranium, designed and operated with aqueous homogeneous fuel in liquid form. It adopts liquid fuel having lots of advantages to achieve high power density and inherent safety. However, it also has some technical limitations in maintaining homogeneous state with relatively large fuel particle at that time. With a lesson of previous experiences, it was evolved to adopt the liquid fuel as the eutectic formation of fuel material with molten salt to solve the issue on the slurry fuel, which is the current MSR concept. This was successfully demonstrated by Aircraft Reactor Experiment (ARE) and Molten Salt Reactor Experiment (MSRE) by Oak Ridge National Laboratory in the 1950s. Recently, liquid-fueled MSR is reconsidered as an alternative of a conventional nuclear power plants with aims of the development of related chemical reprocessing and molten salt technologies, taking advantages of the liquid fuel in safety and economic viewpoint as well as the radioactive waste issue. In a viewpoint of design and analysis of liquid-fueled MSR system, complex system behavior should be considered in the aspects of coupled physics; neutronics and thermal-hydraulics. Different from a solid-fueled reactor, delayed neutron precursors generated in core decay at the different location from the fuel flow, and it affects the overall neutron economy. It means a distribution of the fission source is largely dependent on the velocity field which determines the overall power profile. Moreover, it affects temperature field and varies the density of liquid fuel ultimately. Because of this, Multiphysics approach on the MSR system looks promising on the assessment of the system including important aspects of coupled physics. With aims of growing computational power, considering all physics lying under certain problem can be a feasible option nowadays. However, Multiphysics model itself for the complex system should be assessed not to misinterpret the behavior along with system analysis. In the above context, this work is aimed at developing the integrated design and analysis tool for MSR on the Multiphysics approach, which enables to perform system analysis and model sensitivity analysis simultaneously including all underlying physics based on the adjoint method and its application on the assessment of new conceptual design of MSR: nanofluidic molten salt reactor.

The first part explains the adjoint-based sensitivity analysis method on the Multiphysics approach. Adjoint method is the concept to establish a relatively simple problem having duality with a primal system. The concept of the adjoint formulation is independent of the model/input parameter itself,

ULSAN NATIONAL INSTITUTE OF
SCIENCE AND TECHNOLOGY

such that it has advantages of the calculating a set of the sensitivity of the certain physical system to the numerous parameters with less computational efforts, compared to traditional way of sensitivity analysis, i.e. recalculating perturbed state. To evaluate adjoint-based sensitivity method for Multiphysics problem, a one-dimensional steady-state model of the circulating liquid fuel system and its sensitivity system is established, which consists of one group neutron diffusion equation, balance equations of 6 groups of neutron precursors and 3 groups of decay heat groups, and energy conservation equation. For the condition of Molten Salt Fast Reactor (MSFR) developed by European project SAMOFAR as a representative of liquid-fueled MSR, physical interpretation of the model sensitivity considering coupled effect of two physics are discussed in terms of modeling option and importance of parameter. The second part includes the development of integrated solver within open source Multiphysics toolkit, OpenFOAM, called *msrAdjointFoam*. It consists of neutronics and thermal-hydraulics coupled in the same environment (i.e. internal coupling) and model sensitivity analysis solver based on the adjoint formulation of the local sensitivity of system variable to all input/model parameters. Adjoint sensitivity solver is implemented based on the mathematical derivation of model equations of the system. Validation and verification of the solver are conducted with several benchmark cases and compared with the analytic solution. The last part describes the application of the integrated design and analysis tool for developing a new conceptual design of MSR; Nanofluidic Molten Salt Reactor. The concept of nanofluid itself is for enhancement of the convection heat transfer with the adoption of excellent thermal properties with the nanoparticle. To evaluate the conceptual design of the nanofluidic molten salt reactor, *msrAdjointFoam* was extended to *nanoMsrAdjointFoam* by implementing nanofluid characteristic; dispersion model suggested by Y. Buongiorno based on the concentration of nanoparticle, and its influences on the coupled neutronics and thermal-hydraulics. Using the integrated analysis tool, several design options of the nanofluidic molten salt reactor including decay heat removal system for drain tank are assessed in terms of system performance and safety.

According to the mathematical background of the concept of adjoint sensitivity system, it can be extended to the model sensitivity analysis of any engineering system that can represent in a PDE form. In addition, the sensitivity analysis method on the Multiphysics approach can give a physical insight in economic and straightforward way. Integrated Multiphysics tool developed can help to understand and evaluate the complex system such as a nuclear reactor in a more realistic way without any exaggeration of the prediction of overall system behavior considering all coupled phenomena. In the end, from the practical point of view, the concept of nanofluidic molten salt reactor is expected to be the most feasible reactor option with enhanced safety, reduction of nuclear waste, high proliferation resistance as a future nuclear power.

ULSAN NATIONAL INSTITUTE OF SCIENCE AND TECHNOLOGY

Contents

ULSAN NATIONAL INSTITUTE OF SCIENCE AND TECHNOLOGY

ULSAN NATIONAL INSTITUTE OF SCIENCE AND TECHNOLOGY

Nomenclature

A	Operator matrix of equation
C	Source term in direct sensitivity equation
C_p	Specific heat [J/kg K]
c	Concentration of delayed neutron precursor [$1/m^3$]
D	Diffusion coefficient [1/cm]
d	Energy density of decay heat precursor [J/m^3]
E	Energy [J or eV]
e	Internal energy [J]
F	Operator matrix for neutronics
G	Mass flux [kg/m^2s]
g	Gravitational acceleration [m/s^2]
h	Heat transfer coefficient per unit length [W/m^3K] or indicator of decay heat precursor
K	Temperature dependency terms in direct sensitivity system
k	Multiplication factor [-] or thermal conductivity [W/mK]
L	Loop length [m]
M	Operator matrix
N	The number of state variable or direct sensitivity field of nanoparticle concentration
T	Temperature [K]
u	Velocity [m/s]
P	Weighting functions on state variable in definition of system response
Q	Power density [W/m^3]
R	System response
S	Sensitivity coefficient [-]
x	State variable or one-dimensional coordinate
X	Direct sensitivity field of neutron flux [$1/cm^2s$ / (unit of α)]
Y_i	Direct sensitivity field of ith group of delayed neutron precursors [$1/m^3$ / (unit of α)]
W_i	Direct sensitivity field of ith group of decay heat precursors [J/m^3 / (unit of α)]
Z	Direct sensitivity field of temperature [K / (unit of α)]

ULSAN NATIONAL INSTITUTE OF SCIENCE AND TECHNOLOGY

Greek symbols

α	Input/model parameter or coefficients
β	Fractions of precursors or coefficients
χ	Fraction of neutron energy
ρ	Density [kg/m^3]
ϕ	Neutron flux [1/cm^{2}s]
φ	Concentration of nanoparticle [1/m^3]
λ	Decay constant [1/s] or derivative of state variable with respect to α
ν	Kinematic viscosity [m^2/s]
Σ	Cross section

Subscripts

0	Reference value
C	Non-temperature dependency term
d	Decay heat
f	Fission generation term
i	i-th group of precursor or the number of model and input parameter
j	The number of type of system response
ref	Reference
T	Total
Z	Temperature dependency term

Superscripts

*	adjoint or adjoint sensitivity solution

Abbreviations

ARE	Aircraft Reactor Experiment
CL	Cold Leg

ULSAN NATIONAL INSTITUTE OF SCIENCE AND TECHNOLOGY

DHRS	Decay Heat Removal System
FHR	Fluoride salt-cooled High temperature Reactor
GIF	Generation IV International Forum
HL	Hot Leg
HX	Heat Exchanger
LFTR	Liquid Fluoride Thorium Reactor
LWR	Light Water Reactor
MCFR	Molten Chloride Salt Reactor
MSBR	Molten Salt Breeder Reactor
MSFR	Molten Salt Fast Reactor
MSR	Molten Salt Reactor
MSRE	Molten Salt Reactor Experiment
NPP	Nuclear Power Plant
NRC	Nuclear Regulatory Commission
NSF	The number of neutron generated by fission reaction, $\nu\Sigma_f$
ORNL	Oak Ridge National Laboratory
PIRT	Phenomena Identification Ranking Table
SA	Absorption cross section, Σ_a
SP	Power per fission, $E_f\Sigma_f$
SWaB	Seaborg Waste Burner reactor
TMSR	Thorium Molten Salt Reactor

ULSAN NATIONAL INSTITUTE OF SCIENCE AND TECHNOLOGY

List of Figures

ULSAN NATIONAL INSTITUTE OF SCIENCE AND TECHNOLOGY

ULSAN NATIONAL INSTITUTE OF
SCIENCE AND TECHNOLOGY

List of Tables

ULSAN NATIONAL INSTITUTE OF SCIENCE AND TECHNOLOGY

CHAPTER 1 INTRODUCTION

1.1 Research Background and Motivation

The framework of the Generation IV International Forum (GIF) has been carried out the research and development since 2000 to pursue the nuclear energy as future energy resources, where several reactor types of the nuclear power plant are proposed to achieve the advances in sustainability, reduction of nuclear waste, safety and reliability, proliferation resistance and competitive economies [1]. In addition, the importance of the nuclear safety has been emphasized to protect people and environment from any radioactive hazardous disasters after Fukushima nuclear power plant (NPP) accident in 2011. It means how nuclear reactor can be designed, operated, and managed to mitigate such kind of unpredictable accident in walkway safety concept. It also tells that along with improving existing NPP systems, developing new types of nuclear reactor is required for the next generation of nuclear energy in a long-term perspective.

In retrospect of the history of the nuclear reactor, Fermi's water boiler, the first nuclear reactor fueled with uranium-235 enriched uranium, designed and operated with aqueous homogeneous fuel in liquid form [2]. It adopts liquid fuel having lots of advantages to achieve high power density and neutron economy. In terms of the safety viewpoint, it can achieve a meltdown-proof reactor design with intrinsically safe as well; draining liquid fuel to other region except core maintaining subcritical state and large thermal expansion coefficient for strong negative temperature reactivity feedback coefficient. In addition, Alvin Weinberg who lead homogeneous reactor experiment in 1950s stated that liquid fuel system can achieve much simpler fuel cycle and system itself than solid fueled one as 3P system; a pot, a pipe, and a pump with excellent neutron economy [3]. However, it had some technical limitations in maintaining homogeneous state in a certain concentration of fuel slurry form with relatively large fuel particle and expenses, and required highly enriched fuel, as well as some political issues at that time, such that solid fueled light water reactor (LWR) was selected and most of the nuclear reactors are those types nowadays.

Rethinking the history of nuclear reactor, from Fermi's boiler to nowadays LWR, liquid-fueled nuclear reactor is quite attractive option to achieve both safety and sustainability as a future nuclear energy. In addition, it is the only one which was successfully demonstrated by several series of experiments among generation IV reactor designs as well. With aims of the development of related chemical reprocessing and molten salt technologies, taking advantages of the liquid fuel in safety and economic viewpoint as well as the radioactive waste issue. In a viewpoint of design and analysis of liquid-fueled MSR system, comprehensive understanding of underlying physics and its complex system behavior is required in the aspects of Multiphysics viewpoints.

ULSAN NATIONAL INSTITUTE OF SCIENCE AND TECHNOLOGY

1.2 Review on Molten Salt Reactor and Multiphysics Modeling

Molten Salt Reactor (MSR) is the only reactor among Gen IV reactors that adopts liquid fuel serving as a coolant as well. With a lesson of previous experiences, it was evolved to adopt the liquid fuel as the eutectic formation of fuel material with molten salt, which is the current MSR concept. This was successfully demonstrated by Aircraft Reactor Experiment (ARE) and Molten Salt Reactor Experiment (MSRE) by Oak Ridge National Laboratory (ORNL) in the 1950s. Nowadays, various design work of MSR has been conducted in worldwide from increasing demands on the MSR concept; including national R&D program such as Fluoride salt cooled high temperature reactors (FHR) program of USA, SAMOFAR in framework of Horizon 2020, MOSART program of Russia, Thorium MSR (TMSR) program of China, and many startups such as Transatomic, TerraPower, FLiBe energy in USA, Moltex Energy in UK, Thorium Technical Solution of Japan, etc., and their reactor design is shown in Figure 1-1.

ORNL designed Molten Salt Breeder Reactor (MSBR) based on the precious experiences in demonstration of MSR, but never built. There are two types of MSBR: one is a single-fluid type thermal spectrum MSR with total power of 2250 MW_{th} for the breeder and power reactor [4], and the other is two-fluid type thermal spectrum MSR with total power of 2400 MW_{th} [5], however design work of MSBR is shifted to one-fluid core design [6]. For both types, graphite moderator forms a channel having various diameter along radial direction dividing fuel zone and fuel salt flows along that channel, and reactivity is controlled by graphite control rod. Starting with reference design of single fluid MSBR, FUJI reactor by Thorium Technology Solution of Japan [7] and TMSR-LF (Thorium MSR- Liquid Fuel) by SINAP of China [8] have been developed, LFTR (Liquid Fluoride Thorium Reactor) of FLiBe Energy of USA [9] has been under developed from two-fluid MSBR. They are all graphite-moderated thermal spectrum molten salt reactor using uranium only or uranium-thorium fuel cycle. MSR concept is also adequate for burning minor actinides to solve the issue on the radioactive waste or utilizing thorium efficiently. SWaB (Seaborg Waste Burner) of Seaborg Technologies of Denmark is designed to burn the conventional nuclear waste and power generation of 50 MW_{th} in this stage. It adopts single fluid of lithium fluoride salt, thermal-epithermal spectrum with graphite moderator [10]. MCFR (Molten Chloride salt cooled Fast Reactor) by TerraPower of USA launched their reactor design work [11]. It adopts chloride type salt in fast spectrum operation for uranium and plutonium recycle with 2500 MW_{th} power generation without any internal structures such as moderator and control rod. MSFR (Molten Salt Fast Reactor) developed by EU in frame of EVOL Euratom project, which is two fluid of lithium fluoride fuel and blanket salt in fast spectrum for waste burner, breeding and power generation of 3000 MW_{th}, and its power is adjusted by controlling heat exchanger and flow rate of fuel salt or helium bubbling [12]. Various types of MSR design features are summarized in Table 1-1.

ULSAN NATIONAL INSTITUTE OF SCIENCE AND TECHNOLOGY

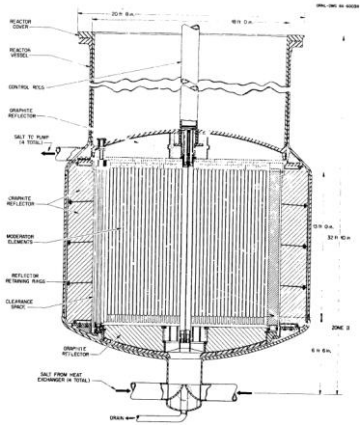

a) MSBR (ORNL) [4]

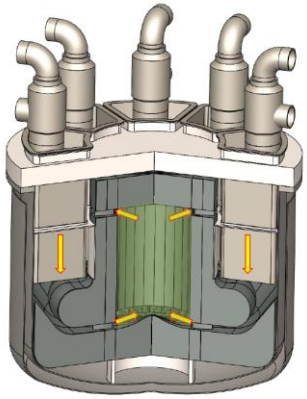

b) MCFR (Terrapower) [11]

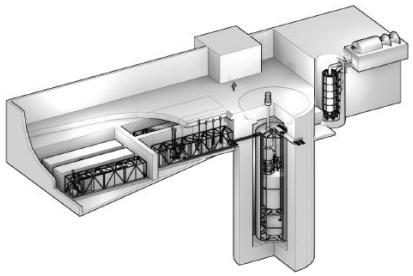

c) LFTR (Flibe Energy) [9]

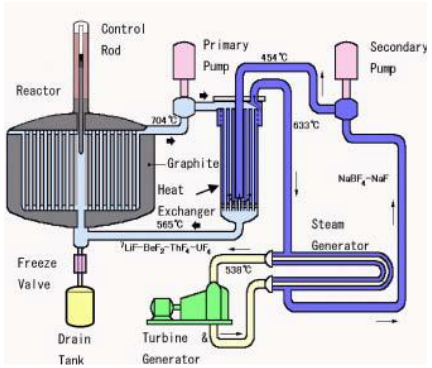

d) FUJI
(Thorium Technology Solutions) [7]

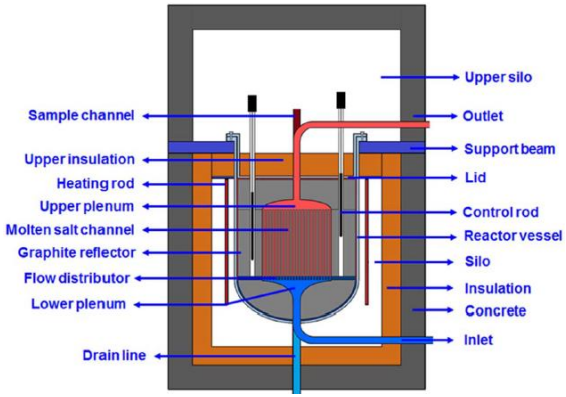

e) TMSR (SINAP) [8]

f) SWaB (Seaborg) [10]

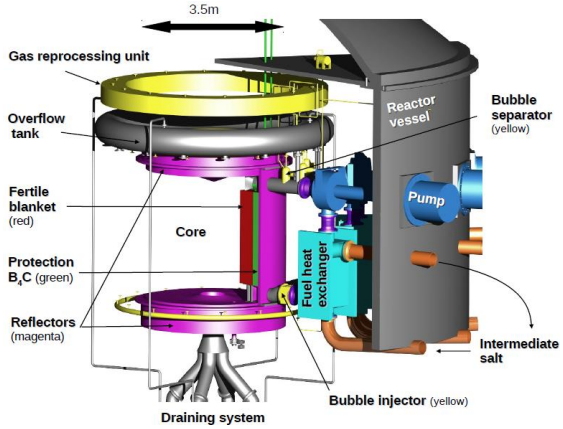

g) MSFR (SAMOFAR) [12]

Figure 1-1 Schematics of various MSR concepts

ULSAN NATIONAL INSTITUTE OF SCIENCE AND TECHNOLOGY

Table 1-1 Design features of liquid-fueled MSR

	MSBR (ORNL)	**MCFR (Terrapower)**	**LFTR (Flibe energy)**	**FUJI (Th. Tech. Sol.)**	**TMSR-LF (SINAP)**	**SWaB (Seaborg)**	**MSFR (SAMOFAR)**
Neutron spectrum	Thermal	Fast	Thermal	Thermal	Thermal	Thermal	Fast
Purpose	Breeding & Power	U-Pu recycle	Breeding & Power	Breeding & Power	Development of thorium energy	Waste burner	Waste burner & Breeding & Power
Type	Single fluid	Single fluid	Two-fluid	Single fluid	Single fluid	Single fluid	Two-fluid
Base salt	FLiBe	NaCl	FLiBe	FLiBe	FLiBe	LiF	LiF
Fuel cycle	U-Th	Pu-Th or U-Pu	U	U-Th	U-Th or Pu-Th	Th	U-Th or ^{enr}U-(Pu-MA)
Total power	2250 MW_{th}	2500 MW_{th}	600 MW_{th}	450 MW_{th}	395 MW_{th}	50 MW_{th}	3000 MW_{th}
Fuel salt volume	48.7 m^3 (19.0 m^3 in core)	N/A	N/A	26.4 m^3 (21.1 m^3 in core)	N/A	5.7 m^3	18 m^3
Reactivity control	• Graphite control rod	• N/A	• Graphite control rod	• Graphite control rod	• N/A	• Power control by HX/flow rate	• Power control by HX or flow rate • Helium bubbling
Shutdown	• Drain fuel salt	• Drain fuel salt	• Shutdown rod • Drain fuel salt	• B_4C emergency shutdown rod • Drain fuel salt	• Fuel salt drainage	• Graphite shutdown rod • Drain fuel salt	• Drain fuel salt
DHRS of drain tank	NaK or LiF-BeF_2 channel	N/A	DRACS loop	Water-steam cooling channel	Sodium heat pipe	TBD	Water cooling channel

ULSAN NATIONAL INSTITUTE OF SCIENCE AND TECHNOLOGY

As described, MSR can be designed in thermal or fast spectrum, molten salt as a both fuel and coolant, or coolant only with solid fuel, salt material as fluoride or chloride salt according to the purpose of the reactor. Most of them adopted the liquid-fueled MSR, where it can be an alternative of a conventional nuclear power plants with aims of the development of related chemical reprocessing and molten salt technologies, taking advantages of the liquid fuel in safety and economic viewpoint as well as the radioactive waste issue. The issue on the design of the MSR is the predicting system behavior of fluid fuel, especially the transport of the delayed neutron precursors along with fuel salt flow. For the solid fuel reactor, delayed neutron precursors can be modeled by balance equations considering produce and lost terms, where they stay at the given position. For instance, point kinetics equation for neutron and delayed precursors modeled by the balance equations expressed as (1-1) and (1-2) can explain the importance of delayed neutron on overall neutron economy [13].

$$\frac{d}{dt}n(t) = S(t) + \frac{(\rho - \beta)}{\Lambda}n(t) + \sum_i \lambda_i C_i(t), \tag{1-1}$$

$$\frac{d}{dt}C_i(t) = \frac{\beta_i}{\Lambda}n(t) - \lambda_i C_i(t) \text{ (,where i=1,2, ... ,6)} \tag{1-2}$$

, where n is the number of the neutron, S is the source of neutron, ρ is the reactivity defined as $(k-1)/k$, Λ is the prompt neutron generation time defined as neutron lifetime divided by multiplication factor, β is the delayed neutron fraction, λ is the decay constant, and C_i is the number of i-th group of delayed neutron precursor, respectively.

From the point kinetic equations, we can easily catch that overall neutron economies are governed by the delayed neutron fraction β. In delayed neutron balance equation for solid fuel, the number of precursors produced and decaying are included along with neutron balance equation. However, for the liquid fuel, it is important to consider the additional influences from flow of liquid fuel; i.e. transport of the delayed neutron precursors. Since the location where they are produced and decaying are different while moving in the system, the distribution determined by the transport of the delayed neutron precursors influences overall neutronics. It affects the total power distribution in reactor that small changes of the temperature field give a feedback on the neutronics in the end. Figure 1-2 shows the relationship between each physics underlying molten salt reactor analysis and tightly coupled features by sharing important phenomena. Therefore, it is important for the analysis of MSR to consider the interactions between strongly coupled physics for analysis of MSR by means of a multiphysics approach, different from conventional solid-fueled nuclear reactor [14].

ULSAN NATIONAL INSTITUTE OF SCIENCE AND TECHNOLOGY

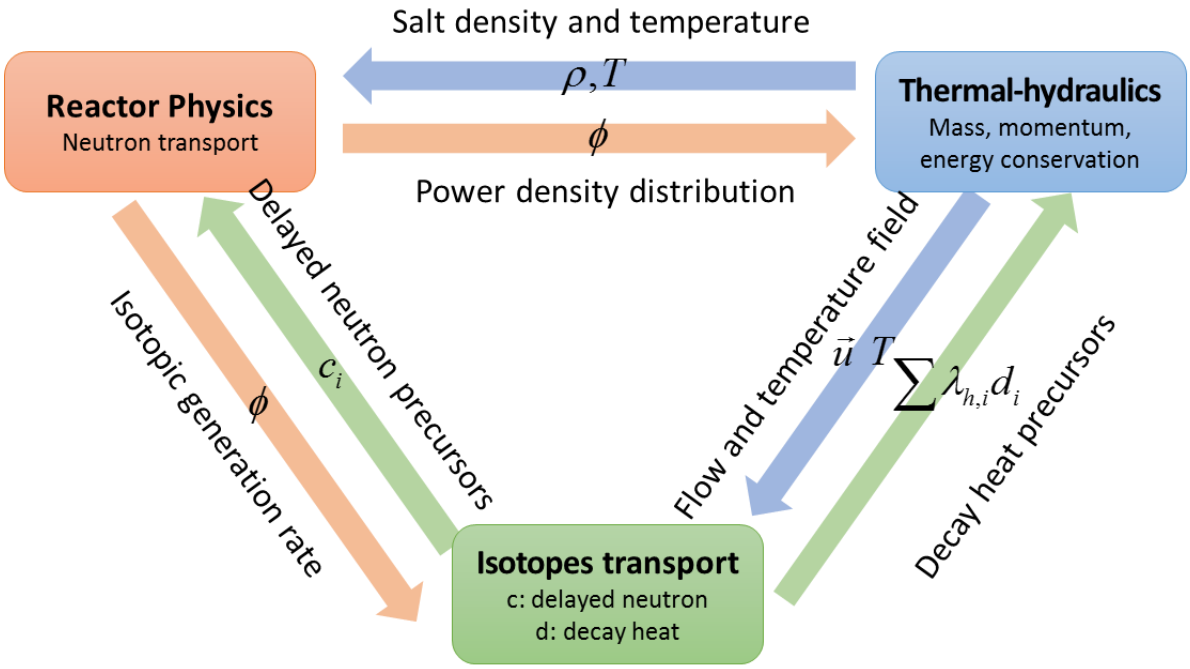

Figure 1-2 Multiphysics system of liquid-fueled molten salt reactor

ULSAN NATIONAL INSTITUTE OF
SCIENCE AND TECHNOLOGY

In fundamental viewpoint of predictive modeling of the system, identification and characterization of the uncertainties underlying simulation processes are required for the computational model prediction [15]. It includes data error and uncertainties of input data, model parameters or initial/boundary conditions, numerical error from discretization and truncation error, and unclear configurations of the physical processes which is modeled. To assess the model accuracy and proposed simulation methodology of the liquid fueled MSR as non-LWR case, US-NRC listed several figure-of-Merits (FoMs) in neutronics and thermal-hydraulics for the preliminary Phenomena Identification and Ranking Table (PIRT) [16]. The reactivity, power distribution and peak power, kinetic parameters, fluence, and primary system gases are chosen in neutronics, and primary system temperature distribution, power distribution and peak power, flow velocity, liquid salt composition and distribution, gas and solid fission products transport and composition are chosen in thermal hydraulics as FoMs based on the important phenomena. Three important viewpoints are considered for the comprehensive understanding of MSR system.

- ✓ Design: What are the important phenomena of the liquid fueled MSR?
- ✓ Model: How important phenomena are included properly in the system analysis?
- ✓ Sensitivity: How much these complex and coupled models influence analysis results?

In other words, results of the safety analysis of the liquid fueled MSR are highly dependent on the what physical processes are modeled, especially for the tightly coupled neutronics and thermal-hydraulics characteristics. For the predictive model on the Multiphysics approach, motion of the delayed neutron precursors considering three-dimensional geometrical flow pattern and uncertainties of the fuel salt properties from temperature and composition variations from depletion are the two most important features to influence the system analysis. Besides, several issues on the safety analysis methodology for liquid fueled MSR are underlying. For instance, safety principle of defense in depth and multiple barrier concept defined for existing LWR is no longer applicable. Second, safety criteria defined for the solid fuel; melting point of solid fuel or peak cladding temperature is not acceptable, such that severe accident scenario should be re-defined and existing safety analysis code is not suitable for liquid fuel system [17]. As an early stage of the systematic assessment of liquid fueled MSR system, unique methodology on the system analysis and sensitivity analysis is required based on the Multiphysics approach first. Moreover, various models of the liquid fuel system should be assessed in the sense that whether suggested models can represent the real situations.

ULSAN NATIONAL INSTITUTE OF SCIENCE AND TECHNOLOGY

1.3 Objectives and Scope

This work aims for the development of the integrated analysis method for the Multiphysics problem; especially for the circulating liquid fuel system including system analysis and its sensitivity with adjoint-based mathematical techniques, which can be extended to general systems. It deals with the researches on the Multiphysics modeling and its sensitivity analysis of the circulating liquid fuel system in deterministic way and its extension to the nanofluidic molten salt reactor analysis to investigate the performance of decay heat removal system. There are three objectives of this work;

1) To establish the adjoint-based sensitivity analysis of the circulating liquid fuel system on the Multiphysics approach;
2) To develop the integrated analysis tool including system analysis and its sensitivity analysis with adjoint based techniques by means of the combining nuclear physics and computational fluid dynamic (CFD) approaches;
3) To evaluate the feasibility of the nanofluidic molten salt reactor concept in case of decay heat removal capability using developed tool.

Chapter 1 briefly reviews the existing status of the R&D of molten salt reactor and its Multiphysics modeling approach, and introduces the motivation, objective, and the scope of this study.

Chapter 2 includes the adjoin-based sensitivity analysis method for Multiphysics problem and its application to the circulating liquid fuel system. One-dimensional primary loop of MSR in steady state is modeled and its Multiphysics behavior and model sensitivity are described in terms of the coupling method and model parameter importance.

Chapter 3 describes the integrated design and analysis solver; *msrAdjointFoam* based on the Multiphysics toolkit, OpenFOAM coupling neutronics, thermal-hydraulics, and species transport physics combined with adjoint based technique. 2D square cavity benchmark simulation and simplified loop geometry under MSFR condition are investigated in terms of system performance evaluation and local sensitivity. Extending the methodology, nanofluid physics is implemented to the solver; called *nanoMsrAdjointFoam*. Application to the nanofluidic molten salt reactor, passive decay heat removal performance of the drain tank using molten salt nanofluid is discussed using developed tool.

Finally, the conclusions and recommendations on this work are described in Chapter 4.

ULSAN NATIONAL INSTITUTE OF SCIENCE AND TECHNOLOGY

CHAPTER 2 ADJOINT-BASED SENSITIVITY ANALYSIS FOR MULTIPHYSICS PROBLEM

2.1 Introduction

For many engineering fields, sensitivity analysis to input parameters is required in system design and analysis. The analysis of engineering systems is a complex task, involving many experimental, modelling and computational aspects: numerical models, sets of linear or non-linear equations representing physical phenomena, uncertainty of input parameters, or data processing with measurements, are just a few examples [18]. It is important to evaluate how much those aspects influence to the system locally or globally to avoid misunderstanding of the system behavior and misinterpretations of analysis results. Objective of the sensitivity analysis is to figure out in a quantitative way the effects of parameter variations on the computational results [19]. Nowadays, the importance of sensitivity analysis keeps increasing as engineering systems of interest are becoming more and more complex, making it difficult to separate the effects of the several parameters describing large scale multiphysics systems.

Adjoint method is a widely used technique to evaluate the system performance and reliability in complex system with its excellent efficiency [20]. It has lots of advantages in case of i) the number of parameter exceeding that of system response functions of interest; ii) large scale systems; and iii) complex systems described by highly non-linear models and equations [19], [21]. These advantages can be applied to multiphysics problems as well, such as the analysis of nuclear reactors, accounting for the contributions from both neutronics and thermal-hydraulics. With aims of Adjoint Sensitivity Analysis Procedure (ASAP) developed by Cacuci [18], several attempts to investigate the systematic sensitivity using adjoint based method for numerous parameters with reduced computational resources.

Recently, the importance of analyzing the sensitivity of generation IV reactor systems is highlighted, considering both neutronics and thermal-hydraulics. Gilli et al. conducted the sensitivity analysis for the solid fueled sodium cooled fast reactor, considering point kinetics model for delayed neutron precursors and energy equations for the fuel and coolant [22]. They adopted first order ASAP for the coupled neutronics and thermal-hydraulics case to investigate the performance of reactor power and maximum cladding temperature at certain point under several accident conditions. In this case, adjoint method for sensitivity analysis only requires the Jacobian information of the nonlinear problem obtained from existing codes. Perko et al. performed the sensitivity analysis for coupled criticality problems with feedback between neutronics and thermal-hydraulics by solving coupled adjoint equations of the one-dimensional slab problem [23]. They considered the steady state power level, reactivity worth, or other important phenomena as system responses of the light water reactor by

ULSAN NATIONAL INSTITUTE OF
SCIENCE AND TECHNOLOGY

solving decoupled adjoint problems for neutronics and other augmented codes in steady state. For the solid fueled nuclear reactor analysis, it is easy to consider the relatively weak coupling between neutronics and thermal-hydraulics, by exchanging temperature information on the solid fuel.

At this viewpoint, MSR is one of the most challenging cases to analyze the sensitivity of the system response to the input or model parameters, due to the effects of fuel flow to tightly coupled neutronics and thermal-hydraulics. Rodigari performed a sensitivity analysis only for neutronics model of molten salt reactor based on the adjoint method, but the effect of circulating fuel salt was included in neutronics precursor balance equation without any temperature feedback [24]. Table 2-1 summarizes the approaches for the local sensitivity analysis of coupled problem related to nuclear reactor in literature.

In this section, adjoint-based sensitivity analysis method is applied on the Multiphysics approach for the general circulating liquid fuel system to develop a model sensitivity analysis method for molten salt reactor. Considering fully-coupled physics effect, the importance of the different parameters affecting the system behaviors is evaluated in deterministic way to provide useful guidelines for design and analysis of circulating liquid fuel system. To verify and validate the developed sensitivity analysis method, numerical studies are performed using MATLAB on the configurations of the one-dimensional closed loop in steady state.

ULSAN NATIONAL INSTITUTE OF SCIENCE AND TECHNOLOGY

Table 2-1 Comparison of sensitivity analysis approach for coupled problem of nuclear reactor

Authors (year)	**Neutronics**	**Thermal-Hydraulics**	**Note**
Gilli et al. (2011) [22]	Point kinetic model w/ neutron precursors balance equation	Energy equations for both fuel and coolant	- Solid fuel (fast reactor) - Transient analysis
Perko et al. (2013) [23]	Two group 1D diffusion equation	Energy equation for fuel	- Solid fuel (light water reactor) - Steady state analysis
Rodigari (2008) [24]	Point kinetic model w/ 6 groups of neutron precursors balance equations	N/A	- Liquid fuel (MSR) - Transient analysis - Flow effect is considered in equations of neutron precursors.
Present study	One group 1D diffusion equation w/ 8 groups of neutron precursors balance equations	Energy equation w/ 3 groups of decay heat precursors balance equations	- Liquid fuel (MSR) - Steady state analysis - Flow effect is considered in equations of neutron precursors and decay heat precursors.

ULSAN NATIONAL INSTITUTE OF SCIENCE AND TECHNOLOGY

2.2 Adjoint-based Sensitivity Analysis Method for Multiphysics Model

2.2.1 Comparison of Sensitivity Analysis Methods

Local sensitivity of system response is defined as a rate of change of system response from the changes of any parameters α, as a first derivative of the system response with respect to α. The conventional way to evaluate the sensitivity of system response is based on the linear perturbation theory, obtained by calculating system response more than twice for the perturbation of each parameter, Δα; so-called recalculation as shown by equation (2-1). Estimating the sensitivity in this way requires to choose proper value of Δα, not much small to avoid misinterpretations of results from computational error, but small enough to satisfy the first order approximation [19].

$$\frac{dR}{d\alpha} \approx \frac{R(\alpha+\Delta\alpha)-R(\alpha)}{\Delta\alpha} \tag{2-1}$$

In general, let system variables $\mathbf{x}=\left[x_1, x_2, x_3, \cdots, x_N\right]$ in vector form and the system equation $\mathbf{F}=\left[F_1(\alpha,\mathbf{x}).F_2(\alpha,\mathbf{x}).\cdots,F_N(\alpha,\mathbf{x})\right]$ satisfying $\mathbf{F}=0$, where each system equation representing single physics problem can be expressed in matrix form as $F_i(\alpha,\mathbf{x})=\mathbf{A}_i x_i-\mathbf{b}_i$. Differentiate system equation F with respect to any input parameter α yields;

$$\frac{d\mathbf{F}}{d\alpha}=\frac{\partial\mathbf{F}}{\partial\alpha}+\frac{\partial\mathbf{F}}{\partial\mathbf{x}}\frac{\partial\mathbf{x}}{\partial\alpha}=0 \quad \text{or} \quad \frac{\partial\mathbf{x}}{\partial\alpha}=\left(\frac{\partial\mathbf{F}}{\partial\mathbf{x}}\right)^{-1}\left(-\frac{\partial\mathbf{F}}{\partial\alpha}\right) \tag{2-2}$$

For the system response R represented as **R**(α,**x**) in (2-3), its sensitivity with respect to α can be expressed with the sensitivity of each variables to the any parameter, $\boldsymbol{\lambda}=\frac{\partial\mathbf{x}}{\partial\alpha}$.

$$\frac{d\mathbf{R}(\alpha,\mathbf{x})}{d\alpha}=\frac{\partial\mathbf{R}}{\partial\alpha}+\frac{\partial\mathbf{R}}{\partial\mathbf{x}}\frac{\partial\mathbf{x}}{\partial\alpha} \tag{2-3}$$

Rewriting (2-3) by substituting $\boldsymbol{\lambda}=\frac{\partial\mathbf{x}}{\partial\alpha}$ and $\frac{\partial\mathbf{x}}{\partial\alpha}=\left(\frac{\partial\mathbf{F}}{\partial\mathbf{x}}\right)^{-1}\left(-\frac{\partial\mathbf{F}}{\partial\alpha}\right)$ in (2-2), the sensitivity of system response R can be expressed as (2-4). In this point, solving the derivatives of system equations for sensitivity analysis; i.e. obtaining λ called direct method.

ULSAN NATIONAL INSTITUTE OF SCIENCE AND TECHNOLOGY

$$\frac{d\mathbf{R}(\alpha,\mathbf{x})}{d\alpha}=\frac{\partial\mathbf{R}}{\partial\alpha}+\frac{\partial\mathbf{R}}{\partial\mathbf{x}}\frac{\partial\mathbf{x}}{\partial\alpha}=\frac{\partial\mathbf{R}}{\partial\alpha}-\frac{\partial\mathbf{R}}{\partial\mathbf{x}}\frac{\partial\mathbf{F}}{\partial\mathbf{x}}^{-1}\frac{\partial\mathbf{F}}{\partial\alpha} \tag{2-4}$$

2.2.2 Adjoint-based Sensitivity Analysis Method

Cacuci [25] firstly developed the adjoint-based sensitivity analysis procedure (ASAP) for the system that can be described in PDEs. Adjoint sensitivity is obtained by taking adjoints of the derivatives of the system variables, which are derived by differentiating system equations with respect to each parameter, such that it is expressed with linearized form to the original problem. On the derivation of adjoint sensitivity system, source terms are determined depending on the solution of main problem and on which parameter is chosen for sensitivity analysis. For the parameter sensitivity, ASAP is considered as the most efficient method for local sensitivity analysis so far [19]. Once the main solutions are obtained from calculations, it is straightforward that the adjoint sensitivity can be easily calculated with relatively less efforts than those from calculating original sensitivity in direct method which requires same resources for primal problem.

The adjoint method can be utilized to analyze a certain complex problem by constructing an adjoint system having a duality with primal system. It is applicable to any system defined with continuous and differentiable real function which is quadratically summable with their derivatives on whole domain [20]. For the system equation, for instance, $Av=f$, the corresponding adjoint equation $A^*v^*=g$ is defined. In this case, A^* is called an adjoint operator to primal system operator, A and v^* is an adjoint solution. Note that g is an arbitrary function that can be defined in form and properties depending on the problem.

$$\left(Av,v^*\right)=\left(v,A^*v^*\right),\ \text{where}\ \ (v,w)=\int_\Omega vw\,d\Omega \tag{2-5}$$

Back to the sensitivity analysis, let corresponding adjoint function to λ be λ^* satisfying Lagrange's identity such that $\left(\frac{\partial\mathbf{F}}{\partial\mathbf{x}}\right)^*=\left(\frac{\partial\mathbf{F}}{\partial\mathbf{x}}\right)^T$ by the definition of Hermitian adjoint matrix.

$$\frac{\partial\mathbf{F}}{\partial\mathbf{x}}^*\boldsymbol{\lambda}^*=\frac{\partial\mathbf{R}}{\partial\mathbf{x}},\ \text{where}\ \left(\frac{\partial\mathbf{F}}{\partial\mathbf{x}}\boldsymbol{\lambda},\boldsymbol{\lambda}^*\right)=\left(\boldsymbol{\lambda},\frac{\partial\mathbf{F}}{\partial\mathbf{x}}^*\boldsymbol{\lambda}^*\right) \tag{2-6}$$

ULSAN NATIONAL INSTITUTE OF
SCIENCE AND TECHNOLOGY

Three methods for evaluating local sensitivity of system; recalculation, direct and the adjoint based method can be summarized in Table 2-2 and its numerical procedure in Figure 2-1. Adjoint-based method becomes powerful in sensitivity analysis for complex system. With only single adjoint function λ^* regardless of the type of parameter, sensitivity of system response $dR/d\alpha$ can be calculated for all parameters. On the other hand, recalculating system response or direct method requires repetitive calculations to obtain solution for each parameter. For instance, let N be the number of parameters included in model, geometry of system, or specifications of system design, and M be the number of system responses of interests. When sensitivities of system response are obtained by recalculation, it requires not only to select a proper $\Delta\alpha$ small enough to prevent misunderstanding of those system, but also to solve the problem for a minimum (N+1)*M times of calculations for a single set of main problems. On the other hand, adjoint-based sensitivity analysis can significantly reduce calculation times as well as computational resources, required to solve the problem M times only.

Considering a large scale and/or complex system analysis having numerous input parameters, it is hard to assess its sensitivity in entire range for all the parameters: this is one of typical difficulties of local sensitivity analysis [26]. In this case, when the adjoint system is derived for the model sensitivity from a small perturbation of model input in terms of derivative of model output on that input parameter, they can be utilized to assess the changes of system response from variation of the input parameters with relatively economic way. Due to the properties of adjoint operators, the adjoint system has the meaning of a linear transformation by projecting the primal system into a dual space defined arbitrarily.

ULSAN NATIONAL INSTITUTE OF SCIENCE AND TECHNOLOGY

Table 2-2 Comparison of the sensitivity analysis methods

	System variables	**Sensitivity, dR/dα**
Recalculation	$\mathbf{x}=\left[x_1, x_2, x_3, \cdots, x_N\right]$	$\frac{d\mathbf{R}}{d\alpha}=\frac{R(\alpha+\Delta\alpha)-R(\alpha)}{\Delta\alpha}$
Direct method	$\frac{d\mathbf{x}}{d\alpha}=\boldsymbol{\lambda}=\left[\frac{dx_1}{d\alpha}, \frac{dx_2}{d\alpha}, \frac{dx_3}{d\alpha}, \cdots, \frac{dx_N}{d\alpha}\right]$, where $\frac{\partial\mathbf{F}}{\partial\mathbf{x}}\lambda=-\frac{\partial\mathbf{F}}{\partial\alpha}$	$\frac{d\mathbf{R}}{d\alpha}=\frac{\partial\mathbf{R}}{\partial\alpha}+\frac{\partial\mathbf{R}}{\partial\mathbf{x}}\boldsymbol{\lambda}$
Adjoint method	$\boldsymbol{\lambda}^*=\left[\lambda_1^*, \lambda_2^*, \lambda_3^*, \cdots, \lambda_N^*\right]$, where $\frac{\partial\mathbf{F}^*}{\partial\mathbf{x}}\boldsymbol{\lambda}^*=\frac{\partial\mathbf{R}}{\partial\mathbf{x}}$	$\frac{d\mathbf{R}}{d\alpha}=\frac{\partial\mathbf{R}}{\partial\alpha}-\boldsymbol{\lambda}^*\frac{\partial\mathbf{F}}{\partial\alpha}$

ULSAN NATIONAL INSTITUTE OF SCIENCE AND TECHNOLOGY

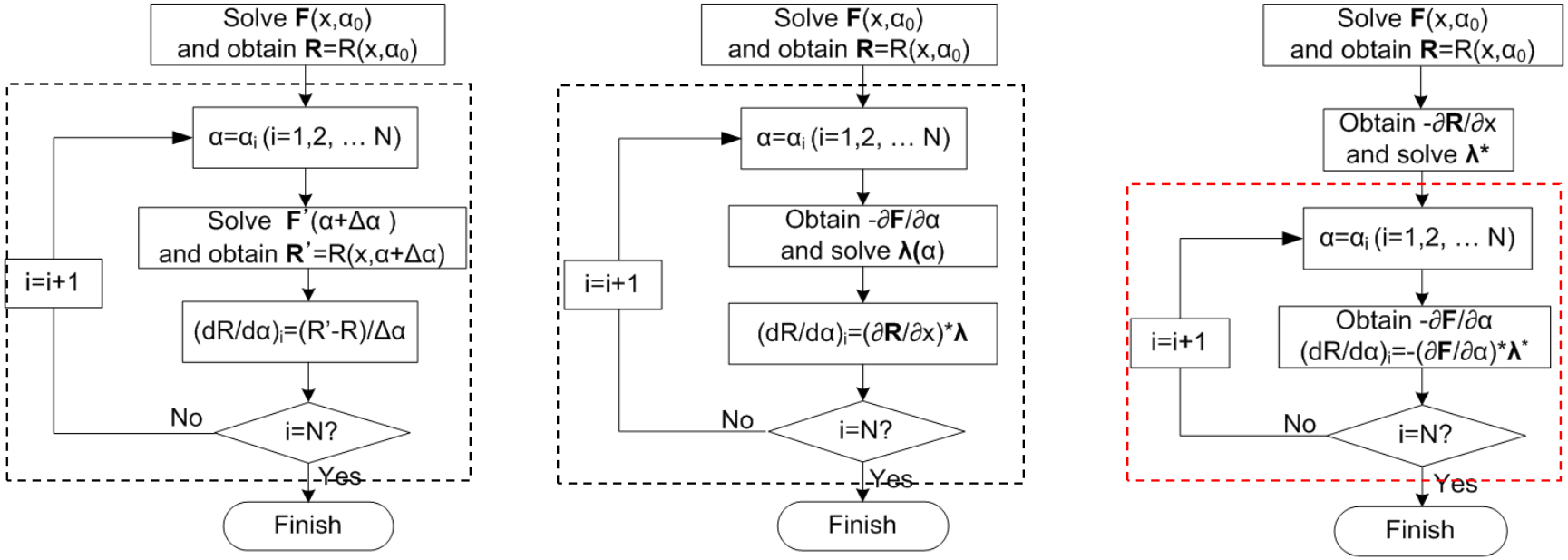

a) Recalculation b) Direct method c) Adjoint method

Figure 2-1 Comparison of flow chart for sensitivity analysis according to method

ULSAN NATIONAL INSTITUTE OF SCIENCE AND TECHNOLOGY

2.3 Model Sensitivity of the Circulating Liquid Fuel System

2.3.1 Multiphysics Model of Circulating Liquid Fuel System

A circulating liquid fuel system as a representative of the liquid-fueled MSR is chosen as a case problem of model sensitivity analysis which includes tightly coupled neutronics and thermal-hydraulics. It consists of the core part, hot leg, cold leg, and heat exchanger, where all parts is connected each other forming a closed loop, shown in Figure 2-2. Multiphysics model of the circulating liquid fuel system is constructed in one-dimensional, steady state including tightly coupled neutronics and thermal-hydraulics. In this chapter, one group neutron diffusion theory is chosen to solve the distribution of neutron flux considering diffusion, absorption, generation by fission reaction, and produced by delayed neutron precursors. To distinguish the region, fission generation term is included only in core region. Thermal-hydraulics model includes energy conservation equation with constant mass flux through the loop with volumetric heat removal term only at the heat exchanger region. Transportations of delayed neutron precursor and decay heat precursor are modeled in balance equations considering diffusion and convection term from the fuel flow. Governing equations are described in (2-7) to (2-10). Each variable has loop continuous boundary conditions as (2-11).

$$\begin{cases} -\dfrac{\partial}{\partial x}\left(D\dfrac{\partial\phi}{\partial x}\right)+\left(\Sigma_a-\dfrac{1-\beta_t}{k_{eff}}\nu\Sigma_f\right)\phi=\displaystyle\sum_{i=1}^{N_c}\lambda_i c_i & \text{for core} \\ -\dfrac{\partial}{\partial x}\left(D\dfrac{\partial\phi}{\partial x}\right)+\Sigma_a\phi=\displaystyle\sum_{i=1}^{N_c}\lambda_i c_i & \text{otherwise} \end{cases} \tag{2-7}$$

$$-\frac{\partial}{\partial x}\left(\frac{G}{\rho}c_i\right)+\frac{\partial}{\partial x}\left(\frac{\nu_T}{Sc_T}\frac{\partial c_i}{\partial x}\right)-\lambda_i c_i+\beta_i\frac{\nu\Sigma_f}{k_{eff}}\phi=0\quad\left(i=1,2,\cdots N_c\right) \tag{2-8}$$

$$-\frac{\partial}{\partial x}\left(\frac{G}{\rho}d_i\right)+\frac{\partial}{\partial x}\left(\frac{\nu_T}{Sc_T}\frac{\partial d_i}{\partial x}\right)-\lambda_{h,i}d_i+\beta_{h,i}E_f\Sigma_f\phi=0\quad\left(i=1,2,\cdots N_d\right) \tag{2-9}$$

$$\begin{cases} GC_p\dfrac{\partial T}{\partial x}=\left(1-\beta_{h,t}\right)E_f\Sigma_f\phi+\displaystyle\sum_{i=1}^{N_d}\lambda_{h,i}d_i\quad\left(i=1,2,\cdots N_d\right) & \text{otherwise} \\ GC_p\dfrac{\partial T}{\partial x}=-\dfrac{hp}{A_c}\left(T-T_w\right)+\left(1-\beta_{h,t}\right)E_f\Sigma_f\phi+\displaystyle\sum_{i=1}^{N_d}\lambda_{h,i}d_i\quad\left(i=1,2,\cdots N_d\right) & \text{for HX} \end{cases} \tag{2-10}$$

$$\begin{cases} \varphi(0)=\varphi(L) \\ \left.\dfrac{d\varphi}{dx}\right|_{x=0}=\left.\dfrac{d\varphi}{dx}\right|_{x=L} \end{cases} \text{,where } \varphi=\phi, c_i, d_i, \text{ and } T \tag{2-11}$$

ULSAN NATIONAL INSTITUTE OF SCIENCE AND TECHNOLOGY

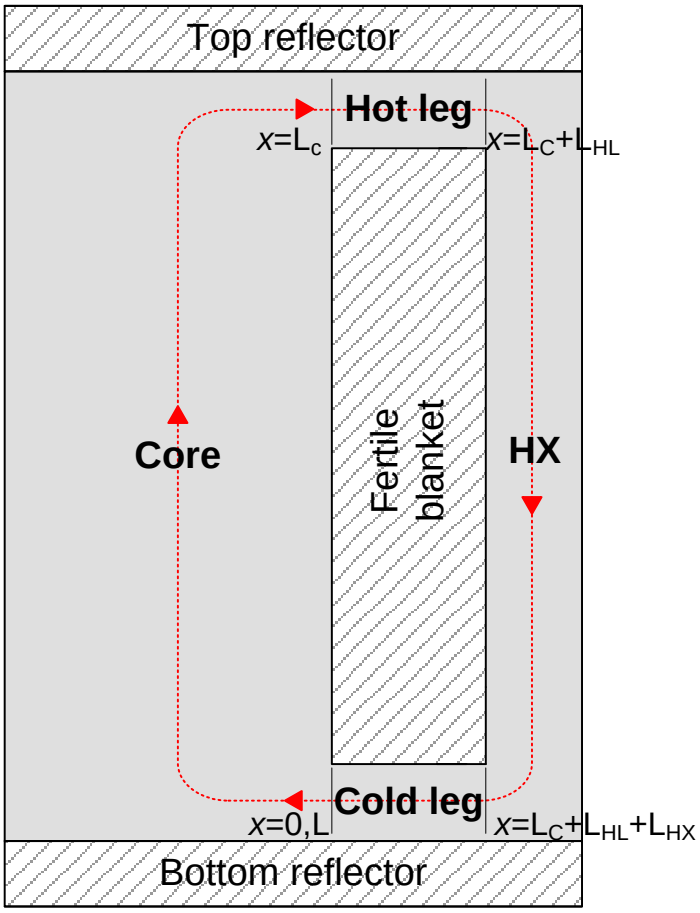

Figure 2-2 Physical domain of a circulating liquid fuel system

ULSAN NATIONAL INSTITUTE OF SCIENCE AND TECHNOLOGY

Since neutron reaction cross section, diffusion coefficient, and thermophysical properties of the liquid fuel are dependent on the temperature field, it is required to include proper coupling models to consider those effects. In this section, nuclear data and liquid properties such as density and specific heat are updated to the logarithmic temperature ratio to the reference temperature and density ratio to reference density to simulate the Doppler effect.

$$\rho = \alpha_\rho T + \beta_\rho \tag{2-12}$$

$$C_p = \alpha_{Cp} T + \beta_{Cp} \tag{2-13}$$

$$\Sigma = \frac{\rho}{\rho_{ref}}\left(\Sigma_0 + \alpha_\Sigma \log\left(\frac{T}{T_{ref}}\right)\right) \tag{2-14}$$

$$D = \frac{\rho_{ref}}{\rho}\left(D_0 + \alpha_D \log\left(\frac{T}{T_{ref}}\right)\right) \tag{2-15}$$

2.3.2 Adjoint-based Sensitivity Analysis of Circulating Liquid Fuel System

To generalize the sensitivity analysis method to Multiphysics system analysis, system response R is defined as the sum of functionals of solutions such as flux, temperature, concentration of all groups of delayed neutron precursors and decay heat precursors in steady state as equation (2-16).

$$R(\alpha,\chi) = \int_0^L P_X \phi dx + \int_0^L P_Z T dx + \int_0^L \sum_{i=1}^{N_c} P_{Yi} c_i dx + \int_0^L \sum_{i=1}^{N_d} P_{Wi} d_i dx = \sum\left(P_\xi, \chi\right) \tag{2-16}$$

, where χ is one of system variable; ϕ, T, c_i or d_i, and P_X, P_Z, P_{Yi}, and P_{Wi} are dependent on the definitions from which type of system response is of interests. For instance, these can be functions related to instrumental or measurement characteristics.

As described in section 2.2.1, sensitivity can be obtained by differentiating system response directly, letting the first derivatives of system variables $\lambda = \frac{d\chi}{d\alpha}$ as (2-17).

$$\begin{aligned}\frac{dR(\alpha,x)}{d\alpha} &= \frac{d}{d\alpha}\left(\sum\left(P_\xi,\chi\right)\right) = \sum\left(\frac{dP_\xi}{d\alpha},\chi\right) + \left(P_\xi, \frac{\partial\chi}{\partial\alpha}\right) \\ &= \frac{\partial R}{\partial\alpha} + \sum\left(P_\xi,\lambda\right)\end{aligned} \tag{2-17}$$

ULSAN NATIONAL INSTITUTE OF SCIENCE AND TECHNOLOGY

The term $\frac{\partial R}{\partial \alpha}$ in (2-17) represents the "direct term" defined by the explicit dependence of system response on parameter α. The remaining term $\sum\left(P_{\xi},\lambda\right)$ are called "indirect terms", which represent the implicit dependences of system response on parameter α [27]. Now, the problem of sensitivity of system response is changed to calculate corresponding λ. In this section, the first derivative of each system variable with respect to any input/model parameter α is denoted as $X=\frac{d\phi}{d\alpha}$, $Z=\frac{dT}{d\alpha}$, $Y_i=\frac{dc_i}{d\alpha}$, and $W_i=\frac{dd_i}{d\alpha}$.

Detailed procedure to derive adjoint sensitivity system and how to treat strongly coupled terms in primal system in its derivation are described in general case. First, direct sensitivity equations are derived by differentiating set of original governing equations with respect to α. Equation for the neutron flux sensitivity, X can be derived by differentiating with respect to α as follows. In this section, the perturbation of k_{eff} is not considered at this moment. (In CHAPTER 3, perturbed k_{eff} will be considered.) First, system equations for neutron flux, each group of delayed neutron precursors, that of decay heat precursors, and temperature are differentiated with respect to the any input or model parameter α.

$$-\frac{\partial}{\partial x}\left(D\frac{\partial X}{\partial x}\right)+\left(\Sigma_a-\frac{1-\beta_t}{k_{eff}}\nu\Sigma_f\right)X-\sum_{i=1}^{N_c}\lambda_i Y_i+K_X Z+K_{X1}\frac{\partial Z}{\partial x}=C_X \tag{2-18}$$

$$K_X=-\frac{\partial\phi}{\partial x}\frac{\partial}{\partial x}\left(\frac{dD}{d\alpha}\right)_Z-\frac{\partial^2\phi}{\partial x^2}\left(\frac{dD}{d\alpha}\right)_Z+\left(\frac{d\Sigma_a}{d\alpha}\right)_Z\phi-\frac{1-\beta_t}{k_{eff}}\left(\frac{d\left(\nu\Sigma_f\right)}{d\alpha}\right)_Z\phi \tag{2-19}$$

$$K_{X1}=-\frac{\partial\phi}{\partial x}\left(\frac{dD}{d\alpha}\right)_Z \tag{2-20}$$

$$\begin{aligned}C_X=&\frac{\partial\phi}{\partial x}\frac{\partial}{\partial x}\left(\frac{dD}{d\alpha}\right)_C+\frac{\partial^2\phi}{\partial x^2}\left(\frac{dD}{d\alpha}\right)_C-\left(\frac{d\Sigma_a}{d\alpha}\right)_C\phi+\frac{d}{d\alpha}\left(\frac{1-\beta_t}{k_{eff}}\right)\nu\Sigma_f\phi\\&+\frac{1-\beta_t}{k_{eff}}\left(\frac{d\left(\nu\Sigma_f\right)}{d\alpha}\right)_C\phi+\sum_{i=1}^{N_c}\frac{d\lambda_i}{d\alpha}c_i\end{aligned} \tag{2-21}$$

In (2-18), K_X, K_{X1} and C_X are determined by the primal solution and dependencies of nuclear data to the temperature sensitivity, Z from updates of nuclear data and salt thermophysical properties of the temperature variations. First of all, sensitivity of salt properties to the arbitrary parameter α can be divided into two terms; temperature sensitivity related term denoted as subscript Z, and other term

ULSAN NATIONAL INSTITUTE OF SCIENCE AND TECHNOLOGY

denoted as subscript C as (2-22) and (2-23).

$$\frac{d\rho}{d\alpha}=\frac{d\alpha_{\rho}}{d\alpha}T+\alpha_{\rho}Z+\frac{d\beta_{\rho}}{d\alpha}=\left(\frac{d\rho}{d\alpha}\right)_{Z}Z+\left(\frac{d\rho}{d\alpha}\right)_{C} \tag{2-22}$$

$$\frac{dC_{p}}{d\alpha}=\frac{d\alpha_{Cp}}{d\alpha}T+\alpha_{Cp}Z+\frac{d\beta_{Cp}}{d\alpha}=\left(\frac{dC_{p}}{d\alpha}\right)_{Z}Z+\left(\frac{dC_{p}}{d\alpha}\right)_{C} \tag{2-23}$$

Sensitivity of nuclear data to the certain parameter α can be expressed in same way.

$$\frac{d\Sigma}{d\alpha}=\left(\frac{d\Sigma}{d\alpha}\right)_{Z}Z+\left(\frac{d\Sigma}{d\alpha}\right)_{C} \tag{2-24}$$

$$\left(\frac{d\Sigma}{d\alpha}\right)_{Z}=\left(\frac{d\rho}{d\alpha}\right)_{Z}\left(\frac{1}{\rho_{ref}}\right)\left(\Sigma_{0}+\alpha_{\Sigma}\log\frac{T}{T_{ref}}\right)+\frac{\rho}{\rho_{ref}}\frac{\alpha_{\Sigma}}{T} \tag{2-25}$$

$$\begin{aligned}\left(\frac{d\Sigma}{d\alpha}\right)_{C}=&\left\{\left(\frac{d\rho}{d\alpha}\right)_{C}\left(\frac{1}{\rho_{ref}}\right)-\frac{\rho}{{\rho_{ref}}^{2}}\frac{d\rho_{ref}}{d\alpha}\right\}\left(\Sigma_{0}+\alpha_{\Sigma}\log\frac{T}{T_{ref}}\right)\\&+\frac{\rho}{\rho_{ref}}\left(\frac{d\Sigma_{0}}{d\alpha}+\frac{d\alpha_{\Sigma}}{d\alpha}\log\frac{T}{T_{ref}}-\frac{\alpha_{\Sigma}}{T_{ref}}\frac{dT_{ref}}{d\alpha}\right)\end{aligned} \tag{2-26}$$

$$\frac{dD}{d\alpha}=\left(\frac{dD}{d\alpha}\right)_{Z}Z+\left(\frac{dD}{d\alpha}\right)_{C} \tag{2-27}$$

$$\left(\frac{dD}{d\alpha}\right)_{Z}=-\frac{\rho_{ref}}{\rho^{2}}\left(\frac{d\rho}{d\alpha}\right)_{Z}\left(D_{0}+\alpha_{D}\log\frac{T}{T_{ref}}\right)+\frac{\rho_{ref}}{\rho}\frac{\alpha_{D}}{T} \tag{2-28}$$

$$\begin{aligned}\left(\frac{dD}{d\alpha}\right)_{C}=&\left\{\frac{d\rho_{ref}}{d\alpha}\left(\frac{1}{\rho}\right)-\frac{\rho_{ref}}{\rho^{2}}\left(\frac{d\rho}{d\alpha}\right)_{C}\right\}\left(D_{0}+\alpha_{D}\log\frac{T}{T_{ref}}\right)\\&+\frac{\rho_{ref}}{\rho}\left(\frac{dD_{0}}{d\alpha}+\frac{d\alpha_{D}}{d\alpha}\log\frac{T}{T_{ref}}-\frac{\alpha_{D}}{T_{ref}}\frac{dT_{ref}}{d\alpha}\right)\end{aligned} \tag{2-29}$$

By differentiating boundary conditions of primal problem in (2-11), corresponding boundary conditions for direct system can be obtained as (2-30).

$$\begin{aligned}&X(0)=X(L)\\&\left.\frac{dX}{dx}\right|_{x=0}=\left.\frac{dX}{dx}\right|_{x=L}\end{aligned} \tag{2-30}$$

ULSAN NATIONAL INSTITUTE OF SCIENCE AND TECHNOLOGY

Direct system equations for sensitivity of temperature Z, sensitivity of delayed neutron precursor Y_i, sensitivity of decay heat precursors W_i, and corresponding boundary conditions can be obtained in same way.

$$\frac{\partial}{\partial x}\left(GC_pZ\right)+K_ZZ+K_{Z1}\frac{\partial Z}{\partial x}-\left(1-\beta_{h,t}\right)E_f\Sigma_fX-\sum_{i=1}^{N_d}\lambda_{h,i}W_i=C_Z \tag{2-31}$$

$$K_Z=\frac{hp}{A_c}-\left(1-\beta_{h,t}\right)\left(\frac{dE_f\Sigma_f}{d\alpha}\right)_Z\phi+G\frac{\partial T}{\partial x}\left(\frac{dC_p}{d\alpha}\right)_Z \tag{2-32}$$

$$K_{Z1}=GT\left(\frac{dC_p}{d\alpha}\right)_Z \tag{2-33}$$

$$\begin{aligned}C_Z=&-\frac{d}{d\alpha}\left(\frac{hp}{A_c}\right)\left(T-T_w\right)+\frac{hp}{A_c}\frac{dT_w}{d\alpha}+\frac{d\left(1-\beta_{h,t}\right)}{d\alpha}E_f\Sigma_f\phi+\left(1-\beta_{h,t}\right)\left(\frac{dE_f\Sigma_f}{\partial\alpha}\right)_C\phi\\&-\frac{dG}{d\alpha}\left(C_p\frac{\partial T}{\partial x}+\frac{\partial C_p}{\partial x}T\right)-GT\frac{\partial}{\partial x}\left(\frac{dC_p}{d\alpha}\right)_C-G\left(\frac{dC_p}{d\alpha}\right)_C\frac{\partial T}{\partial x}+\sum_{i=1}^{N_d}\frac{d\lambda_{h,i}}{d\alpha}d_i\end{aligned} \tag{2-34}$$

$$\begin{aligned}&Z\left(0\right)=Z\left(L\right)\\&\left.\frac{dZ}{dx}\right|_{x=0}=\left.\frac{dZ}{dx}\right|_{x=L}\end{aligned} \tag{2-35}$$

$$-\frac{\partial}{\partial x}\left(\frac{G}{\rho}Y_i\right)+\frac{\partial}{\partial x}\left(\frac{\nu_T}{Sc_T}\frac{\partial Y_i}{\partial x}\right)-\lambda_iY_i+\beta_i\frac{\nu\Sigma_f}{k_{eff}}X+K_{Yi}Z+K_{Yi1}\frac{\partial Z}{\partial x}=C_{Yi} \tag{2-36}$$

$$K_{Yi}=-\frac{2G}{\rho^3}c_i\frac{\partial\rho}{\partial x}\left(\frac{d\rho}{d\alpha}\right)_Z+\frac{G}{\rho^2}\frac{\partial c_i}{\partial x}\left(\frac{d\rho}{d\alpha}\right)_Z+\frac{\beta_i}{k_{eff}}\left(\frac{d\nu\Sigma_f}{d\alpha}\right)_Z\phi \tag{2-37}$$

$$K_{Yi1}=\frac{G}{\rho^2}c_i\left(\frac{d\rho}{d\alpha}\right)_Z \tag{2-38}$$

$$\begin{aligned}C_{Yi}=&\frac{dG}{d\alpha}\left(\frac{\partial c_i}{\partial x}\frac{1}{\rho}-\frac{1}{\rho^2}\frac{\partial\rho}{\partial x}c_i\right)+\frac{2G}{\rho^3}c_i\frac{\partial\rho}{\partial x}\left(\frac{d\rho}{d\alpha}\right)_C-\frac{G}{\rho^2}\left(\frac{\partial}{\partial x}\left(\frac{d\rho}{d\alpha}\right)_C c_i+\left(\frac{d\rho}{d\alpha}\right)_C\frac{\partial c_i}{\partial x}\right)\\&-\frac{d}{d\alpha}\left(\frac{\nu_T}{Sc_T}\right)\frac{\partial^2c_i}{\partial x^2}+\frac{d\lambda_i}{d\alpha}c_i-\left(\frac{d\beta_i}{d\alpha}\frac{\nu\Sigma_f}{k_{eff}}\phi+\frac{\beta_i}{k_{eff}}\left(\frac{d\nu\Sigma_f}{d\alpha}\right)_C\phi\right)\end{aligned} \tag{2-39}$$

$$\begin{aligned}&Y_i\left(0\right)=Y_i\left(L\right)\\&\left.\frac{dY_i}{dx}\right|_{x=0}=\left.\frac{dY_i}{dx}\right|_{x=L}\end{aligned} \tag{2-40}$$

ULSAN NATIONAL INSTITUTE OF SCIENCE AND TECHNOLOGY

$$-\frac{\partial}{\partial x}\left(\frac{G}{\rho}W_i\right)+\frac{\partial}{\partial x}\left(\frac{\nu_T}{Sc_T}\frac{\partial W_i}{\partial x}\right)-\lambda_{h,i}W_i+\beta_{h,i}E_f\Sigma_f X+K_{Wi}Z+K_{Wi1}\frac{\partial Z}{\partial x}=C_{Wi} \tag{2-41}$$

$$K_{Wi}=-\frac{2G}{\rho^3}d_i\frac{\partial\rho}{\partial x}\left(\frac{d\rho}{d\alpha}\right)_Z+\frac{G}{\rho^2}\frac{\partial d_i}{\partial x}\left(\frac{d\rho}{d\alpha}\right)_Z+\beta_{h,i}\left(\frac{dE_f\Sigma_f}{d\alpha}\right)_Z\phi \tag{2-42}$$

$$K_{Wi1}=\frac{G}{\rho^2}d_i\left(\frac{d\rho}{d\alpha}\right)_Z \tag{2-43}$$

$$\begin{aligned}C_{Wi}=&\frac{dG}{d\alpha}\left(\frac{\partial d_i}{\partial x}\frac{1}{\rho}-\frac{1}{\rho^2}\frac{\partial\rho}{\partial x}d_i\right)+\frac{2G}{\rho^3}d_i\frac{\partial\rho}{\partial x}\left(\frac{d\rho}{d\alpha}\right)_C-\frac{G}{\rho^2}\left(\frac{\partial}{\partial x}\left(\frac{d\rho}{d\alpha}\right)_C d_i+\left(\frac{d\rho}{d\alpha}\right)_C\frac{\partial d_i}{\partial x}\right)\\&-\frac{d}{d\alpha}\left(\frac{\nu_T}{Sc_T}\right)\frac{\partial^2 d_i}{\partial x^2}+\frac{d\lambda_{h,i}}{d\alpha}d_i-\left(\frac{d\beta_{h,i}}{d\alpha}E_f\Sigma_f\phi+\beta_{h,i}\left(\frac{dE_f\Sigma_f}{d\alpha}\right)_C\phi\right)\end{aligned} \tag{2-44}$$

$$\begin{aligned}&W_i(0)=W_i(L)\\&\left.\frac{dW_i}{dx}\right|_{x=0}=\left.\frac{dW_i}{dx}\right|_{x=L}\end{aligned} \tag{2-45}$$

And then, multiplying adjoint sensitivity solution denoted as superscript * to each direct sensitivity equations above and integrating them into whole domain is required for linear transformation to obtain the corresponding adjoint sensitivity equation.

$$\begin{aligned}&\int_0^L X^*\left(-\frac{\partial}{\partial x}\left(D\frac{\partial X}{\partial x}\right)+\left(\Sigma_a-\frac{1-\beta_t}{k_{eff}}\nu\Sigma_f\right)X-\sum_{i=1}^{N_C}\lambda_i Y_i+K_X Z+K_{X1}\frac{\partial Z}{\partial x}\right)dx\\&=\int_0^L X^* C_X dx\end{aligned} \tag{2-46}$$

$$\begin{aligned}&\int_0^L\sum_{i=1}^{N_c}Y_i^*\left(-\frac{\partial}{\partial x}\left(\frac{G}{\rho}Y_i\right)+\frac{\partial}{\partial x}\left(\frac{\nu_T}{Sc_T}\frac{\partial Y_i}{\partial x}\right)-\lambda_i Y_i+\beta_i\frac{\nu\Sigma_f}{k_{eff}}X+K_{Yi}Z+K_{Yi1}\frac{\partial Z}{\partial x}\right)dx\\&=\int_0^L\sum_{i=1}^{N_c}Y_i^* C_{Yi}dx\end{aligned} \tag{2-47}$$

$$\begin{aligned}&\int_0^L Z^*\left(\frac{\partial}{\partial x}\left(GC_pZ\right)+K_Z Z+K_{Z1}\frac{\partial Z}{\partial x}-(1-\beta_t)E_f\Sigma_f X-\sum_{i=1}^{N_d}\lambda_{h,i}W_i\right)dx\\&=\int_0^L Z^* C_Z dx\end{aligned} \tag{2-48}$$

$$\begin{aligned}&\int_0^L\sum_{i=1}^{N_d}W_i^*\left(-\frac{\partial}{\partial x}\left(\frac{G}{\rho}W_i\right)+\frac{\partial}{\partial x}\left(\frac{\nu_T}{Sc_T}\frac{\partial W_i}{\partial x}\right)-\lambda_{h,i}W_i+\beta_{h,i}E_f\Sigma_f X+K_{Wi}Z+K_{Wi1}\frac{\partial Z}{\partial x}\right)dx\\&=\int_0^L\sum_{i=1}^{N_d}W_i^* C_{Wi}dx\end{aligned} \tag{2-49}$$

ULSAN NATIONAL INSTITUTE OF SCIENCE AND TECHNOLOGY

The first derivatives to the temperature sensitivity Z are included in (2-46), (2-47), and (2-48). They can be easily converted to Z by calculating integration terms. For instance, terms including $\frac{\partial Z}{\partial x}$ for X in (2-46) can be calculated by setting proper boundary conditions of adjoint solution X^* with already determined boundary conditions of KX_1 and Z. Then, the first term in RHS of (2-50) becomes zero.

$$\int_0^L X^*\left(K_{X1}\frac{\partial Z}{\partial x}\right)dx = \left[X^* K_{X1} Z\right]_0^L - \int_0^L \frac{\partial\left(K_{X1}X^*\right)}{\partial x} Z dx \tag{2-50}$$

$$X^*(0) = X^*(L) \tag{2-51}$$

With same procedure, equations (2-46) to (2-49) are rewritten with converted terms of $\frac{\partial Z}{\partial x}$ as below.

$$\int_0^L X^*\left(-\frac{\partial}{\partial x}\left(D\frac{\partial X}{\partial x}\right)+\left(\Sigma_a - \frac{1-\beta_t}{k_{eff}}\nu\Sigma_f\right)X - \sum_{i=1}^{N_c}\lambda_i Y_i + K_X Z\right)dx - \int_0^L \frac{\partial\left(K_{X1}X^*\right)}{\partial x} Z dx \tag{2-52}$$

$$\begin{aligned}&\int_0^L \sum_{i=1}^{N_c} Y_i^*\left(-\frac{\partial}{\partial x}\left(\frac{G}{\rho}Y_i\right)+\frac{\partial}{\partial x}\left(\frac{\nu_T}{Sc_T}\frac{\partial Y_i}{\partial x}\right)-\lambda_i Y_i + \beta_i\frac{\nu\Sigma_f}{k_{eff}}X + K_{Yi}Z\right)dx \\ &-\int_0^L \sum_{i=1}^{N_c}\left(\frac{\partial\left(K_{Yi1}Y_i^*\right)}{\partial x}Z\right)dx\end{aligned} \tag{2-53}$$

$$\int_0^L Z^*\left(\frac{\partial}{\partial x}\left(GC_p Z\right)+K_Z Z + K_{Z1}\frac{\partial Z}{\partial x} - \left(1-\beta_t\right)E_f\Sigma_f X - \sum_{i=1}^{N_d}\lambda_{h,i}W_i\right)dx \tag{2-54}$$

$$\begin{aligned}&\int_0^L \sum_{i=1}^{N_d} W_i^*\left(-\frac{\partial}{\partial x}\left(\frac{G}{\rho}W_i\right)+\frac{\partial}{\partial x}\left(\frac{\nu_T}{Sc_T}\frac{\partial W_i}{\partial x}\right)-\lambda_{h,i}W_i + \beta_{h,i}E_f\Sigma_f X + K_{Wi}Z\right)dx \\ &-\int_0^L \sum_{i=1}^{N_d}\left(\frac{\partial\left(K_{Wi1}W_i^*\right)}{\partial x}Z\right)dx\end{aligned} \tag{2-55}$$

According to the definition of adjoint formulation, equations (2-52) to (2-55) can be rearranged by separating adjoint solutions of neutron flux sensitivity, X^*, temperature sensitivity Z^*, each group of delayed neutron precursor sensitivity Y_i^*, and decay heat group sensitivities W_i^* with proper boundary conditions. For instance, calculating the first integration term in (2-52) by integration rules can be expressed as follows.

ULSAN NATIONAL INSTITUTE OF SCIENCE AND TECHNOLOGY

$$\int_0^L X^*\left(-\frac{\partial}{\partial x}\left(D\frac{\partial X}{\partial x}\right)\right)dx = -\left[X^*\left(D\frac{\partial X}{\partial x}\right)\right]_0^L + \left[\left(D\frac{\partial X^*}{\partial x}\right)X\right]_0^L - \int_0^L \frac{\partial}{\partial x}\left(D\frac{\partial X^*}{\partial x}\right)X\,dx \tag{2-56}$$

The first and second integrated terms in (2-56) becomes zero by setting proper boundary conditions of X^*, then the only last term remained, and it finally satisfies the definition of adjoint operator. Now, equation (2-52) can be rewritten as follows.

$$\int_0^L X\left(-\frac{\partial}{\partial x}\left(D\frac{\partial X^*}{\partial x}\right)+\left(\Sigma_a-\frac{1-\beta_t}{k_{eff}}\nu\Sigma_f\right)X^*\right)dx+\int_0^L X^*\left(-\sum_{i=1}^{N_c}\lambda_i Y_i+K_X Z\right)dx$$
$$-\int_0^L \frac{\partial\left(K_{X1}X^*\right)}{\partial x}Z\,dx \tag{2-57}$$

In same manner, (2-53), (2-54), and (2-55) can be expressed as follows.

$$\int_0^L \sum_{i=1}^{N_c} Y_i\left(\frac{\partial}{\partial x}\left(\frac{G}{\rho}Y_i^*\right)+\frac{\partial}{\partial x}\left(\frac{\nu_T}{Sc_T}\frac{\partial Y_i^*}{\partial x}\right)-\lambda_i Y_i^*\right)dx+\int_0^L \sum_{i=1}^{N_c} Y_i^*\left(\beta_i\frac{\nu\Sigma_f}{k_{eff}}X+K_{Yi}Z\right)dx$$
$$-\int_0^L \sum_{i=1}^{N_c}\left(\frac{\partial\left(K_{Yi1}Y_i^*\right)}{\partial x}Z\right)dx \tag{2-58}$$

$$\int_0^L Z\left(-\frac{\partial}{\partial x}\left(GC_pZ^*\right)+K_Z Z^*-K_{Z1}\frac{\partial Z^*}{\partial x}\right)dx+\int_0^L Z^*\left(-\left(1-\beta_t\right)E_f\Sigma_f X-\sum_{i=1}^{N_d}\lambda_{h,i}W_i\right)dx \tag{2-59}$$

$$\int_0^L \sum_{i=1}^{N_d} W_i\left(\frac{\partial}{\partial x}\left(\frac{G}{\rho}W_i^*\right)+\frac{\partial}{\partial x}\left(\frac{\nu_T}{Sc_T}\frac{\partial W_i^*}{\partial x}\right)-\lambda_{h,i}W_i^*\right)dx+\int_0^L \sum_{i=1}^{N_d} W_i^*\left(\beta_{h,i}E_f\Sigma_f X+K_{Wi}Z\right)dx$$
$$-\int_0^L \sum_{i=1}^{N_d}\left(\frac{\partial\left(K_{Wi1}W_i^*\right)}{\partial x}Z\right)dx \tag{2-60}$$

ULSAN NATIONAL INSTITUTE OF SCIENCE AND TECHNOLOGY

Rearranging equations with (2-58), (2-59), and (2-60), final form of the adjoint sensitivity equations can be obtained by adding (2-52) to (2-55).

$$\int_0^L X\left(-\frac{\partial}{\partial x}\left(D\frac{\partial X^*}{\partial x}\right)+\left(\Sigma_a-\frac{1-\beta_t}{k_{eff}}\nu\Sigma_f\right)X^*-(1-\beta_t)E_f\Sigma_f Z^*+\sum_{i=1}^{N_c}Y_i^*\left(\beta_i\frac{\nu\Sigma_f}{k_{eff}}\right)+\sum_{i=1}^{N_d}W_i^*\left(\beta_{h,i}E_f\Sigma_f\right)\right)dx$$

$$+\int_0^L Z\left(-\frac{\partial}{\partial x}\left(GC_pZ^*\right)+K_ZZ^*-K_{Z1}\frac{\partial Z^*}{\partial x}+K_XX^*+\sum_{i=1}^{N_c}K_{Yi}Y_i^*+\sum_{i=1}^{N_d}K_{Wi}W_i^*-\frac{\partial\left(K_{X1}X^*\right)}{\partial x}-\sum_{i=1}^{N_c}\left(\frac{\partial\left(K_{Yi1}Y_i^*\right)}{\partial x}\right)-\sum_{i=1}^{N_d}\left(\frac{\partial\left(K_{Wi1}W_i^*\right)}{\partial x}\right)\right)dx$$

$$+\int_0^L\sum_{i=1}^{N_c}Y_i\left(\frac{\partial}{\partial x}\left(\frac{G}{\rho}Y_i^*\right)+\frac{\partial}{\partial x}\left(\frac{\nu_T}{Sc_T}\frac{\partial Y_i^*}{\partial x}\right)-\lambda_iY_i^*-\lambda_iX^*\right)dx \qquad (2\text{-}61)$$

$$+\int_0^L\sum_{i=1}^{N_d}W_i\left(\frac{\partial}{\partial x}\left(\frac{G}{\rho}W_i^*\right)+\frac{\partial}{\partial x}\left(\frac{\nu_T}{Sc_T}\frac{\partial W_i^*}{\partial x}\right)-\lambda_{h,i}W_i^*-\lambda_{h,i}Z^*\right)dx$$

$$=\int_0^L X^*C_Xdx+\int_0^L Z^*C_Zdx+\int_0^L\sum_{i=1}^{N_c}Y_i^*C_{Yi}dx+\int_0^L\sum_{i=1}^{N_d}W_i^*C_{Wi}dx$$

Let the expressions of LHS in integral terms of the equation (2-61) as weighting functions, P_ξ, where ξ=X, Y_i, W_i, and Z.

$$-\frac{\partial}{\partial x}\left(D\frac{\partial X^*}{\partial x}\right)+\left(\Sigma_a-\frac{1-\beta_t}{k_{eff}}\nu\Sigma_f\right)X^*-(1-\beta_t)E_f\Sigma_fZ^*+\sum_{i=1}^{N_c}Y_i^*\left(\beta_i\frac{\nu\Sigma_f}{k_{eff}}\right)+\sum_{i=1}^{N_d}W_i^*\left(\beta_{h,i}E_f\Sigma_f\right)=P_X \qquad (2\text{-}62)$$

$$-\frac{\partial}{\partial x}\left(GC_pZ^*\right)+K_ZZ^*-K_{Z1}\frac{\partial Z^*}{\partial x}+K_XX^*+\sum_{i=1}^{N_c}K_{Yi}Y_i^*+\sum_{i=1}^{N_d}K_{Wi}W_i^*-\frac{\partial\left(K_{X1}X^*\right)}{\partial x}-\sum_{i=1}^{N_c}\left(\frac{\partial\left(K_{Yi1}Y_i^*\right)}{\partial x}\right)-\sum_{i=1}^{N_d}\left(\frac{\partial\left(K_{Wi1}W_i^*\right)}{\partial x}\right)=P_Z \qquad (2\text{-}63)$$

$$\frac{\partial}{\partial x}\left(\frac{G}{\rho}Y_i^*\right)+\frac{\partial}{\partial x}\left(\frac{\nu_T}{Sc_T}\frac{\partial Y_i^*}{\partial x}\right)-\lambda_iY_i^*-\lambda_iX^*=P_{Yi} \qquad (2\text{-}64)$$

$$\frac{\partial}{\partial x}\left(\frac{G}{\rho}W_i^*\right)+\frac{\partial}{\partial x}\left(\frac{\nu_T}{Sc_T}\frac{\partial W_i^*}{\partial x}\right)-\lambda_{h,i}W_i^*-\lambda_{h,i}Z^*=P_{Wi} \qquad (2\text{-}65)$$

ULSAN NATIONAL INSTITUTE OF SCIENCE AND TECHNOLOGY

Equations (2-62) to (2-65) are adjoint sensitivity equations. Equivalent form of the indirect term of the sensitivity of the system response can be expressed with adjoint sensitivity solutions as below.

$$\begin{aligned}&\int_0^L P_X X dx + \int_0^L P_Z Z dx + \int_0^L \sum_{i=1}^{N_c} P_{Yi} Y_i dx + \int_0^L \sum_{i=1}^{N_d} P_{Wi} W_i dx \\ &= \int_0^L X^* C_X dx + \int_0^L Z^* C_Z dx + \int_0^L \sum_{i=1}^{N_c} Y_i^* C_{Yi} dx + \int_0^L \sum_{i=1}^{N_d} W_i^* C_{Wi} dx\end{aligned} \tag{2-66}$$

$$\frac{\partial R}{\partial \alpha} = \sum\left(P_\xi, \lambda\right) = \sum\left(C_\xi, \lambda^*\right) \tag{2-67}$$

Equation (2-67) is the final expression of the adjoint based sensitivity analysis. Reminding the system response R and its sensitivity, it represents the indirect term of the sensitivity of R. Corresponding P_X, P_{Yi}, P_{Wi}, and P_Z are now taking a role of the source terms in adjoint equations, where they contain the information of system response: type of the system response or specific position that want to be investigated. Instead, new functionals representing sensitivity or R are defined with source terms of C_X, C_Z, C_{Yi}, and C_{Wi}, which are derived from direct sensitivity equations. Only transformation of equations mathematically without any assumptions are considered to get equivalent form of sensitivity of R with adjoint solutions.

ULSAN NATIONAL INSTITUTE OF SCIENCE AND TECHNOLOGY

2.3.3 Validation of Adjoint-based Sensitivity Analysis Method

To validate the developed adjoint-based sensitivity analysis method for the circulating liquid fuel system, typical liquid-fueled MSR design, MSFR condition is selected as a case problem. Considering design features of MSFR in steady state, specifications of the 1D case problem is summarized in Table 2-3.

To compute all equations including governing equations, original sensitivity and adjoint sensitivity equations for flux, temperature, 8 groups of neutron precursors and 3 groups of decay heat groups, MATLAB scripts are written to solve above discretized forms of equations numerically. A set of primal equations are discretized with second order central differencing scheme as follows.

$$D_i \frac{\left.\frac{d\phi}{dx}\right|_{i+1/2} - \left.\frac{d\phi}{dx}\right|_{i-1/2}}{\Delta x} + \left(\Sigma_{a,i} - \frac{(1-\beta_t)}{k_{eff}} \nu\Sigma_{f,i} \right) \phi_i = \sum_{i=1}^{8} \lambda_i c_{i,i} \tag{2-68}$$

$$-\frac{\left.\frac{G}{\rho} c_i\right|_{i+1} - \left.\frac{G}{\rho} c_i\right|_{i-1}}{2\Delta x} + \frac{\nu_T}{Sc_T} \frac{c_{i,i-1} - 2c_{i,i} + c_{i,i+1}}{\Delta x^2} - \lambda_i c_{i,i} + \beta_i \frac{\nu\Sigma_f}{k_{eff}} \phi_i = 0 \tag{2-69}$$

$$-\frac{\left.\frac{G}{\rho} d_i\right|_{i+1} - \left.\frac{G}{\rho} d_i\right|_{i-1}}{2\Delta x} + \frac{\nu_T}{Sc_T} \frac{d_{i,i-1} - 2d_{i,i} + d_{i,i+1}}{\Delta x^2} - \lambda_{h,i} d_{i,i} + \beta_i E_f \Sigma_f \phi_i = 0 \tag{2-70}$$

$$GC_{p,i} \frac{T_{i+1} - T_{i-1}}{2\Delta x} + \frac{hp}{A_c} (T_i - T_w) = (1-\beta_{h,t}) E_f \Sigma_f \phi_i + \sum_{i=1}^{3} \lambda_{h,i} d_{i,i} \tag{2-71}$$

Due to the criteria to derive adjoint functions where primal ones should be defined as continuous and differentiable in all domain [20], fission generation term, $\nu\Sigma_f$ included only in core region in flux equation and heat transfer coefficient of heat exchanger, h only for HX region in energy conservation equation are set as a quadratic function of position, to avoid discontinuity of first and second derivative of the main solutions. At this moment, neutron diffusion equation is treated as a fixed source problem, and multiplication factor in steady state is set as neutron flux and concentration level of precursor achieves the target nominal power closely, so that this steady state model can be easily extended to the dynamic model for circulating liquid fuel system as well.

ULSAN NATIONAL INSTITUTE OF SCIENCE AND TECHNOLOGY

Table 2-3 Specifications of case problem representing MSFR

Parameter	**Value**	**cf.**
L_C, L_{HX}	2.06 m	
L_{hl}, L_{cl}	1.95 m	
Core diameter	1.5 m	Considered only for calculating total power
Channel diameter (including HL, CL, HX)	0.5 m	
Nominal power	3000 MW	
Mass flux, G	10,200 kg/m^{2}s	
Heat transfer coefficient per unit length, h	9.0E+6 W/m^{3}K	Sufficiently large to maintain inlet temperature as 923 K
Wall temperature of primary side, T_w	853 K	

ULSAN NATIONAL INSTITUTE OF
SCIENCE AND TECHNOLOGY

Main solutions; flux, temperature, concentration of each group of neutron precursors and decay heat precursors are shown in Figure 2-3, which shows reasonable agreement in their magnitude and distribution in loop with those using OpenFOAM Multiphysics solver developed for MSFR [28]. Due to the flow effects of the fuel salt, delayed neutron precursors and decay heat groups are accumulated at the core outlet, which indicates the dependencies of the distribution of the important variables governing all neutron economy. Their distributions are determined by their characteristics; i.e. various decay constant and fraction for each group along with their transport. In addition, temperature distribution determined by the prescribed velocity field and power distribution also affects the overall neutronics by reactivity feedback on the variations of the cross-sectional data or diffusion coefficient as well as thermophysical properties of the salt. Such kind of the phenomena from coupled physics need to be assessed how much the models adopted reflect the reality of the circulating liquid fuel system.

The type of input/model parameters are chosen as considered coupling options including estimated correlations of cross section and diffusion coefficient and library data for kinetic constants of delayed neutron and decay heat precursors, and design parameters such as the features of heat exchanger and flow rate. Table 2-4 lists all parameters considered for the circulating liquid fuel system analysis, and Table 2-5 shows the kinetic constants of delayed neutron adopted from JEFF-3.1 library and estimated ones for decay heat precursors [29]. Based on the distribution of neutron flux, temperature, each group of delayed neutron precursor and decay heat precursor in closed loop at steady state, sensitivity of the input/model parameter to the system responses are calculated.

ULSAN NATIONAL INSTITUTE OF SCIENCE AND TECHNOLOGY

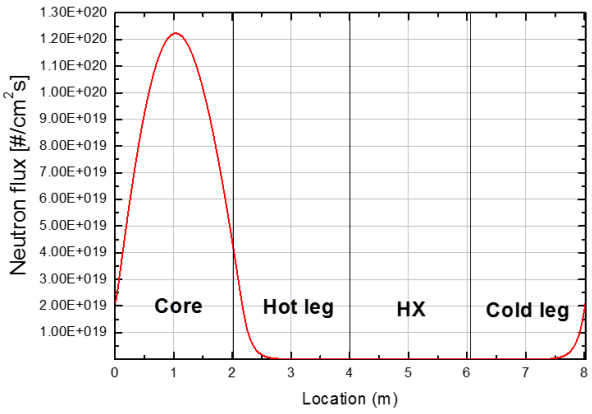

a) Neutron flux

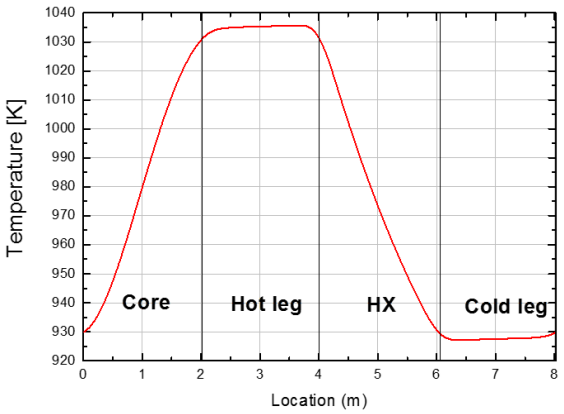

b) Temperature

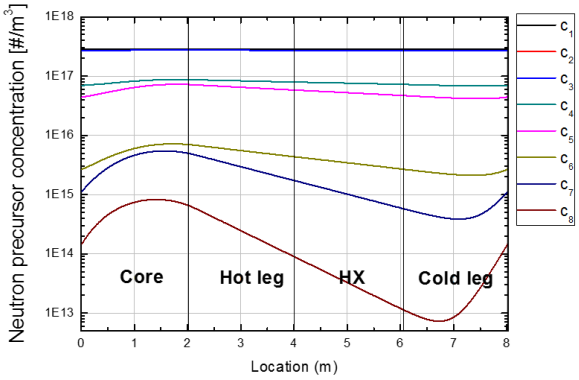

c) Delayed neutron precursors (8 groups)

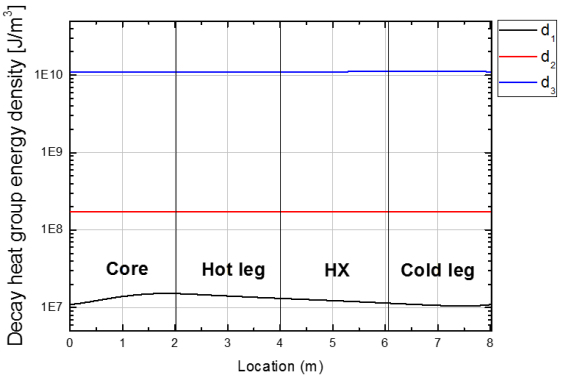

d) Decay heat precursors (3 groups)

Figure 2-3 Steady state solution of circulating liquid fuel system

ULSAN NATIONAL INSTITUTE OF SCIENCE AND TECHNOLOGY

Table 2-4 Parameters for all types of system responses

Category	Parameters	Note
Coefficients for updates of nuclear data	$\alpha_{\Sigma a}$, Σ_{a0} for absorption XS, $\alpha_{\nu\Sigma f}$, $\nu\Sigma_{f0}$ for fission generation, $\alpha_{Ef\Sigma f}$, $E_f\Sigma_{f0}$ for fission energy, α_D, D_0 for diffusion coefficient	$\Sigma = \rho^* \left(\Sigma_0 + \alpha_\Sigma \log\left(\frac{T}{T_{ref}} \right) \right)$ $D = \frac{1}{\rho^*} \left(D_0 + \alpha_D \log\left(\frac{T}{T_{ref}} \right) \right)$
Coefficients for updates of salt properties	α_ρ, β_ρ for salt density, α_{Cp}, β_{Cp} for salt specific heat	$\rho = \alpha_\rho T + \beta_\rho$ $C_p = \alpha_{Cp} T + \beta_{Cp}$
Reference values	Reference density and temperature to determine ratio	T_{ref}, ρ_{ref} $\rho^* = \frac{\rho}{\rho_{ref}}$
Decay constants and fractions	λ_i and β_i for neutron precursors $\lambda_{h,i}$ and $\beta_{h,i}$ for decay heat precursors	8 groups for c_i 3 groups for d_i
Reactor design parameter	Mass flux, G Heat transfer coefficient of HX, h Wall temperature of primary side, T_w	

ULSAN NATIONAL INSTITUTE OF
SCIENCE AND TECHNOLOGY

Table 2-5 Kinetic constants of delayed neutron and decay heat precursors [29]

Parameter	Values	
λ_1 / β_1	1.24667E-02	22.2E-05
λ_2 / β_2	2.82917E-02	48.1E-05
λ_3 / β_3	4.25244E-02	40.5E-05
λ_4 / β_4	1.33042E-01	64.5E-05
λ_5 / β_5	2.92467E-01	102.1E-05
λ_6 / β_6	6.66488E-01	17.7E-05
λ_7 / β_7	1.63478	22.3E-05
λ_8 / β_8	3.5546	5.40E-05
$\lambda_{h,1}$ / $\beta_{h,1}$	0.1973	1.10E-02
$\lambda_{h,2}$ / $\beta_{h,2}$	0.0168	1.28E-02
$\lambda_{h,3}$ / $\beta_{h,3}$	3.58E-04	3.58E-02

ULSAN NATIONAL INSTITUTE OF SCIENCE AND TECHNOLOGY

Based on the primal solutions, the sensitivity of system response P is compared for all parameters first. P is the simplest type of system response without having any direct terms in sensitivity expression, which is suitable to verify and validate the adjoint sensitivity analysis method for coupled problem. System response P and its sensitivity to arbitrary parameter α, $dP/d\alpha$ are defined as equation (2-72) and (2-74), respectively.

$$P = \sum(1, \varphi_i) = (1, \phi) + \sum_{i=1}^{8}(1, c_i) + \sum_{i=1}^{3}(1, d_i) + (1, T) \tag{2-72}$$

$$\frac{dP}{d\alpha} = \sum\left(1, \frac{d\varphi_i}{da}\right) = \left(1, \frac{d\phi}{d\alpha}\right) + \sum_{i=1}^{8}\left(1, \frac{dc_i}{da}\right) + \sum_{i=1}^{3}\left(1, \frac{dd_i}{da}\right) + \left(1, \frac{dT}{d\alpha}\right) \tag{2-73}$$

Table 2-6 shows the summary of the comparison of sensitivity of system response P by three methods as described; recalculation, direct method, and adjoint method. Deviation between results from recalculation and adjoint sensitivity solution is under 9.43 %. Among all 39 parameters, there are ones which have largest deviations of sensitivity by recalculation and adjoint sensitivity method; for instance, mass flux G, coefficients of specific heat of salt, α_{Cp} and β_{Cp}. The reason of relatively large deviations is the point why the adjoint sensitivity method is powerful to analyze sensitivity of the system response. In this work, sensitivity of system response is defined as the first derivative; gradient of the system response from changes of the parameter. To obtain the trend of system response changes, small changes of input or model parameters should be first defined for the recalculation method. And then, solving primal equations are repeated for original and perturbed parameter to get the changes of the system response. At this moment, sensitivity of system response is dependent on the approximated perturbed amount of the parameter. For instance, when assumed values are too small to catch the changes of system response properly or too large to track the changes of system response at the given point, it might yield misinterpretations of analyzing the system response behavior. In this viewpoint, adjoint sensitivity analysis method can be a best option to understand the characteristics of the system from the small perturbations of the parameters at the designed values.

From the comparison results on the sensitivity of P to all parameters by recalculation, direct method, and adjoint method, it is revealed that the adjoint sensitivity analysis method applied to the circulating liquid fuel system analysis is properly extended for the coupled system and applicable for the sensitivity analysis for this system.

ULSAN NATIONAL INSTITUTE OF SCIENCE AND TECHNOLOGY

Table 2-6 Comparison of sensitivity of system response P

Parameter, α	Reference value	Sensitivity, $dP/d\alpha$			Deviation
		Recalculation* (R)	Direct method (D)	Adjoint method (A)	(A-R)/R [%]
G	10,200	4.7721E+14	4.7874E+14	4.3221E+14	9.43
h	9.00E+5	4.8061E+13	4.8058E+13	4.7650E+13	0.85
T_w	853	-3.6743E+17	-3.5665E+17	-3.4917E+17	4.97
λ_1	1.2467E-02	-1.8235E+20	-1.8237E+20	-1.8278E+20	-0.23
λ_2	2.8292E-02	-7.6511E+19	-7.6518E+19	-7.6714E+19	-0.27
λ_3	4.2524E-02	-2.8305E+19	-2.8305E+19	-2.8398E+19	-0.33
λ_4	1.3304E-01	-3.9468E+18	-3.9479E+18	-3.9868E+18	-1.01
λ_5	2.9247E-01	-2.0386E+17	-2.0404E+17	-1.9546E+17	4.12
λ_6	6.6649E-01	2.1218E+17	2.1198E+17	2.1011E+17	0.97
λ_7	1.6348E+00	2.6478E+17	2.6476E+17	2.6357E+17	0.46
λ_8	3.5546E+00	3.1685E+16	3.1690E+16	3.1475E+16	0.66
β_1	2.2200E-04	1.2754E+22	1.2754E+22	1.2757E+22	-0.02
β_2	4.8100E-04	7.0277E+21	7.0277E+21	7.0353E+21	-0.11
β_3	4.0500E-04	5.5256E+21	5.5257E+21	5.5361E+21	-0.19
β_4	6.4500E-04	3.5703E+21	3.5704E+21	3.5864E+21	-0.45
β_5	1.0210E-03	3.2390E+21	3.2390E+21	3.2588E+21	-0.61
β_6	1.7700E-04	3.5233E+21	3.5226E+21	3.5480E+21	-0.70
β_7	2.2300E-04	4.7701E+21	4.7696E+21	4.8037E+21	-0.70
β_8	5.4000E-05	6.4095E+21	6.4097E+21	6.4486E+21	-0.61
$\lambda_{h,1}$	1.9730E-01	9.8649E+16	9.8602E+16	9.5473E+16	3.22
$\lambda_{h,2}$	1.6800E-02	7.3781E+16	7.3723E+16	7.3144E+16	0.86
$\lambda_{h,3}$	3.5800E-04	-1.6172E+20	-1.6197E+20	-1.5287E+20	5.45
$\beta_{h,1}$	1.1000E-02	-4.7721E+19	-4.7730E+19	-4.6595E+19	2.36
$\beta_{h,2}$	1.2800E-02	-4.9407E+19	-4.9404E+19	-4.7882E+19	3.09
$\beta_{h,3}$	1.8600E-02	-4.6310E+19	-4.6310E+19	-4.6570E+19	-0.56
α_ρ	-0.882	6.2325E+19	6.2327E+19	6.0930E+19	2.24
β_ρ	4982.96	6.3044E+16	6.3046E+16	6.1643E+16	2.22
α_{Cp}	2.78	3.8426E+18	3.8525E+18	3.5654E+18	7.21
β_{Cp}	-1111	3.9686E+15	3.9791E+15	3.6882E+15	7.06
ρ_0	4124.87	-6.2491E+16	-6.2493E+16	-6.1031E+16	2.34
Σ_{a0}	0.689269	-1.3596E+22	-1.3601E+22	-1.3639E+22	-0.32
$\alpha_{\Sigma a}$	0.007842	-1.2606E+21	-1.2607E+21	-1.2644E+21	-0.30
$E_f\Sigma_{f0}$	9.57E-12	-5.1829E+30	-5.1828E+30	-5.0967E+30	1.66
$\alpha_{Ef\Sigma f}$	-2.06E-13	-4.2975E+29	-4.2956E+29	-4.2946E+29	0.07
$\nu\Sigma_{f0}$	0.753492	1.2591E+22	1.2587E+22	1.2616E+22	-0.20
$\alpha_{\nu\Sigma f}$	-0.017001	1.1668E+21	1.1668E+21	1.1700E+21	-0.28
D_0	0.01172	-1.9435E+22	-1.9435E+22	-1.9184E+22	1.29
α_D	-5.98E-05	-1.7970E+21	-1.7971E+21	-1.7908E+21	0.35
T_{ref}	900	3.5379E+17	3.5380E+17	3.5472E+17	-0.26

ULSAN NATIONAL INSTITUTE OF SCIENCE AND TECHNOLOGY

2.3.4 Importance of Modeling Options

In circulating liquid fuel system, it is important to evaluate the variation of reactivity or power level and distribution with temperature feedback from changes of nuclear data and fuel thermophysical properties. Sometimes, fuel thermo-physical properties or nuclear data are set as constant values without considering their dependence on temperature. From the model or experimentally measured correlations, different results may be obtained if such dependence is considered. In this section, 3 cases are categorized depending on the temperature feedback to the salt thermophysical properties and/or nuclear data as follows.

- ✓ Case 1: all properties as constants

  , such that $\rho = \rho_0 = \rho(\alpha)$, $C_p = C_{p0} = C_p(\alpha)$ for salt properties,

  $\Sigma = \Sigma_0 = \Sigma(\alpha)$, $D = D_0 = D(\alpha)$ for nuclear data are considered.

- ✓ Case 2: updates of nuclear data from temperature variation only

  , such that $\rho = \rho_0 = \rho(\alpha)$, $C_p = C_{p0} = C_p(\alpha)$ for salt properties,

  $\Sigma = \Sigma_0 + \alpha_\Sigma \log\left(\frac{T}{T_{ref}}\right) = \Sigma(\alpha, T)$, $D = D_0 + \alpha_D \log\left(\frac{T}{T_{ref}}\right) = D(\alpha, T)$ for nuclear data are considered.

- ✓ Case 3: updates of nuclear data and salt properties from temperature variation

  , such that $\rho = \alpha_\rho T + \beta_\rho = \rho(\alpha, T)$, $C_p = \alpha_{Cp} T + \beta_{Cp} = C_p(\alpha, T)$ for salt properties

  $\Sigma = \frac{\rho}{\rho_{ref}}\left(\Sigma_0 + \alpha_\Sigma \log\left(\frac{T}{T_{ref}}\right)\right) = \Sigma(\alpha, T)$, $D = \frac{\rho_{ref}}{\rho}\left(D_0 + \alpha_D \log\left(\frac{T}{T_{ref}}\right)\right) = D(\alpha, T)$ for nuclear data are considered.

ULSAN NATIONAL INSTITUTE OF SCIENCE AND TECHNOLOGY

Sensitivity coefficient S indicates the importance of parameter on the system response R normalized by the magnitude of parameter and system response as. (2-74).

$$S = \frac{dR}{d\alpha}\frac{\alpha}{R} \tag{2-74}$$

Table 2-7 and Table 2-8 show the comparisons of sensitivity and sensitivity coefficient to all parameters in different modeling options, respectively. In terms of sensitivity magnitude dP/dα in all three cases, the most sensitive parameter to the system response is the fission energy generation term; $E_f\Sigma_{f0}$ and $\alpha_{E_f\Sigma_f}$. In fact, temperature is directly influenced by their values through the source term in energy conservation equation, regardless of modeling option. In addition, diffusion term; D_0 and α_D and Σ_{a0} and $\alpha_{\Sigma a}$ are also some of the dominant parameters, having a strong effect on the neutron flux distribution. The lowest sensitivity is obtained to the reactor design parameters; mass flux, heat transfer coefficient and wall temperature on primary side of the heat exchanger. However, in terms of the sensitivity coefficient, wall temperature is one of the parameters having large sensitivity coefficient, except in case 1.

Likewise, sensitivity of system response to certain parameter is determined from the modeling options about considering variations of nuclear data and salt properties from temperature. Especially for the reactor design parameters, for instance, sensitivity to the reactor design parameters have big changes after including updates of nuclear data or salt properties; the sign of their values changes from positive to negative number. Salt properties have low dependencies to system response in case 1 and 2, but their values increase when considering updates of salt properties in case 3. It is found that the variation of nuclear data and/or salt properties have affected system response significantly, regarding the temperature feedback effect. Kinetic constants of neutron precursor group remain almost constant in any cases. On the other hand, kinetic constants of decay heat precursor show an increase of sensitivity when the dependence of nuclear data or salt properties is considered. Two-most important parameters in terms of sensitivity coefficient are fission energy terms in all cases, but their importance decreases in case 2 and 3. Salt properties such as density and specific heat capacity of fuel salt seems not to be important in case 1.

ULSAN NATIONAL INSTITUTE OF SCIENCE AND TECHNOLOGY

Table 2-7 Comparison of sensitivity of P according to the modeling options

Category	Parameter	Sensitivity dP/dα		
		Case 1	Case 2	Case 3
T/H design parameter	G	-3.0355E+14	4.0039E+14	4.3221E+14
	h	-1.3418E-03	4.4179E+13	4.7650E+13
	T_w	8.0040E+00	-3.3475E+17	-3.4917E+17
Kinetic constants	λ_1	-2.3215E+20	-1.8461E+20	-1.8278E+20
	λ_2	-9.6820E+19	-7.7241E+19	-7.6714E+19
	λ_3	-3.5590E+19	-2.8538E+19	-2.8398E+19
	λ_4	-4.3994E+18	-3.9455E+18	-3.9868E+18
	λ_5	8.4348E+17	-1.5321E+17	-2.3082E+17
	λ_6	4.8852E+17	2.2287E+17	2.1011E+17
	λ_7	5.6790E+17	2.7550E+17	2.6357E+17
	λ_8	6.7559E+16	3.2850E+16	3.1475E+16
	β_1	1.8171E+22	1.2899E+22	1.2757E+22
	β_2	1.0935E+22	7.1404E+21	7.0353E+21
	β_3	9.0482E+21	5.6327E+21	5.5361E+21
	β_4	6.6564E+21	3.6740E+21	3.5864E+21
	β_5	6.3967E+21	3.3488E+21	3.2588E+21
	β_6	7.1937E+21	3.6528E+21	3.5480E+21
	β_7	9.9146E+21	4.9533E+21	4.8037E+21
	β_8	1.3422E+22	6.6586E+21	6.4486E+21
	$\lambda_{h,1}$	-6.7045E+08	8.5809E+16	9.5473E+16
	$\lambda_{h,2}$	-1.0765E+11	1.1795E+17	7.3144E+16
	$\lambda_{h,3}$	-3.4448E+14	1.7292E+17	-1.5287E+20
	$\beta_{h,1}$	1.1985E+10	-4.3320E+19	-4.6595E+19
	$\beta_{h,2}$	1.4075E+11	-4.4870E+19	-4.7882E+19
	$\beta_{h,3}$	6.6049E+12	-4.5021E+19	-4.6570E+19
Salt properties	α_ρ	7.5063E+14 (ρ=const.)	3.7412E+14 (ρ=const.)	6.0930E+19
	β_ρ			6.1643E+16
	α_{Cp}	7.5063E+14 (C_p=const.)	3.5303E+15 (C_p=const.)	3.5654E+18
	β_{Cp}			3.6882E+15
Nuclear data	ρ_0	-	-	-6.1031E+16
	Σ_{a0}	-2.8669E+22 (Σ_a=const.)	-1.4134E+22	-1.3639E+22
	$\alpha_{\Sigma a}$		-1.3257E+21	-1.2644E+21
	$E_f\Sigma_{f0}$	1.3035E+22 ($E_f\Sigma_f$=const.)	-4.7467E+30	-5.0967E+30
	$\alpha_{Ef\Sigma f}$		-3.9993E+29	-4.2946E+29
	$\nu\Sigma_{f0}$	2.6528E+22 ($\nu\Sigma_f$=const.)	1.3075E+22	1.2616E+22
	$\alpha_{\nu\Sigma f}$		1.2268E+21	1.1700E+21
	D_0	-4.0517E+22 (D=const.)	-1.9781E+22	-1.9184E+22
	α_D		-1.8630E+21	-1.7908E+21
	T_{ref}	-	3.6775E+17	3.5472E+17

ULSAN NATIONAL INSTITUTE OF SCIENCE AND TECHNOLOGY

Table 2-8 Comparison of sensitivity coefficient of P according to the modeling options

Category	Parameter	Sensitivity coefficient, S		
		Case 1	Case 2	Case 3
T/H design parameter	G	-1.2111E-02	1.9891E-02	2.0225E-02
	h	-4.7239E-18	1.9366E-01	2.0983E-01
	T_w	2.6706E-17	-1.3908E+00	-1.4573E+00
Kinetic constants	λ_1	-1.1321E-02	-1.1210E-02	-1.1150E-02
	λ_2	-1.0715E-02	-1.0644E-02	-1.0620E-02
	λ_3	-5.9199E-03	-5.9108E-03	-5.9086E-03
	λ_4	-2.2895E-03	-2.5566E-03	-2.5952E-03
	λ_5	9.6496E-04	-2.1825E-04	-3.2976E-04
	λ_6	1.2736E-03	7.2349E-04	6.8520E-04
	λ_7	3.6316E-03	2.1937E-03	2.1083E-03
	λ_8	9.3936E-04	5.6874E-04	5.4742E-04
	β_1	1.5779E-02	1.3947E-02	1.3857E-02
	β_2	2.0574E-02	1.6728E-02	1.6558E-02
	β_3	1.4334E-02	1.1111E-02	1.0970E-02
	β_4	1.6794E-02	1.1542E-02	1.1318E-02
	β_5	2.5547E-02	1.6653E-02	1.6280E-02
	β_6	4.9806E-03	3.1490E-03	3.0728E-03
	β_7	8.6484E-03	5.3800E-03	5.2414E-03
	β_8	2.8350E-03	1.7513E-03	1.7039E-03
	$\lambda_{h,1}$	-5.1743E-13	8.2460E-05	9.2167E-05
	$\lambda_{h,2}$	-7.0740E-12	9.6516E-06	6.0126E-06
	$\lambda_{h,3}$	-4.8240E-10	3.0151E-07	-2.6778E-04
	$\beta_{h,1}$	5.1567E-13	-2.3209E-03	-2.5078E-03
	$\beta_{h,2}$	7.0471E-12	-2.7973E-03	-2.9988E-03
	$\beta_{h,3}$	4.8055E-10	-4.0786E-03	-4.2383E-03
Salt properties	α_ρ	1.1898E-02 (ρ=const.)	7.3625E-03 (ρ=const.)	-2.6295E-01
	β_ρ			1.5029E+00
	α_{Cp}	-4.4568E-19 (C_p=const.)	2.6910E-02 (C_p=const.)	4.8497E-02
	β_{Cp}			-2.0050E-02
Nuclear data	ρ_0	-	-	-1.2318E+00
	Σ_{a0}	-7.7534E+01 (Σ_a=const.)	-4.7451E+01	-4.5998E+01
	$\alpha_{\Sigma a}$		-5.0637E-02	-4.8516E-02
	$E_f\Sigma_{f0}$	7.8460E+01 ($E_f\Sigma_f$=const.)	4.7985E+01	4.6514E+01
	$\alpha_{Ef\Sigma f}$		-1.0158E-01	-9.7330E-02
	$\nu\Sigma_{f0}$	4.8983E-10 ($\nu\Sigma_f$=const.)	-2.2125E-01	-2.3865E-01
	$\alpha_{\nu\Sigma f}$		4.0126E-04	4.3288E-04
	D_0	-1.8920E+00 (D=const.)	-1.1291E+00	-1.1001E+00
	α_D		5.4263E-04	5.2399E-04
	T_{ref}	-	1.6120E+00	1.5621E+00

ULSAN NATIONAL INSTITUTE OF SCIENCE AND TECHNOLOGY

Figure 2-4 shows the comparison of sensitivity and sensitivity coefficient in absolute value according to the case 1 to 3. Obviously, sensitivity and sensitivity coefficient obtained from recalculation, direct and adjoint method are well agreed each other in same condition. All of parameters shows the variation of sensitivity of system response according to modeling options (case 1 to 3), although their values are not changed. Most of parameters related to the energy undergoing big changes from the modeling options. In detail, importance of parameters is totally different compared to the case 1: constant salt properties and nuclear data and case 2: constant salt properties and temperature dependencies of the nuclear data, such as heat transfer coefficient (htc), wall temperature (Tw) of the heat exchanger, λ_{h1} to λ_{h3}, β_{h1} to β_{h3}, reference value of specific heat of the fuel salt (Cp0), and reference value of the fission energy generation term, $E_f\Sigma_{f0}$ (SP0). They are said to be thermal-hydraulic parameters but considerations of the temperature feedback on the nuclear data of cross section or diffusion coefficient only influence the overall system behavior and temperature changes ultimately, giving higher importance of these parameter on the system response. In addition, reference value of density (rho0) and cross-sectional data such as $\Sigma a0$ (SA0) and $\alpha\Sigma a$ (alpha_SA) for absorption cross section, $E_f\Sigma_{f0}$ (SP0) and $\alpha E_f\Sigma_f$ (alpha_SP) for fission energy generation, $\nu\Sigma f0$ (NSF0) and $\alpha\nu\Sigma f$ (alpha_NSF) for fission neutron generation terms changes their importance when considering the temperature dependencies of the salt properties from case 2 to case 3. It is interesting that parameters closely related to the thermal hydraulics impact on the system behavior when considering temperature dependencies of the nuclear data, and those related to the neutronics do as well considering temperature dependencies of the salt thermophysical properties. These results represent how much important the Multiphysics modeling on the system analysis is; the case when the coupling options; how to model the tightly coupled physics and exchanging information between both physics such as neutronics and thermal-hydraulics in the circulating liquid fuel system.

ULSAN NATIONAL INSTITUTE OF SCIENCE AND TECHNOLOGY

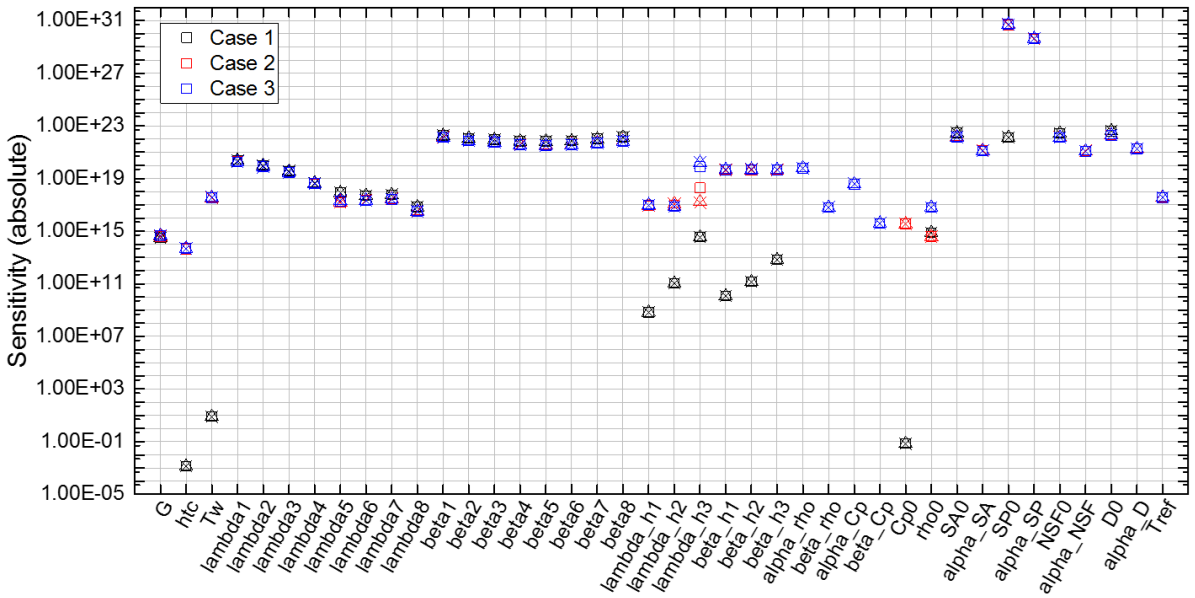

a) Sensitivity, dP/dα (absolute value)

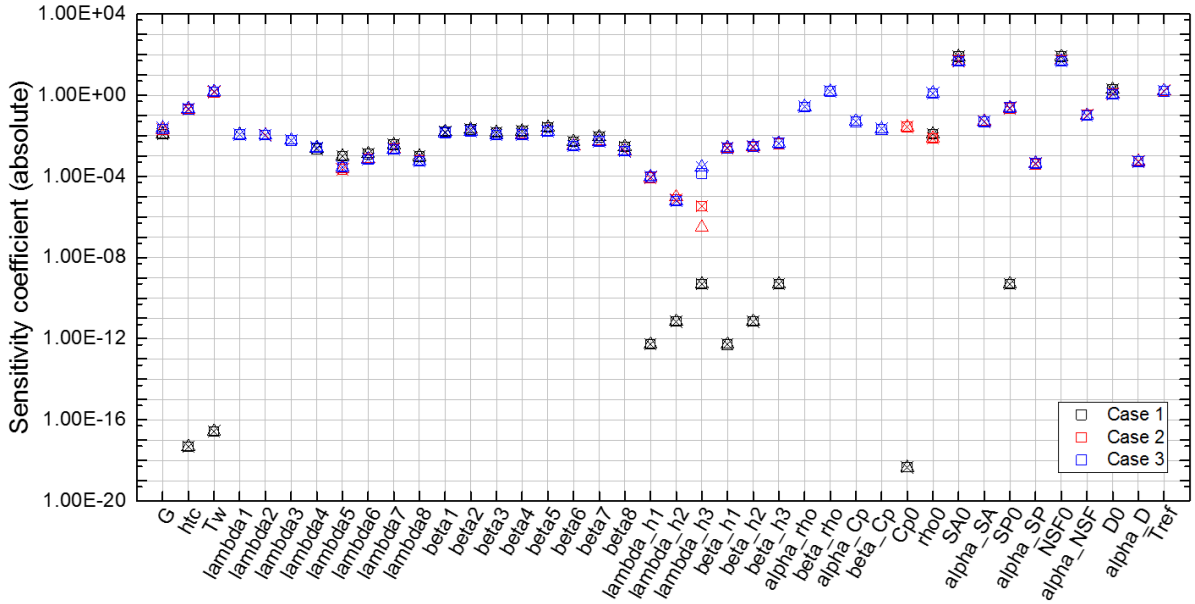

b) Sensitivity coefficient, S (absolute value)

Figure 2-4 Comparison of importance of parameters according to the modeling options

(×: recalculation / △: direct / □: adjoint)

ULSAN NATIONAL INSTITUTE OF SCIENCE AND TECHNOLOGY

2.3.5 Local Sensitivity Analysis of the Circulating Liquid Fuel System

2.3.5.1 Changes of sensitivity from parameter perturbation

In this section, the variation of sensitivity of system response to all parameters is estimated from small perturbation of parameter values in case 3, in which the dependence of both the nuclear data and thermophysical properties on temperature is considered. Perturbed ratio means the ratio of the amount of changed parameter values to the original values. To analyze effects of parameters to system response, sensitivity and sensitivity coefficient to each parameter is evaluated from ±10% perturbation of parameter values. Figure 2-5 shows the ratio of changes in sensitivity of system response P from the changes of values of parameter in case 3. Normalized sensitivity is defined as the ratio of sensitivity for perturbed parameter value to that in reference value, S/S_0. Each plot indicates relative changes of sensitivity coefficients expressed in terms of normalized sensitivity coefficient. Small perturbation about ±10 % of their values are considered for most parameters, however, D_0 and Σ_{a0}, $\nu\Sigma_{f\,0}$, $E_f\Sigma_{f\,0}$ considered ±1 % of their value perturbations due to their highly sensitive characteristics, since changes of system response is too big to be assessed in first derivative between such amount of perturbation of values.

For all cases, variations of sensitivities of all parameters using adjoint method are well predicted compared with those from direct method within ± 0.3 % of deviation. Most of parameters show linear changes of the sensitivity coefficient as parameter perturbation, except coefficients of salt specific heat capacity, α_{Cp} and β_{Cp}. Parameters related to the specific heat capacity of salt show nonlinear change in sensitivity values. For the parameters having linear change of sensitivity, their slopes of changes from small amount of parameter value changes are not related to the magnitude of their value. For example, decay constants of neutron precursor group 5, λ_5 shows largest slope of changes in normalized sensitivity coefficient among other decay constants. Since neutron precursor group 5 has the largest fractions β, not decay constants, it is highly dependent on the neutron flux than others. Normalized sensitivity coefficients from perturbation of values of $\nu\Sigma_{f\,0}$ and $\alpha_{\nu\Sigma f}$ increased as parameter value increases, but others have negative slope in changes of normalized sensitivity coefficient.

ULSAN NATIONAL INSTITUTE OF SCIENCE AND TECHNOLOGY

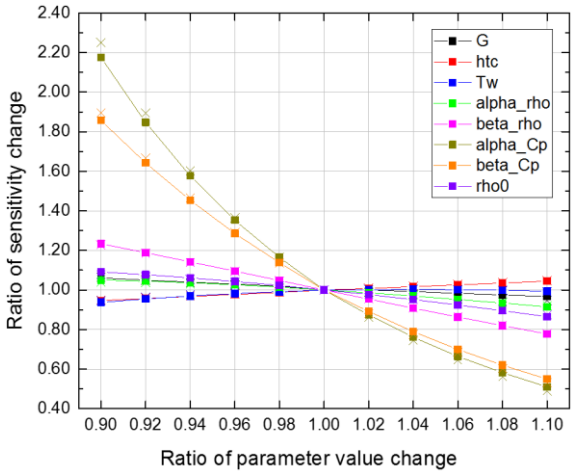

a) T/H parameters

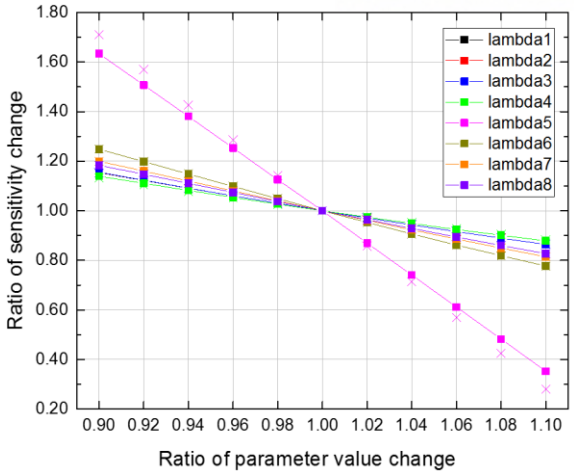

b) λ_i of neutron precursors

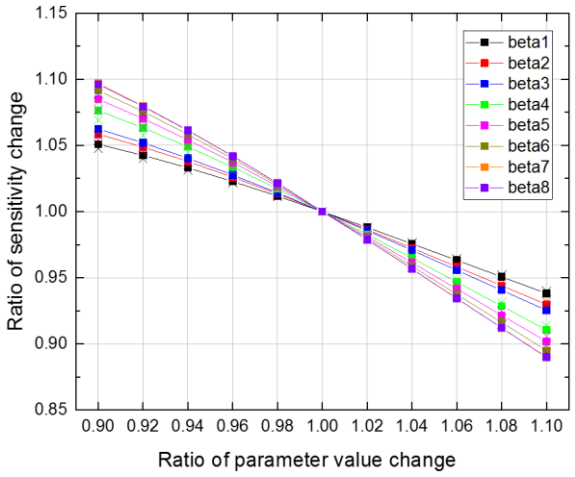

c) β_i for neutron precursors

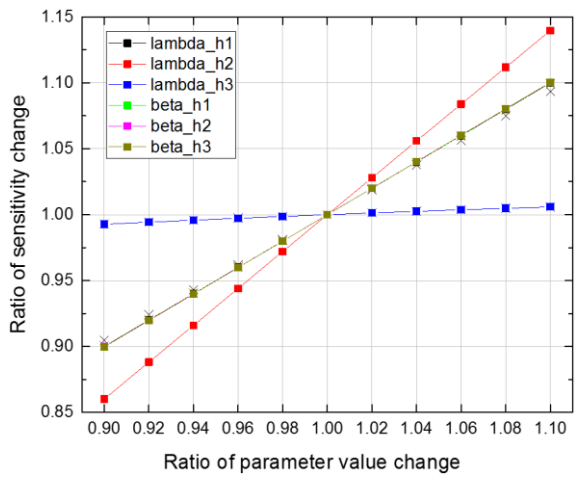

d) $\lambda_{h,i}$ and $\beta_{h,i}$ of decay heat groups

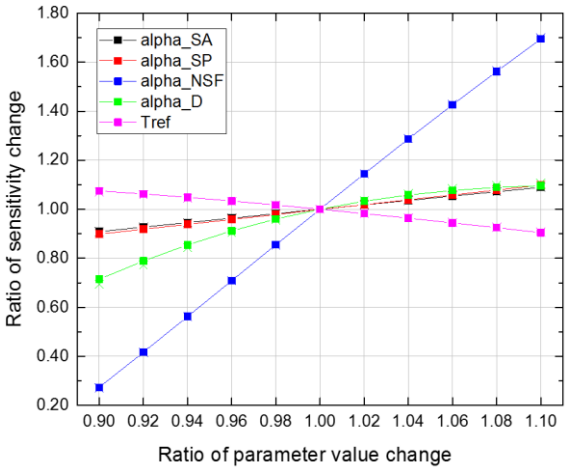

e) Nuclear data: α_D, α_Σ, T_{ref}

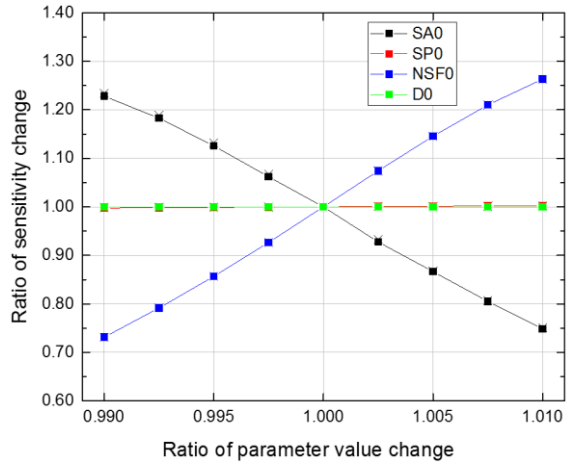

f) Nuclear data: D_0, Σ_0

Figure 2-5 Variations of sensitivity of P from parameter perturbations

(×: direct, ■: adjoint)

ULSAN NATIONAL INSTITUTE OF SCIENCE AND TECHNOLOGY

Along with normalized sensitivity coefficient, ratio of sensitivity and the slope of changes of sensitivity according to the perturbation of parameter are compared. Ratio of sensitivity indicates how much the magnitude of sensitivity value changes, and slope describes how much it is sensitive to parameter value respectively in (2-75) and (2-76).

$$\text{Ratio} = \Delta\left(\frac{dR}{d\alpha}\right) / \left(\frac{dR}{d\alpha}\right)_0 \tag{2-75}$$

$$\text{Slope} = \Delta\left(\frac{dR}{d\alpha}\right) / \Delta\alpha \tag{2-76}$$

Figure 2-6 and Table 2-9 show the comparison of ratio and slope for sensitivity changes from parameter value perturbation within ±10 % in absolute value. Wall temperature of heat exchanger, T_w shows the highest change ratio of sensitivity, which means it is the most sensitive parameter to system response P. Parameters related to the fission energy generation terms; $\nu\Sigma_{f0}$ and $\alpha_{\nu\Sigma f}$, have the two-highest slopes. However, they have relatively low values of change ratio of sensitivity; it means that their influences on the sensitivity of system response is not much dependent on the changes of parameter values, but on the magnitude of their values. The parameter that has the highest ratio is not always matched with that having the highest slope.

ULSAN NATIONAL INSTITUTE OF SCIENCE AND TECHNOLOGY

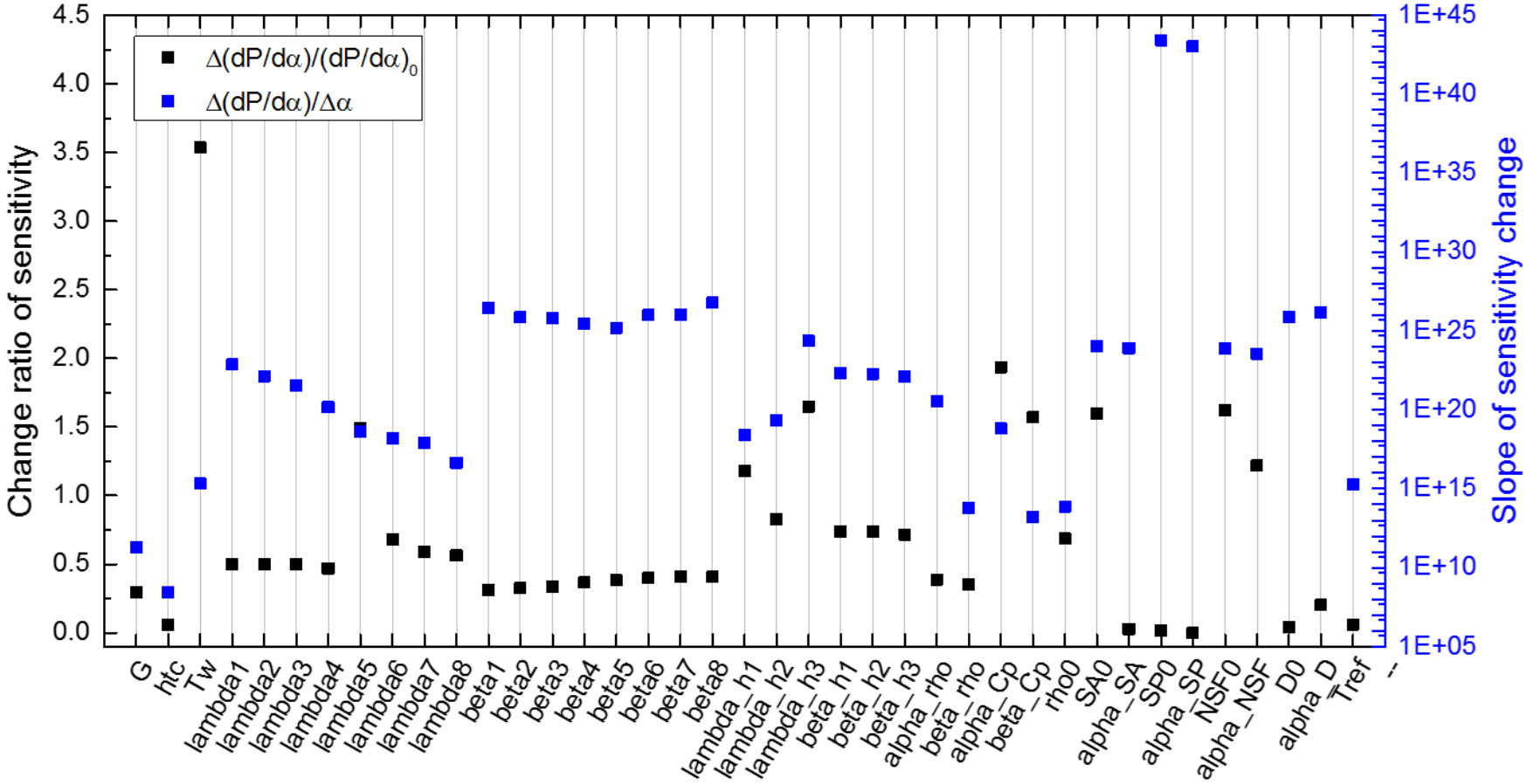

Figure 2-6 Summary of changes of sensitivity of P from perturbations

ULSAN NATIONAL INSTITUTE OF SCIENCE AND TECHNOLOGY

Table 2-9 Changes of sensitivity of P from parameter perturbations

Parameter	Reference value	dP/dα at ref. value	Δ(dP/dα)*	Change ratio [%]
T_w	853	-3.5908E+17	1.2688E+18	-353.333
α_{Cp}	2.78	3.5654E+18	-6.8989E+18	-193.499
λ_{h3}	0.000358	-1.5287E+20	2.6723E+20	-174.809
$\nu\Sigma_0$	0.753492	1.2616E+22	2.0498E+22	162.474
Σ_{a0}	0.689269	-1.3639E+22	2.1816E+22	-159.958
β_{Cp}	-1111	3.6882E+15	-5.7857E+15	-156.869
λ_5	0.29247	-2.3044E+17	3.4426E+17	-149.393
$\alpha_{\nu\Sigma}$	-0.017	1.1700E+21	1.4271E+21	121.968
λ_{h1}	0.1973	9.6588E+16	-1.1367E+17	-117.688
λ_{h2}	0.0168	7.0974E+16	-5.8684E+16	-82.685
β_{h2}	0.0128	-4.7882E+19	3.5293E+19	-73.708
β_{h1}	0.011	-4.6595E+19	3.4249E+19	-73.505
β_{h3}	0.0186	-4.6570E+19	3.3321E+19	-71.552
ρ_0	4124.87	-6.1031E+16	4.1779E+16	-68.456
λ_6	0.66649	2.1011E+17	-1.4290E+17	-68.008
λ_7	1.6348	2.6357E+17	-1.5614E+17	-59.242
λ_8	3.5546	3.1475E+16	-1.7715E+16	-56.285
λ_2	0.028292	-7.6714E+19	3.8373E+19	-50.021
λ_3	0.042524	-2.8398E+19	1.4186E+19	-49.955
λ_1	0.012467	-1.8278E+20	9.1187E+19	-49.889
λ_4	0.13304	-3.9868E+18	1.8649E+18	-46.777
β_7	0.000223	4.8037E+21	-1.9638E+21	-40.882
β_8	0.000054	6.4486E+21	-2.6352E+21	-40.864
β_6	0.000177	3.5480E+21	-1.4140E+21	-39.854
α_ρ	-0.882	6.0930E+19	-2.3690E+19	-38.881
β_5	0.001021	3.2588E+21	-1.2463E+21	-38.243
β_4	0.000645	3.5864E+21	-1.3126E+21	-36.598
β_ρ	4982.96	6.1643E+16	-2.1679E+16	-35.169
β_3	0.000405	5.5361E+21	-1.8659E+21	-33.705
β_2	0.000481	7.0353E+21	-2.3046E+21	-32.757
β_1	0.000222	1.2757E+22	-3.9800E+21	-31.199
G	10200	4.0524E+14	-1.1946E+14	-29.478
α_D	-6E-05	-1.7908E+21	-3.6328E+20	-20.286
T_{ref}	900	3.5472E+17	-2.1818E+16	-6.151
h	900000	4.7650E+13	-2.8281E+12	-5.935
D_0	0.01172	-1.9184E+22	8.1235E+20	-4.235
$\alpha_{\Sigma a}$	0.007842	-1.2644E+21	3.6939E+19	-2.921
$E_f\Sigma_{f0}$	9.57E-12	-5.0967E+30	1.0140E+29	-1.990
$\alpha_{E_f\Sigma_f}$	-2.1E-13	-4.2946E+29	2.5177E+25	-0.006

ULSAN NATIONAL INSTITUTE OF SCIENCE AND TECHNOLOGY

2.3.5.2 Sensitivity analysis of various system responses

Adjoint-based sensitivity analysis method derived for Multiphysics models of circulating liquid fuel system can be also applied to the sensitivity analysis of various system responses such as fission power Q_f and decay heat Q_d., where their definition and sensitivities are defined as (2-77) to (2-82).

$$Q_f = \left(\left(1-\beta_{h,t}\right) E_f \Sigma_f, \phi \right) \tag{2-77}$$

$$\frac{dQ_f}{d\alpha} = \frac{\partial Q_f}{\partial \alpha} + \left(\left(1-\beta_{h,t}\right) E_f \Sigma_f, X \right) + \left(\left(1-\beta_{h,t}\right) \left(\frac{\partial E_f \Sigma_f}{\partial \alpha} \right)_Z \phi, Z \right) \tag{2-78}$$

$$\frac{\partial Q_f}{\partial \alpha} = \left(\left\{ \frac{\partial \left(1-\beta_{h,t}\right)}{\partial \alpha} E_f \Sigma_f + \left(1-\beta_{h,t}\right) \left(\frac{\partial E_f \Sigma_f}{\partial \alpha} \right)_C \right\}, \phi \right) \tag{2-79}$$

$$Q_d = \sum_{i=1}^{3} \left(\lambda_{h,i}, d_i \right) \tag{2-80}$$

$$\frac{dQ_d}{d\alpha} = \frac{\partial Q_d}{\partial \alpha} + \sum_{i=1}^{8} \left(\lambda_{h,i}, W_i \right) \tag{2-81}$$

$$\frac{\partial Q_d}{\partial \alpha} = \sum_{i=1}^{8} \left(\frac{d\lambda_{h,i}}{d\alpha}, d_i \right) \tag{2-82}$$

Derivative of fission power to α having subscript Z indicates temperature sensitivity-dependent term, and that with subscript C indicates temperature sensitivity-independent term. Indirect sensitivity of fission power $\frac{\partial Q_f}{\partial \alpha}$, and that of decay power $\frac{\partial Q_d}{\partial \alpha}$ can be evaluated with the adjoint method.

Figure 2-7 shows the comparison of sensitivity and sensitivity coefficient of the fission power and decay power in absolute value. Among parameters, absorption cross section (SA0) and fission generation term (NSF0) fission energy term have two-largest sensitivity coefficients for fission and decay power. It indicates that terms directly related to the neutron flux have strong influences on the behavior of the circulating liquid fuel system. Following them, wall temperature and heat transfer coefficient of heat exchanger have high importance as well, since they determine the temperature distribution of the system. Kinetic constants of delayed neutron precursors have less important in terms of indirect sensitivity, but their actual importance to fission power includes the direct terms of sensitivity to fractions of neutron precursors. On the other hand, influences of kinetic constants of decay heat groups to decay power becomes powerful including only their indirect sensitivities.

ULSAN NATIONAL INSTITUTE OF SCIENCE AND TECHNOLOGY

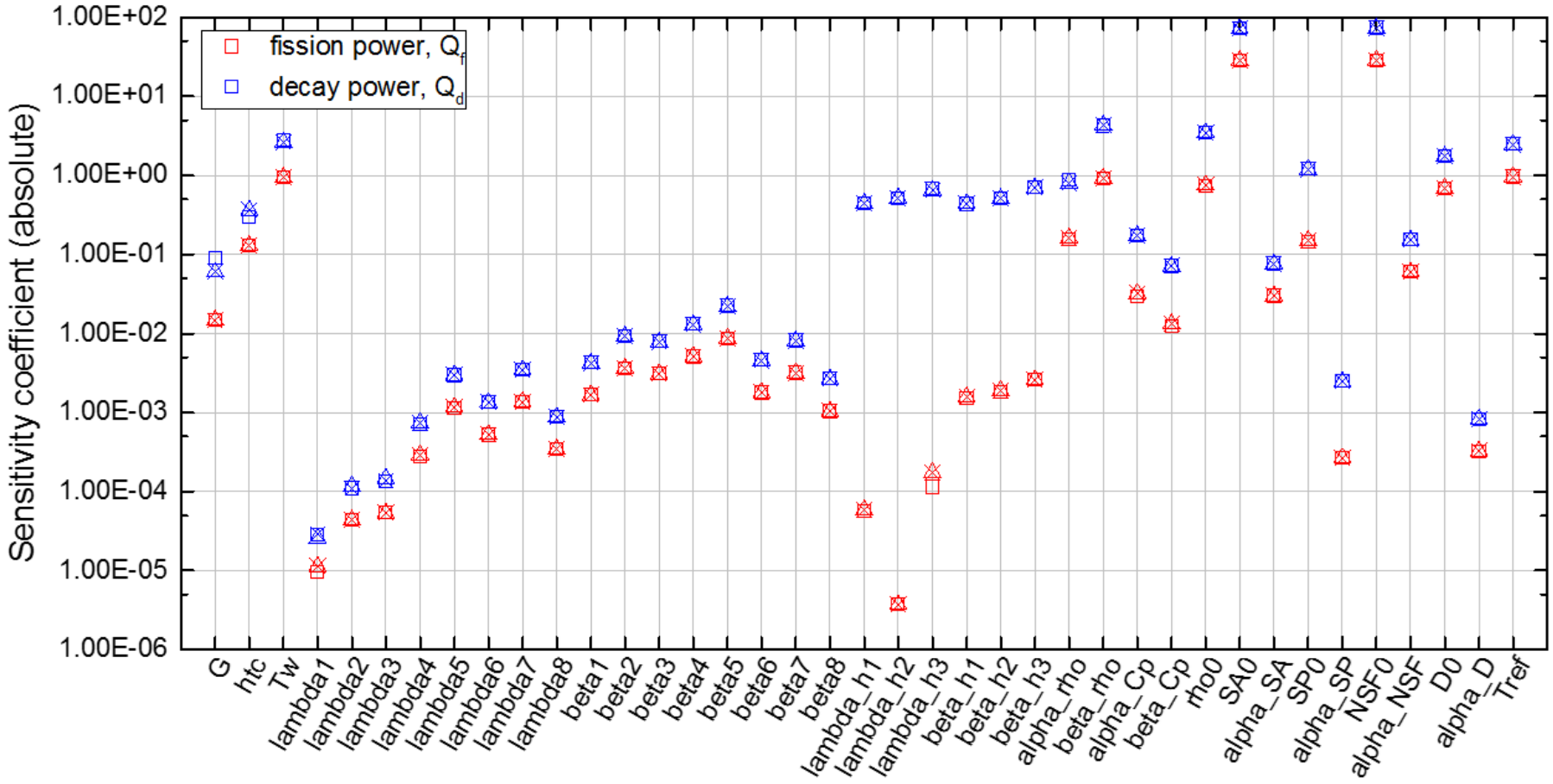

Figure 2-7 Sensitivity of fission power and decay power to the input/model parameters

(×: recalculation / □: Direct / △: adjoint method)

ULSAN NATIONAL INSTITUTE OF SCIENCE AND TECHNOLOGY

In summary, adjoint-based sensitivity analysis method is particularly informative for the Multiphysics systems. For the system variable x and system response R, sensitivity of system response using adjoint sensitivity solution is obtained as follows.

$$\frac{\partial F}{\partial x}\lambda^* = \frac{\partial R}{\partial x} \text{ such that } \frac{dR}{d\alpha} = \left(\frac{\partial R}{\partial x}, \lambda\right) = \left(\lambda^*, -\frac{\partial F}{\partial \alpha}\right) \tag{2-83}$$

It includes all coupled physics modeling in deterministic way and not to have approximations on the sensitivity analysis in repeating calculations in efficient way. It is a gradient based sensitivity analysis method on obtaining derivatives of system variables to parameter. In this viewpoint, adjoint sensitivity field λ^* indicates the local importance of the sensitivity of system variable on the response. With adjoint sensitivity solution, influences of each variables can be separated on the sensitivity analysis. Sensitivity of system response $dR/d\alpha$ includes information of both system response expressed as $\frac{\partial R}{\partial x}$ and dependencies of system on the parameter $\frac{\partial F}{\partial \alpha}$ in (2-83).

Figure 2-8 shows the accuracy of the sensitivities of all parameters by adjoint method comparing with those by recalculation. Recalculating system response requires to approximation on the amount of small perturbation of parameter. The reason why the deviations of sensitivities obtained from recalculation and adjoint method exists at this point. It means that obtaining sensitivity by recalculation method should have several trial-and-error to find proper values of $\Delta\alpha$, and it will increase the burden required for the sensitivity analysis. In addition, once its weighting functions like P_X, P_Z, P_{Yi}, and P_{Wi} are decided from system response of interests, adjoint solutions are calculated only once from a set of adjoint sensitivity equations, regardless to which parameter is selected. These features can be a strong advantage to analyze the sensitivity of complex, large scale system, such as nuclear reactors, strongly reducing the computational resources compared to the recalculation. Figure 2-9 shows the time elapsed in sensitivity computations of the sensitivity of system response P using recalculation and adjoint method. For instance, computational time for obtaining 39 parameter's importance using adjoint method significantly reduces by 66.3 times for the same case.

Finally, the adjoint based sensitivity analysis method extended to the coupled problem has strong advantages with accurate sensitivity information without trial-and-error process of recalculation in efficient way. Based on the adjoint sensitivity method extended to the system having coupled physics such as circulating liquid fuel system, the integrated analysis tool including system analysis as well as its sensitivity for the liquid fueled MSR is developed, described in following chapter.

ULSAN NATIONAL INSTITUTE OF SCIENCE AND TECHNOLOGY

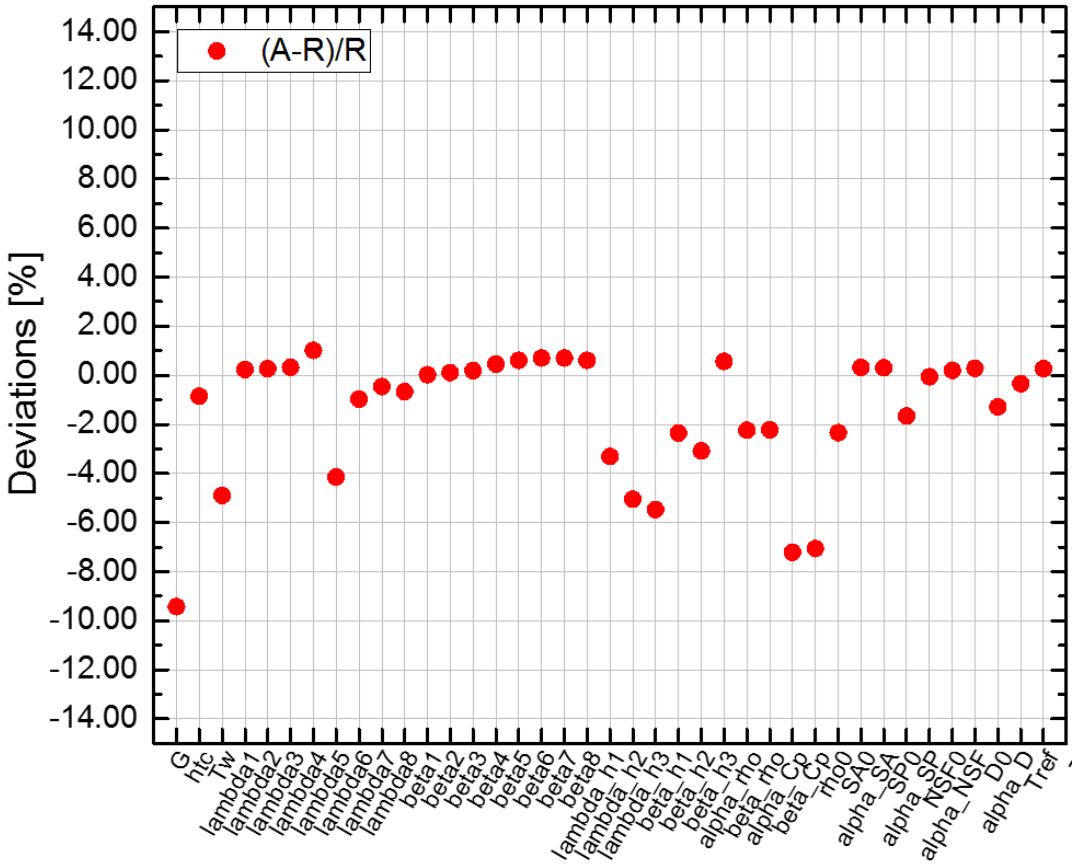

Figure 2-8 Accuracy of the adjoint sensitivity method (A) comparing recalculation method (R)

ULSAN NATIONAL INSTITUTE OF
SCIENCE AND TECHNOLOGY

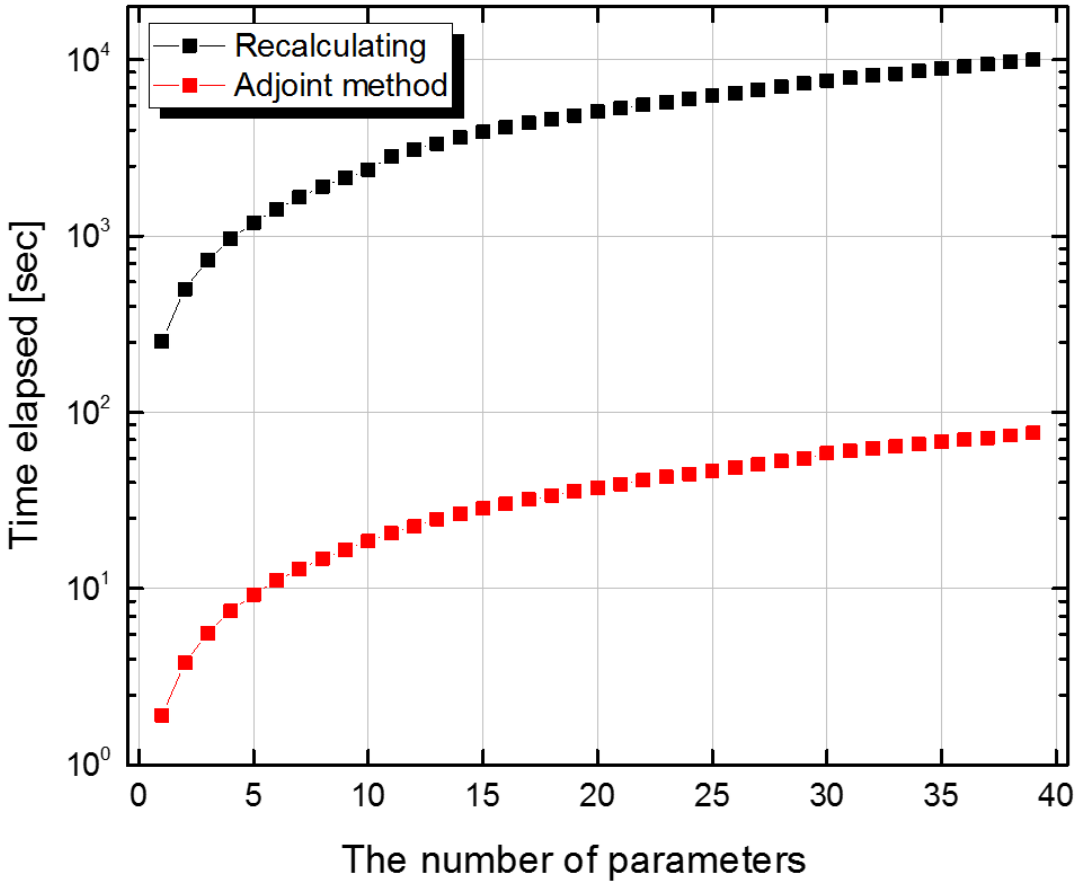

Figure 2-9 Comparison of computation times on sensitivity analysis

ULSAN NATIONAL INSTITUTE OF SCIENCE AND TECHNOLOGY

CHAPTER 3 DEVELOPMENT OF INTEGRATED MULTIPHYSICS SOLVER FOR MOLTEN SALT REACTOR

3.1 Introduction

As increasing demands of the development of MSR and its related technologies, the development of the advanced simulation tool for MSR on the integrated Multiphysics modeling has been started to help comprehensive physics and systematic analysis of MSR. In fact, a single physics of MSR, for instance, reactor physics cannot be separated alone due to its tightly coupled effects from thermal-hydraulics, mass transport, thermo-chemical, etc. Considering all together, much of efforts have been conducted to simulate the MSR on the Multiphysics approach nowadays, summarized in Table 3-1.

Wang et al. extended SIMMER-III to simulate the liquid fueled MSR, which is available for the conventional nuclear power plant severe accident analysis. They adopts neutronics and thermal-hydraulics coupling by solving two dimensional diffusion equation and Navier-Stokes equation the homogeneous approach in cross section treatment in steady state for MOSART analysis [30]. Lindsay et al. developed Moltre solver based on the MOOSE platform to solve multigroup diffusion theory with heterogeneous approach and prescribed velocity and energy conservation for thermal-hydraulics, and they validated tool by MSRE simulation [31]. In earnest, computational fluid dynamics (CFD) approaches are combined with neutronics by solving the all physics in same environment considering three dimensional geometric effects on the system behavior. Starting with Cammi et al. [14], Multiphysics solver to simulate the primary loop system behavior in single phase [25] and two-phase flow with salt and helium bubbling [30], based on the open source Multiphysics toolkit, OpenFOAM.

State of the art of the Multiphysics modeling approach for the liquid fueled molten salt reactor is the combination of the CFD techniques with neutronics with coupling models; how to model the reactivity feedback and transport of delayed neutron precursors and its influences on the system behavior. In this section, it is described that how to implement the developed adjoint-based sensitivity analysis method into OpenFOAM Multiphysics solver and numerical tests to investigate the input/model parameter importance.

ULSAN NATIONAL INSTITUTE OF SCIENCE AND TECHNOLOGY

Table 3-1 Modeling approaches to Multiphysics analysis tool for nuclear reactor

	Extended SIMMER-III [30]	**Moltre** [31]	**COMSOL Multiphysics®** [14]	**Gen-Foam** [32]	**Multiphysics solver** [28], [33]
Institute, country	KIT, Germany	INL, USA	Politecnico di Milano, Italy	PSI, Switzerland	Politecnico di Milano, Italy
Platform	SIMMER	MOOSE	COMSOL	OpenFOAM	OpenFOAM
Analysis type	Steady state, 2D	Transient, 2D/3D	Transient, 2D axial-symmetric	Transient, 3D (subscale model)	Transient, 3D
Neutronics & XS treatment	• Homogeneous approach	• Multigroup (2-24) diffusion theory • Heterogeneous approach	• Two group diffusion theory • Heterogeneous approach	• Multigroup (~33) diffusion theory • Heterogeneous approach	• Multigroup diffusion theory • Homogeneous approach
Thermal-Hydraulics	Navier-Stokes equations	Prescribed uniform velocity Energy conservation	Navier-Stokes equations (RANS/k-ε model)	Navier-Stokes equations (RANS/k-ε model)	Navier-Stokes Equations (RANS/ k-ε model)
Reactor	MOSART	MSRE	MSBR	Generic nuclear reactor (Normally SFR)	MSFR
Features	• Steady state extension of SIMMER-III	• Group constants from SCALE	• Group constants from SCALE	• Thermo-mechanics • Group constants from SERPENT-2	• Group constants from SERPENT-2 • Extended to two-phase Eulerian-Eulerian

ULSAN NATIONAL INSTITUTE OF SCIENCE AND TECHNOLOGY

First of all, adjoint technique is widely used one to approximate the perturbed solution to the unperturbed problem in nuclear reactor calculation. Based on the perturbation theory, the amount of the perturbation of multiplication factor, k_{eff} which easily affected by reactor geometry or fuel composition can be estimated with adjoint transport equation on the neutron flux [34]. For instance, typical eigenvalue problem in matrix form as (3-1), where A is the operator, φ is the eigenfunction, and λ is the eigenvalue. Perturbed state can be expressed with superscript $'$ as (3-2).

$$A\varphi = \lambda\varphi \tag{3-1}$$

$$A'\varphi' = \lambda'\varphi', \text{ where } A' = A + \delta A,\ \varphi' = \varphi + \delta\varphi, \text{ and } \lambda' = \lambda + \delta\lambda \tag{3-2}$$

To construct the corresponding adjoint system to eigenvalue problem, adjoint operator A^* is introduced. Since the operator A is a self-adjoint operator for typical eigenvalue problem, $\lambda^*=\lambda$.

$$A^*\varphi^* = \lambda\varphi^* \tag{3-3}$$

According to the definition of the adjoint formulation expressed as;

$$\left(A\varphi, \varphi^*\right) = \left(\varphi, A^*\varphi^*\right) \tag{3-4}$$

Adjoint relationship can be also applied to perturbed state equation as well.

$$\left(\varphi^*, A'\varphi'\right) = \left(\varphi^*, \lambda'\varphi'\right) \tag{3-5}$$

LHS and RHS of (3-5) can be expanded as follows.

$$\left(\varphi^*, A'\varphi'\right) = \left(\varphi^*, A\varphi'\right) + \left(\varphi^*, \delta A\varphi'\right) = \left(A^*\varphi^*, \varphi'\right) + \left(\varphi^*, \delta A\varphi'\right) = \lambda\left(\varphi^*, \varphi'\right) + \left(\varphi^*, \delta A\varphi'\right) \tag{3-6}$$

$$\left(\varphi^*, \lambda'\varphi'\right) = \lambda\left(\varphi^*, \varphi'\right) + \delta\lambda\left(\varphi^*, \varphi'\right) \tag{3-7}$$

Then, the perturbed eigenvalue, δλ can be expressed with adjoint eigenfunctions without any approximation. This means the changes of the eigenvalues can be approximated with adjoint functions without calculating the perturbed state.

ULSAN NATIONAL INSTITUTE OF SCIENCE AND TECHNOLOGY

$$\left(\varphi^*, \delta A\varphi'\right) = \delta\lambda\left(\varphi^*, \varphi'\right) \text{ and } \delta\lambda = \frac{\left(\varphi^*, \delta A\varphi'\right)}{\left(\varphi^*, \varphi'\right)} \tag{3-8}$$

Applying same procedure for the two group neutron diffusion equations and delayed neutron precursor equation for static fuel in steady state, expressed in (3-15) to (3-9) and its matrix form as (3-10).

$$\beta_0 \frac{1}{k_{eff}} \nu_1 \Sigma_{f1} \phi_1 + \beta_0 \frac{1}{k_{eff}} \nu_2 \Sigma_{f2} \phi_2 - \lambda c = 0 \tag{3-9}$$

$$\begin{pmatrix} -\nabla \cdot D_1 + \Sigma_{a1} + \Sigma_{s21} & -\Sigma_{s12} & -\chi_1 \lambda \\ -\Sigma_{s21} & -\nabla \cdot D_2 + \Sigma_{a2} + \Sigma_{s12} & -\chi_2 \lambda \\ 0 & 0 & \lambda \end{pmatrix} \begin{pmatrix} \phi_1 \\ \phi_2 \\ c \end{pmatrix}$$
$$= \frac{1}{k_{eff}} \begin{pmatrix} \chi_1 (1-\beta_0) \nu_1 \Sigma_{f1} & \chi_1 (1-\beta_0) \nu_2 \Sigma_{f2} & 0 \\ \chi_2 (1-\beta_0) \nu_1 \Sigma_{f1} & \chi_2 (1-\beta_0) \nu_2 \Sigma_{f2} & 0 \\ \beta_0 \nu_1 \Sigma_{f1} & \beta_0 \nu_2 \Sigma_{f2} & 0 \end{pmatrix} \begin{pmatrix} \phi_1 \\ \phi_2 \\ c \end{pmatrix} \text{ or } M\varphi = \frac{1}{k_{eff}} F\varphi \tag{3-10}$$

Adjoint equation of (3-10) can be done by taking transpose of the matrix M and F.

$$\begin{pmatrix} -\nabla \cdot D_1 + \Sigma_{a1} + \Sigma_{s21} & -\Sigma_{s21} & 0 \\ -\Sigma_{s12} & -\nabla \cdot D_2 + \Sigma_{a2} + \Sigma_{s12} & 0 \\ -\chi_1 \lambda & -\chi_2 \lambda & \lambda \end{pmatrix} \begin{pmatrix} \phi_1^* \\ \phi_2^* \\ c^* \end{pmatrix}$$
$$= \frac{1}{k_{eff}^*} \begin{pmatrix} \chi_1 (1-\beta_0) \nu_1 \Sigma_{f1} & \chi_2 (1-\beta_0) \nu_1 \Sigma_{f1} & \beta_0 \nu_1 \Sigma_{f1} \\ \chi_1 (1-\beta_0) \nu_2 \Sigma_{f2} & \chi_2 (1-\beta_0) \nu_2 \Sigma_{f2} & \beta_0 \nu_2 \Sigma_{f2} \\ 0 & 0 & 0 \end{pmatrix} \begin{pmatrix} \phi_1^* \\ \phi_2^* \\ c^* \end{pmatrix} \text{ or } M^*\varphi = \frac{1}{k_{eff}} F^*\varphi \tag{3-11}$$

Expanding (3-11), adjoint equations of 2 group neutron flux and delayed neutron precursors can be expressed as follows.

$$-\nabla \cdot D_1 \nabla \phi_1 = \chi_1 (1-\beta_0) \frac{1}{k_{eff}^*} \nu_1 \Sigma_{f1} \phi_1^* + \chi_2 (1-\beta_0) \frac{1}{k_{eff}^*} \nu_1 \Sigma_{f1} \phi_2^* - \Sigma_{a1} \phi_1^* + \Sigma_{s21} \phi_2^* - \Sigma_{s21} \phi_1^* + \beta_0 \nu_1 \Sigma_{f1} c^* \tag{3-12}$$

$$-\nabla \cdot D_2 \nabla \phi_2 = \chi_1 (1-\beta_0) \frac{1}{k_{eff}^*} \nu_2 \Sigma_{f2} \phi_1^* + \chi_2 (1-\beta_0) \frac{1}{k_{eff}^*} \nu_2 \Sigma_{f2} \phi_2^* - \Sigma_{a2} \phi_2^* + \Sigma_{s12} \phi_1^* - \Sigma_{s12} \phi_2^* + \beta_0 \nu_2 \Sigma_{f2} c^* \tag{3-13}$$

$$-\chi_1 \lambda \phi_1^* - \chi_2 \lambda \phi_2^* + \lambda c^* = 0 \tag{3-14}$$

ULSAN NATIONAL INSTITUTE OF SCIENCE AND TECHNOLOGY

In this stage, the unit of the adjoint solution changes according to the adjoint neutron flux; i.e. dimensionless one, which indicates the importance of the neutrons in each energy group. Therefore, the physical meaning of the adjoint solution delayed neutron precursor c^* implies the importance as well. The governing equations of the circulating liquid fuel system including all coupled physics of neutronics and thermal-hydraulics can be expressed with adjoint formulations by transposing matrix of operator.

$$-\nabla\cdot D_1\nabla\phi_1=\chi_1\left(1-\beta_0\right)\frac{1}{k_{eff}}\nu_1\Sigma_{f1}\phi_1+\chi_1\left(1-\beta_0\right)\frac{1}{k_{eff}}\nu_2\Sigma_{f2}\phi_2-\Sigma_{a1}\phi_1+\Sigma_{s12}\phi_2-\Sigma_{s21}\phi_1+\chi_1\lambda c \tag{3-15}$$

$$-\nabla\cdot D_2\nabla\phi_2=\chi_2\left(1-\beta_0\right)\frac{1}{k_{eff}}\nu_1\Sigma_{f1}\phi_1+\chi_2\left(1-\beta_0\right)\frac{1}{k_{eff}}\nu_2\Sigma_{f2}\phi_2-\Sigma_{a2}\phi_2+\Sigma_{s21}\phi_1-\Sigma_{s12}\phi_2+\chi_2\lambda c \tag{3-16}$$

$$-\nabla\left(\vec{u}c\right)+\beta_0\frac{1}{k_{eff}}\nu_1\Sigma_{f1}\phi_1+\beta_0\frac{1}{k_{eff}}\nu_2\Sigma_{f2}\phi_2-\lambda c=0 \tag{3-17}$$

$$-\nabla\left(\vec{u}d\right)+\beta_0E_{f1}\Sigma_{f1}\phi_1+\beta_0E_{f2}\Sigma_{f2}\phi_2-\lambda_h d=0 \tag{3-18}$$

$$\rho C_p\nabla\left(\vec{u}T\right)=\left(1-\beta_0\right)E_{f1}\Sigma_{f1}\phi_1+\left(1-\beta_0\right)E_{f2}\Sigma_{f2}\phi_2+\lambda_h d \tag{3-19}$$

$$\begin{aligned}-\nabla\cdot D_1\nabla\phi_1^*=&\chi_1\left(1-\beta_0\right)\frac{1}{k_{eff}}\nu_1\Sigma_{f1}\phi_1^*+\chi_1\left(1-\beta_0\right)\frac{1}{k_{eff}}\nu_2\Sigma_{f2}\phi_2^*-\Sigma_{a1}\phi_1^*+\Sigma_{s21}\phi_2^*-\Sigma_{s21}\phi_1^*\\&+\beta_0\nu_1\Sigma_{f1}c^*-\beta_0E_{f1}\Sigma_{f1}d^*+\left(1-\beta_0\right)E_{f1}\Sigma_{f1}T^*\end{aligned} \tag{3-20}$$

$$\begin{aligned}-\nabla\cdot D_2\nabla\phi_2^*=&\chi_2\left(1-\beta_0\right)\frac{1}{k_{eff}}\nu_1\Sigma_{f1}\phi_1^*+\chi_2\left(1-\beta_0\right)\frac{1}{k_{eff}}\nu_2\Sigma_{f2}\phi_2^*-\Sigma_{a2}\phi_2^*+\Sigma_{s12}\phi_1^*-\Sigma_{s12}\phi_2^*\\&+\beta_0\nu_2\Sigma_{f2}c^*-\beta_0E_{f2}\Sigma_{f2}d^*+\left(1-\beta_0\right)E_{f2}\Sigma_{f2}T^*\end{aligned} \tag{3-21}$$

$$\nabla\left(\vec{u}c^*\right)+\chi_1\lambda\phi_1^*+\chi_2\lambda\phi_2^*-\lambda c^*=0 \tag{3-22}$$

$$-\nabla\left(\vec{u}d^*\right)-\lambda_h d^*-\lambda_h T^*=0 \tag{3-23}$$

$$-\rho C_p\nabla\left(\vec{u}T^*\right)=0 \tag{3-24}$$

Likewise, adjoint decay heat precursor d^*, and adjoint temperature T^* change their units of their original ones. All adjoint formulations becomes related to the importance weighted forms. With taking adjoints of system equations, adjoints of decay heat precursor and temperature represent the importance of the neutron flux per unit energy of salt, where d* indicates the importance of neutron flux on the decay heat, T* does on the overall system temperature. Table 3-2 summarizes the changes of unit of major parameters when taking adjoint of the original equations.

ULSAN NATIONAL INSTITUTE OF
SCIENCE AND TECHNOLOGY

Table 3-2 Changes of unit of adjoint formulation for circulating liquid fuel system

	Primal solution	**Adjoint solution**
Neutron flux	# / cm^2 s	-
Delayed neuron precursor	# / m^3	-
Decay heat precursor	W/m^3	1 / J
Temperature	K	1 / J

ULSAN NATIONAL INSTITUTE OF SCIENCE AND TECHNOLOGY

With adjoint formulations of the overall system variables of the circulating liquid fuel system, the perturbed eigenvalue in steady state can be estimated, which is the most efficient way to calculate the sensitivity system as well.

In CHAPTER 2, adjoint based sensitivity procedure are adjusted to analyze one dimensional loop in constant mass flux condition, without momentum conservation equation. To extend this approach and implement this combining with Multiphysics solver for the circulating liquid fuel systems, adjoint sensitivity system can be generalized in matrix form. By taking derivative of the system equation $M\varphi = \frac{1}{k_{eff}} F\varphi$ where φ includes all system variables that can be expressed in eigenvalue problem, and any system response which can be expressed in linear functionals with weighting functions as $R = (P, \varphi)$ with respect to the certain model parameter α as follows.

$$\frac{\partial}{\partial \alpha}(M\varphi) = \frac{\partial}{\partial \alpha}\left(\frac{1}{k_{eff}} \mathrm{F}\varphi\right) \tag{3-25}$$

$$\frac{\partial R}{\partial \alpha} = \frac{\partial}{\partial \alpha}\left[(P, \varphi)\right] = \left(\frac{dP}{d\alpha}, \varphi\right) + (P, \mathrm{x}), \text{ where } \mathrm{x} = \frac{\partial \varphi_i}{\partial \alpha} \tag{3-26}$$

$$\left(\mathrm{M} - \frac{1}{k_{eff}} \mathrm{F}\right) \mathrm{x} = -\left(\frac{dM}{d\alpha}\varphi - \frac{d\left(1/k_{eff}\right)}{d\alpha} \mathrm{F}\varphi - \frac{1}{k_{eff}} \frac{d\mathrm{F}}{d\alpha}\varphi\right) \text{ or } A\mathrm{x} = C \tag{3-27}$$

Then, analyzing sensitivity of R for the given α is now changing to the calculating x described in the first derivative of system variables with respect to α. C in (3-27) is defined with the unperturbed state of the solution and includes the perturbation of the multiplication factor. For the changes of k_{eff} from the variations of the parameter, it can be approximated by taking adjoint functions of the state variable φ according to the general perturbation theory [18]. For the perturbed state of variable and parameters in matrix form with superscript M′, F′, and φ′, and adjoint equation before perturbation expressing superscript *,

$$M'\varphi' = \frac{1}{k'_{eff}} F'\varphi' \tag{3-28}$$

$$M^*\varphi^* = \frac{1}{k_{eff}} F^*\varphi^* \tag{3-29}$$

ULSAN NATIONAL INSTITUTE OF SCIENCE AND TECHNOLOGY

By multiplying adjoint function φ* on both sides of the equation (3-28), integrating both sides for the whole domain and considering the nature of the adjoint operator, the amount of k_{eff} changes can be expressed with approximating φ′≈φ as (3-30).

$$\Delta\left(\frac{1}{k_{eff}}\right)=\frac{-\frac{1}{k_{eff}}\left(\varphi^{*},\delta F\varphi\right)+\left(\varphi^{*},\delta M\varphi\right)}{\left(\varphi^{*},F'\varphi\right)} \tag{3-30}$$

Then, the derivatives of the eigenvalue to the certain input parameter can be expressed with small perturbation of the α in first order. Finally, we can obtain C as follows.

$$\frac{d\left(1/k_{eff}\right)}{d\alpha}\cong\frac{\Delta\left(1/k_{eff}\right)}{\Delta\alpha} \tag{3-31}$$

$$C=-\frac{dM}{d\alpha}\varphi+\frac{-\frac{1}{k_{eff}}\left(\varphi^{*},\delta F\varphi\right)+\left(\varphi^{*},\delta M\varphi\right)}{\left(\varphi^{*},\mathrm{F}'\varphi\right)\Delta\alpha}\varphi+\frac{1}{k_{eff}}\frac{d\mathrm{F}}{d\alpha}\varphi \tag{3-32}$$

Constructing the adjoint sensitivity system is made by taking a transpose of A in (3-27) for the direct sensitivity system variable x. Then, final form of the adjoint sensitivity system can be derived in generalized form. Figure 3-1 shows the overall procedure of the adjoint sensitivity analysis for various parameters and system responses.

$$\mathrm{A}^{*}\mathrm{x}^{*}=\mathrm{P}\text{, where }\ P=\frac{\partial R}{\partial\varphi}\ \text{ then }\ \left(\mathrm{Ax},\mathrm{x}^{*}\right)=\left(\mathrm{x},\mathrm{A}^{*}\mathrm{x}^{*}\right)=\left(\mathrm{C},\mathrm{x}^{*}\right)=\left(\mathrm{x},\mathrm{P}\right) \tag{3-33}$$

Once Multiphysics solver calculates primal equation of the system, sensitivity of system response for given parameter can be obtained by adjoint sensitivity solver, which means both solution and its sensitivity can be analyzed simultaneously. In the following section, the overview of the integrated Multiphysics solver for the circulating liquid fuel system about how to implement both Multiphysics solver and adjoint sensitivity solver will be described.

ULSAN NATIONAL INSTITUTE OF SCIENCE AND TECHNOLOGY

$A\varphi = \frac{1}{k_{eff}}\varphi$ % Original solution, $\varphi=\phi_1, \phi_2$, c, d, T

$A^*\varphi^* = \frac{1}{k_{eff}}^* \varphi^*$ % Note that $(1/k_{eff})^*=1/k_{eff}$

for i=1:N % the number of parameters, α

for j=1:M % the number of system response, R

$P_j = \frac{\partial R_j}{\partial \varphi}$ % Depend on the response type (R_j)

$A^* x_j^* = P_j$ % Adjoint sensitivity solution

end

$C_i = -\left(\left(\frac{dA}{d\alpha} \right)_i \varphi - \frac{\left(\varphi^*, \delta A_i \varphi \right)}{\left(\varphi^*, \varphi \right) \Delta \alpha_i} \varphi \right)$ % Depend on the parameter type (α_i)

$\left(\frac{dR_j}{d\alpha_i} \right) = \left(x_i, P_j \right) = \left(C_i, x_j^* \right)$ % sensitivity of system response w.r.t. α, $dR/d\alpha$

end

Figure 3-1 Procedure of adjoint sensitivity analysis for circulating liquid fuel system

ULSAN NATIONAL INSTITUTE OF SCIENCE AND TECHNOLOGY

3.2 Integrated Multiphysics Solver for Molten Salt Reactor

3.2.1 Solver Description

In CHAPTER 2, only energy conservation equation under constant mass flux condition is considered. Now, the adjoint based sensitivity analysis method to the system of all coupled physics underlying the circulating liquid fuel system is extended to multi-dimensional case and calculating momentum equation by combining neutronics and computational fluid dynamics (CFD), which is the state of the art at the current stage of Multiphysics approach.

Neutronics part can consist of multigroup neutron diffusion equations and delayed neutron precursor balance equations. For the conditions of interests, user can choose the number of energy group or neutron or delayed neutron and decay heat precursors. For instance, one group neutron diffusion equation and balance equations of 8 groups of delayed neutron precursor, c_i and 3 groups of decay heat precursor, d_i are considered to compare the sensitivities in one-dimensional case and multi-dimensional case with momentum conservation equations.

$$-\nabla\cdot\left(D\nabla\phi\right)+\left(\Sigma_a-\frac{1-\beta_t}{k_{eff}}\nu\Sigma_f\right)\phi=\sum_{i=1}^{8}\lambda_i c_i \tag{3-34}$$

$$-\nabla\left(\vec{u}c_i\right)+\nabla\cdot\left(\frac{\nu_T}{Sc_T}\nabla c_i\right)-\lambda_i c_i+\beta_i\frac{\nu\Sigma_f}{k_{eff}}\phi=0\quad\left(i=1,2,\cdots 8\right) \tag{3-35}$$

$$-\nabla\left(\vec{u}d_i\right)+\nabla\cdot\left(\frac{\nu_T}{Sc_T}\nabla d_i\right)-\lambda_{h,i}d_i+\beta_{h,i}E_f\Sigma_f\phi=0\quad\left(i=1,2,3\right) \tag{3-36}$$

Along with neutronics part, thermal-hydraulic part includes the conserved form of mass, momentum, and energy conservation equations are expressed as follows. S_m in (3-38) is momentum source and S_E in (3-39) describe the heat source, respectively.

$$\frac{\partial\rho}{\partial t}+\nabla\cdot\left(\rho U\right)=0 \tag{3-37}$$

$$\frac{\partial\left(\rho U\right)}{\partial t}+\nabla\cdot\left(\rho U\otimes U\right)=-\nabla p+\rho g+\nabla\cdot\left(\mu_{eff}\left(\nabla U+\nabla U^T\right)\right)-\nabla\left(\frac{2}{3}\mu_{eff}\left(\nabla\cdot U\right)\right)+\rho S_m \tag{3-38}$$

$$\frac{\partial}{\partial t}\left(\rho e+\frac{1}{2}\rho\left|U\right|^2\right)+\nabla\cdot\left(\rho U\left(e+\frac{1}{2}\rho\left|U\right|^2\right)\right)=\nabla\cdot\left(\alpha\nabla e\right)+\rho\left(U\cdot g\right)-\nabla\cdot\left(pU\right)+\rho S_E \tag{3-39}$$

ULSAN NATIONAL INSTITUTE OF SCIENCE AND TECHNOLOGY

According to the velocity field and power density distribution, both neutronics and thermal-hydraulics become tightly coupled each other. To solve neutronics and thermal-hydraulics in same environment, first steady state neutronics models are calculated as eigenvalue problem, and power iteration method is used to update the k_{eff} properly. From the neutron flux distribution and decay heat precursors, power density from fission and decay heat is determined.

$$Q_f = \left(1-\beta_{h,t}\right) E_f \Sigma_f \phi \tag{3-40}$$

$$Q_d = \sum_{i=1}^{3} \lambda_{h,i} d_i \tag{3-41}$$

Since above governing equations are solved numerically, pressure-velocity coupling approach can be utilized then it must satisfy the mass continuity, instead of possible numerical errors from solving continuity equation [35]. Typical pressure-velocity algorithms for continuity equation and momentum equations are SIMPLE (Semi-Implicit Method for Pressure-Linked Equations) for steady state and PIMPLE which is a merged PISO-SIMPLE (Pressure Implicit Split Operator-SIMPLE) algorithm. In this work, SIMPLE algorithm is adopted to solve thermal-hydraulics governing equations. Semi-discretized form of momentum equation, continuity equation, and corresponding pressure equation are as follows, where f is a face, p is a point, and S is outward pointing face area [36].

$$\vec{U}_p = \frac{H\left(\vec{U}\right)}{a_p} - \frac{\nabla p}{a_p}, \text{ where } H\left(\vec{U}\right) = -\sum_n a_n \vec{U}_n + \frac{\vec{U}_o}{\Delta t} \tag{3-42}$$

$$\sum_f \vec{S} \cdot \vec{U}_f = 0 \tag{3-43}$$

$$\nabla \cdot \left(\frac{1}{a_p} \nabla p \right) = \nabla \cdot \left(\frac{H\left(\vec{U}\right)}{a_p} \right) = \sum_f \vec{S} \left(\frac{H\left(\vec{U}\right)}{a_p} \right)_f \tag{3-44}$$

Then, nuclear data including cross section and diffusion coefficient, and thermophysical properties of fuel salt dependent on the temperature field are updated. Density, specific heat, and thermal conductivity of fuel salt are modeled as linear dependencies with temperature as follows.

$$\rho = \alpha_\rho T + \beta_\rho \tag{3-45}$$

$$C_p = \alpha_{Cp} T + \beta_{Cp} \tag{3-46}$$

$$k = \alpha_k T + \beta_k \tag{3-47}$$

ULSAN NATIONAL INSTITUTE OF SCIENCE AND TECHNOLOGY

Updates of cross section and diffusion coefficient are modeled with density changes as well as temperature from Doppler effect. The constant terms and coefficients can be evaluated by means of another means; for instance, Monte Carlo and burnup code, SERPENT [37].

$$\Sigma = \frac{\rho}{\rho_{ref}}\left(\Sigma_0 + \alpha_\Sigma \log\left(\frac{T}{T_{ref}}\right)\right) \tag{3-48}$$

$$D = \frac{\rho_{ref}}{\rho}\left(D_0 + \alpha_D \log\left(\frac{T}{T_{ref}}\right)\right) \tag{3-49}$$

After obtaining converged solution for all system variables; velocity, pressure, temperature, neutron flux and distribution of each group of delayed neutron precursor and decay heat precursor, now adjoint sensitivity system is solved. Corresponding adjoint sensitivity system equations are as follows, where $X = \frac{\partial \phi}{\partial \alpha}$, $Y_i = \frac{\partial c_i}{\partial \alpha}$, $W_i = \frac{\partial d_i}{\partial \alpha}$, $Z = \frac{\partial T}{\partial \alpha}$, and superscript * means adjoint sensitivity solution. From strong nonlinear characteristic of $\nabla \cdot (\rho U \otimes U)$ in momentum conservation equation, velocity field is freeze in adjoint sensitivity system. P_X, P_{Yi}, P_{Wi} and P_Z is defined as system response of interests. From direct sensitivity system $A\mathrm{x} = C$, final form of adjoint sensitivity system is derived as (3-50) to (3-53).

$$\begin{aligned} &-\nabla \cdot \left(D \nabla X^*\right) + \left(\Sigma_a - \frac{1-\beta_t}{k_{eff}} \nu\Sigma_f\right) X^* \\ &\quad + \sum_{i=1}^{8} \beta_i \frac{\nu\Sigma_f}{k_{eff}} Y_i^* + \sum_{i=1}^{3} \beta_{h,i} E_f \Sigma_f W_i^* - \left(1-\beta_{h,t}\right) E_f \Sigma_f Z^* = P_X \end{aligned} \tag{3-50}$$

$$\nabla \cdot \left(\vec{u} Y_i^*\right) + \nabla \cdot \left(\frac{\nu_T}{Sc_T} \nabla Y_i^*\right) - \lambda_i Y_i^* - \lambda_i X^* = P_{Yi} \quad (i = 1, 2, \cdots 8) \tag{3-51}$$

$$\nabla \cdot \left(\vec{u} W_i^*\right) + \nabla \cdot \left(\frac{\nu_T}{Sc_T} \nabla W_i^*\right) - \lambda_{h,i} W_i^* - \lambda_{h,i} Z^* = P_{Wi} \quad (i = 1, 2, 3) \tag{3-52}$$

$$-\nabla \cdot \left(\vec{u} Z^*\right) + \nabla \cdot \left(\alpha \nabla Z^*\right) + K_Z Z^* + K_X X^* + \sum_{i=1}^{8} K_{Yi} Y_i^* + \sum_{i=1}^{3} K_{Wi} W_i^* - \nabla \cdot \left(K_{X1} X^*\right) = P_Z \tag{3-53}$$

Extending two group neutron diffusion equation considered, direct sensitivity and adjoint sensitivity system can be expressed in matrix form as (3-54) and (3-55), respectively.

ULSAN NATIONAL INSTITUTE OF SCIENCE AND TECHNOLOGY

✓ Direct sensitivity system, $Ax = C$, where $\mathrm{x} = \left[X_1 = \frac{d\phi_1}{d\alpha}, X_2 = \frac{d\phi_2}{d\alpha}, Y = \frac{dc}{d\alpha}, W = \frac{dd}{d\alpha}, Z = \frac{dT}{d\alpha} \right]$

$$\begin{pmatrix} -\nabla\cdot D_1\nabla - \chi_1\frac{1}{k_{eff}}(1-\beta_0)\nu_1\Sigma_{f1} + \Sigma_{a1} + \Sigma_{s21} & -\chi_1\frac{1}{k_{eff}}(1-\beta_0)\nu_2\Sigma_{f2} - \Sigma_{s12} & -\chi_1\lambda & 0 & K_{X1} + \nabla\cdot K_{X11} \\ -\chi_2\frac{1}{k_{eff}}(1-\beta_0)\nu_1\Sigma_{f1} - \Sigma_{s21} & -\nabla\cdot D_2\nabla - \chi_2\frac{1}{k_{eff}}(1-\beta_0)\nu_2\Sigma_{f2} + \Sigma_{a2} + \Sigma_{s12} & -\chi_2\lambda & 0 & K_{X2} + \nabla\cdot K_{X12} \\ \beta_0\frac{1}{k_{eff}}\nu_1\Sigma_{f1} & \beta_0\frac{1}{k_{eff}}\nu_2\Sigma_{f2} & \nabla\vec{u} + \nabla\cdot\frac{\nu_T}{Sc_T} - \lambda & 0 & K_Y \\ \beta_{h0}E_{f1}\Sigma_{f1} & \beta_{h0}E_{f2}\Sigma_{f2} & 0 & \nabla\vec{u} + \nabla\cdot\frac{\nu_T}{Sc_T} - \lambda_h & K_W \\ -(1-\beta_{h0})E_{f1}\Sigma_{f1} & -(1-\beta_{h0})E_{f1}\Sigma_{f1} & 0 & -\lambda_h & \rho C_p\nabla\vec{u} - \nabla\cdot k\nabla + K_Z \end{pmatrix} \begin{pmatrix} X_1 \\ X_2 \\ Y \\ W \\ Z \end{pmatrix} = \begin{pmatrix} C_{X1} \\ C_{X2} \\ C_Y \\ C_W \\ C_Z \end{pmatrix} \quad (3\text{-}54)$$

✓ Adjoint sensitivity field; $A^*\mathrm{x}^* = P$, where $A^* = A^T$

$$\begin{pmatrix} -\nabla\cdot D_1\nabla - \chi_1\frac{1}{k_{eff}}(1-\beta_0)\nu_1\Sigma_{f1} + \Sigma_{a1} + \Sigma_{s21} & -\chi_2\frac{1}{k_{eff}}(1-\beta_0)\nu_1\Sigma_{f1} - \Sigma_{s21} & \beta_0\frac{1}{k_{eff}}\nu_1\Sigma_{f1} & \beta_{h0}E_{f1}\Sigma_{f1} & -(1-\beta_{h0})E_{f1}\Sigma_{f1} \\ -\chi_1\frac{1}{k_{eff}}(1-\beta_0)\nu_2\Sigma_{f2} - \Sigma_{s12} & -\nabla\cdot D_2\nabla - \chi_2\frac{1}{k_{eff}}(1-\beta_0)\nu_2\Sigma_{f2} + \Sigma_{a2} + \Sigma_{s12} & \beta_0\frac{1}{k_{eff}}\nu_2\Sigma_{f2} & \beta_{h0}E_{f2}\Sigma_{f2} & -(1-\beta_{h0})E_{f2}\Sigma_{f2} \\ -\chi_1\lambda & -\chi_2\lambda & \vec{u}\cdot\nabla + \nabla\cdot\frac{\nu_T}{Sc_T}\nabla - \lambda & 0 & 0 \\ 0 & 0 & 0 & \vec{u}\cdot\nabla + \nabla\cdot\frac{\nu_T}{Sc_T}\nabla - \lambda_d & -\lambda_h \\ K_{X1} - K_{X11}\cdot\nabla & K_{X2} - K_{X12}\cdot\nabla & K_Y & K_W & -\rho C_p\vec{u}\cdot\nabla - \nabla\cdot k\nabla + K_Z \end{pmatrix} \begin{pmatrix} X_1^* \\ X_2^* \\ Y^* \\ W^* \\ Z^* \end{pmatrix} = \begin{pmatrix} P_{X1} \\ P_{X2} \\ P_Y \\ P_W \\ P_Z \end{pmatrix} \quad (3\text{-}55)$$

ULSAN NATIONAL INSTITUTE OF
SCIENCE AND TECHNOLOGY

Since the direct sensitivity equation is obtained by differentiating the primal equation with respect to the input/model parameter of interests α, the unit of the direct sensitivity solution x is determined by the unit of α. Different from the adjoint solution φ^* indicating the importance of the neutron such as the weighting function, the physical meaning of the adjoint sensitivity field x^* underlies to their units. For instance, the unit of the adjoint neutron sensitivity X^* and the adjoint delayed neutron precursor Y^* are determined by the source term C in (3-54). Since C functions are derived from the procedures of the differentiating the primal equations, adjoint neutron flux sensitivity X^* have the same unit with the neutron flux. On the other hand, the unit of the adjoint decay heat precursor sensitivity W^* and adjoint temperature sensitivity Z^* is the neutron flux per unit energy of the fuel salt. At this point, the physical meaning of the adjoint sensitivity solution is derived; how much important the variable itself is on the sensitivity of the system response for the certain parameter α. Table 3-3 summarizes the unit of adjoint solution φ^*, direct sensitivity field x, and adjoint sensitivity field x^*.

Finally, the system analysis module calculating the primal and adjoint equations, and the sensitivity analysis module calculating the adjoint sensitivity equations are described. *msrAdjointFoam* solver consists on the Multiphysics approach for the integrated analysis for the molten salt reactor and further, it can be introduced to the analysis of general liquid fuel system. Figure 3-2 shows the flow chart of the *msrAdjointFoam* including overall procedure of system analysis and sensitivity analysis.

ULSAN NATIONAL INSTITUTE OF SCIENCE AND TECHNOLOGY

Table 3-3 Unit of direct and adjoint sensitivity field

	Adjoint solution, φ^*	**Direct sensitivity, x (/ (unit of α))**	**Adjoint sensitivity, x^* (/ unit of α))**
Neutron flux	-	# / cm^2 s	# / cm^2 s
Delayed neuron precursor	-	# / m^3	# / cm^2 s
Decay heat precursor	1 / J	W/m^3	(# / cm^2 s) / J
Temperature	1 / J	K	(# / cm^2 s) / J

ULSAN NATIONAL INSTITUTE OF SCIENCE AND TECHNOLOGY

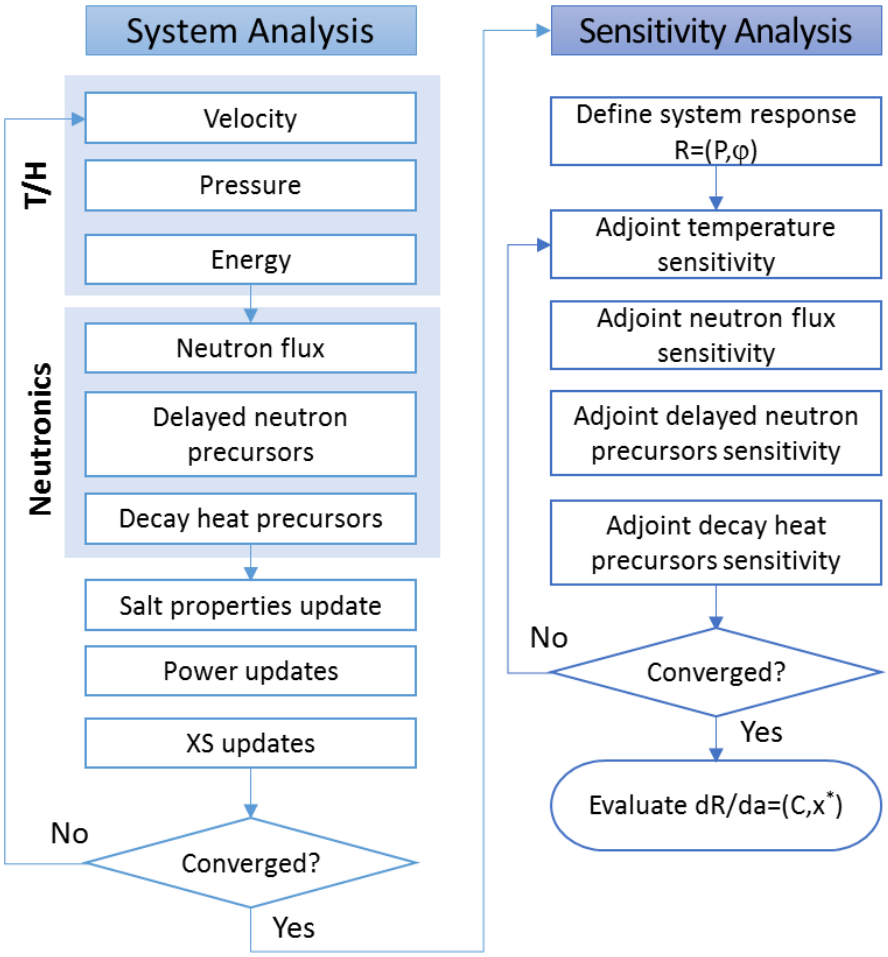

Figure 3-2 Flowchart of *msrAdjointFoam* for steady state calculation

ULSAN NATIONAL INSTITUTE OF
SCIENCE AND TECHNOLOGY

3.2.2 Sensitivity Analysis of the Molten Salt Reactor

msrAdjointFoam solver has a capability to analyze system behavior and model sensitivity on the system response simultaneously including coupled physics phenomena. Depending on the which model is adopted to each physics to describe important phenomena of the system, this solver can be extended under same structure. To figure out the application area of the solver, two case studies are performed; one is CNRS benchmark of two-dimensional square cavity case, and the other is MSFR steady state case. Except Multiphysics tools listed in Table 3-1, code-to-code validation is hard to explain the difference of the results for the complex modeling issue with different modeling approach. Besides, there is few information reported on the Multiphysics model sensitivity, especially for the molten salt reactor. First case investigated the physical phenomena of fuel salt flow and the validation of the solver. And then, simplified primary loop of MSFR in steady state is simulated to investigate the importance of the system response predicted from the input or model parameters in the design viewpoint.

3.2.2.1 CNRS benchmark: 2D square cavity

In the framework of EU EVOL project, development of a purpose-made benchmark was initiated at LPSC/CNRS/Grenoble to solve the issue on challenging Multiphysics coupling and time integration issue, called CNRS benchmark [38] It covers the verification of single physics; neutronics or thermal-hydraulics only, and validation of the modeling on the steady state coupling strategy; one way or fully coupled. Unfortunately, these works are still on-going, such that the comparison of the results will be performed in near future. At first, same domain and conditions are adopted without the turbulence model to configure the Multiphysics coupling and physical phenomena comprehensively using *msrAdjointFoam* for the further comparison with CNRS benchmark results.

CNRS benchmark problem deals with 2 m × 2 m square cavity domain filled with fuel salt flow under natural or forced convection condition, shown in Figure 3-3. Fuel salt is selected as fluoride salt with uranium-235 eutectic salt with FLiBe, whose composition and thermophysical properties are listed in Table 3-4.

ULSAN NATIONAL INSTITUTE OF SCIENCE AND TECHNOLOGY

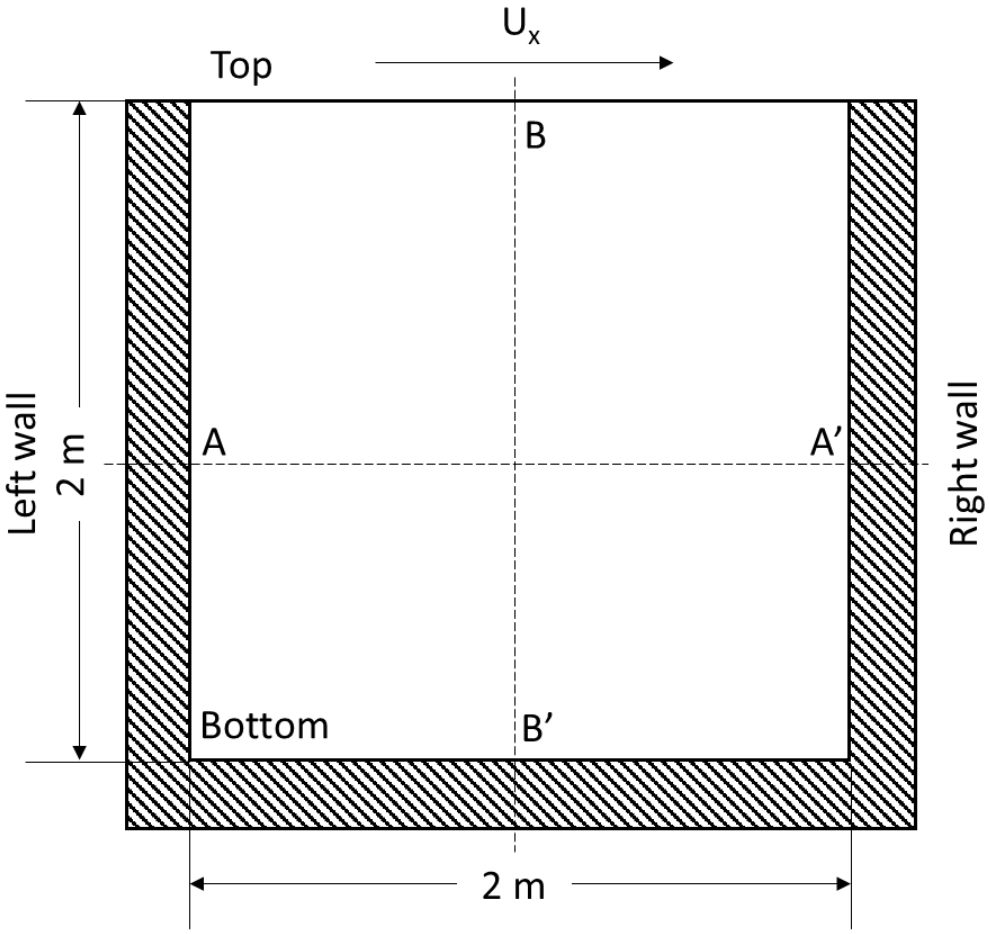

Figure 3-3 2D Domain of CNRS benchmark

ULSAN NATIONAL INSTITUTE OF SCIENCE AND TECHNOLOGY

Table 3-4 Salt composition and thermophysical properties of CNRS benchmark [38]

Parameter	**Values**
Salt composition (% isotope)	^{6}Li – 2.11488 / ^{7}Li – 26.0836 ^{9}Be – 14.0992 / ^{19}F - 56.3696 ^{235}U – 1.30545
Density	2000 kg/m^3
Kinematic viscosity	0.025 m^2/s
Specific heat capacity	3075 J/kg K
Prandtl number	7.0
Schmidt number	20.0
Thermal expansion coefficient	2.0×10^{-4} /K

ULSAN NATIONAL INSTITUTE OF SCIENCE AND TECHNOLOGY

In this case, 2 group neutron diffusion equations and one group of delayed neutron and decay heat group balance equations along with Navier-Stokes equations in steady state are considered as (3-56) to (3-62). Two group neutron diffusion equations consider the fast and thermal spectrum of neutron energy range, indicated subscript 1 and 2, with fission generation from each group of neutrons, absorption, scattering, generation from delayed neutron precursor. Transport equations for both delayed neutron and decay heat precursor contains the convection and diffusion term from fuel motion along with produced and decayed. Fission or decay heat generation are included in the energy conservation equation as a source term.

$$-\nabla\cdot D_1\nabla\phi_1=\chi_1\left(1-\beta_0\right)\frac{1}{k_{eff}}\nu_1\Sigma_{f1}\phi_1+\chi_1\left(1-\beta_0\right)\frac{1}{k_{eff}}\nu_2\Sigma_{f2}\phi_2-\Sigma_{a1}\phi_1+\Sigma_{s12}\phi_2-\Sigma_{s21}\phi_1+\chi_1\lambda c \tag{3-56}$$

$$-\nabla\cdot D_2\nabla\phi_2=\chi_2\left(1-\beta_0\right)\frac{1}{k_{eff}}\nu_1\Sigma_{f1}\phi_1+\chi_2\left(1-\beta_0\right)\frac{1}{k_{eff}}\nu_2\Sigma_{f2}\phi_2-\Sigma_{a2}\phi_2+\Sigma_{s21}\phi_1-\Sigma_{s12}\phi_2+\chi_2\lambda c \tag{3-57}$$

$$-\nabla\left(\vec{uc}\right)+\nabla\cdot\left(\frac{\nu_T}{Sc_T}\nabla c\right)+\beta_0\frac{1}{k_{eff}}\nu_1\Sigma_{f1}\phi_1+\beta_0\frac{1}{k_{eff}}\nu_2\Sigma_{f2}\phi_2-\lambda c=0 \tag{3-58}$$

$$-\nabla\left(\vec{ud}\right)+\nabla\cdot\left(\frac{\nu_T}{Sc_T}\nabla d\right)+\beta_0E_{f1}\Sigma_{f1}\phi_1+\beta_0E_{f2}\Sigma_{f2}\phi_2-\lambda_h d=0 \tag{3-59}$$

$$\frac{\partial\rho}{\partial t}+\nabla\cdot\left(\rho\vec{u}\right)=0 \tag{3-60}$$

$$\nabla\cdot\left(\rho\vec{u}\otimes\vec{u}\right)=-\nabla p+\rho\vec{g}+\nabla\cdot\left(\mu_{eff}\left(\nabla\vec{u}+\nabla\vec{u}^T\right)\right)-\nabla\left(\frac{2}{3}\mu_{eff}\left(\nabla\cdot\vec{u}\right)\right)+\rho S_m \tag{3-61}$$

$$\nabla\cdot\left(\rho\vec{u}\left(e+\frac{1}{2}\rho|\vec{u}|^2\right)\right)=\nabla\cdot\left(\alpha\nabla e\right)+\rho\left(\vec{u}\cdot\vec{g}\right)-\nabla\cdot\left(p\vec{u}\right)+\rho\left[\left(1-\beta\right)\left(E_{f1}\Sigma_{f1}\phi_1+E_{f2}\Sigma_{f2}\phi_2\right)+\lambda_h d\right] \tag{3-62}$$

By modeling dependencies of nuclear data to the temperature field and density changes based on the Boussinesq approximation, physical phenomena from coupled physics are considered. Reference values and coefficients are calculated by deterministic codes from [38] as summarized in Table 3-5.

$$\Sigma=\Sigma_0+\alpha_\Sigma\left(T-T_{ref}\right)\frac{\rho}{\rho_{ref}} \tag{3-63}$$

$$D=D_0\frac{\rho}{\rho_{ref}} \tag{3-64}$$

$$\frac{\rho}{\rho_{ref}}=1-\beta\left(T-T_{ref}\right) \tag{3-65}$$

ULSAN NATIONAL INSTITUTE OF SCIENCE AND TECHNOLOGY

Table 3-5 Reference values and coefficients in 2D cavity problem

Parameter	**Value**	**Parameter**	**Value**
$D_{1\ ref}$	1.67E-02 m	ν_1	2.54
$D_{2\ ref}$	1.33E-02 m	ν_2	2.43
$\Sigma_{a1\ ref}$	2.49E-01 m^{-1}	E_{f1}	3.20435E-11 J
$\Sigma_{a2\ ref}$	9.18E-01 m^{-1}	E_{f2}	3.20435E-11 J
$\alpha_{\Sigma a1}$	7.76E-07 $m^{-1}\,K^{-1}$	χ_1	0.99
$\alpha_{\Sigma a2}$	7.97E-07 $m^{-1}\,K^{-1}$	χ_2	0.01
$\Sigma_{f1\ ref}$	1.15E-01 m^{-1}	β_0	0.00657
$\Sigma_{f2\ ref}$	4.04E-01 m^{-1}	λ	0.416 s^{-1}
$\alpha_{\Sigma f1}$	-1.63E-06 $m^{-1}\,K^{-1}$	β_{h0}	2.0E-02
$\alpha_{\Sigma f2}$	-2.83E-06 $m^{-1}\,K^{-1}$	λ_h	0.19 s^{-1}
Σ_{s12}	0.0 m^{-1}	T_{ref}	900 K
Σ_{s21}	1.73 m^{-1}	ρ_{ref}	2000 kg/m^3

ULSAN NATIONAL INSTITUTE OF SCIENCE AND TECHNOLOGY

For the primal solution, corresponding adjoint equations of neutron flux, delayed neutron precursors, decay heat precursors, and temperature are derived as (3-66) to (3-70). For the adjoint solution of the temperature T^*, it is obtained from the temperature equation which can be expressed from the internal energy equation. Note that the adjoint solution of the velocity field is not considered but freeze velocity field is considered in this study. Due to the high nonlinearity of the Navier-Stokes equations for the case of the changing thermophysical properties of the fluid, it may cause the wrong solution for the adjoint solutions for all variables.

$$-\nabla\cdot D_1\nabla\phi_1^* = \chi_1(1-\beta_0)\frac{1}{k_{eff}}\nu_1\Sigma_{f1}\phi_1^* + \chi_1(1-\beta_0)\frac{1}{k_{eff}}\nu_2\Sigma_{f2}\phi_2^* - \Sigma_{a1}\phi_1^* + \Sigma_{s21}\phi_2^* - \Sigma_{s21}\phi_1^* + \beta_0\nu_1\Sigma_{f1}c^* - \beta_0 E_{f1}\Sigma_{f1}d^* + (1-\beta_0)E_{f1}\Sigma_{f1}T^* \tag{3-66}$$

$$-\nabla\cdot D_2\nabla\phi_2^* = \chi_2(1-\beta_0)\frac{1}{k_{eff}}\nu_1\Sigma_{f1}\phi_1^* + \chi_2(1-\beta_0)\frac{1}{k_{eff}}\nu_2\Sigma_{f2}\phi_2^* - \Sigma_{a2}\phi_2^* + \Sigma_{s12}\phi_1^* - \Sigma_{s12}\phi_2^* + \beta_0\nu_2\Sigma_{f2}c^* - \beta_0 E_{f2}\Sigma_{f2}d^* + (1-\beta_0)E_{f2}\Sigma_{f2}T^* \tag{3-67}$$

$$\nabla\left(\vec{u}c^*\right) + \nabla\cdot\left(\frac{\nu_T}{Sc_T}\nabla c^*\right)\chi_1\lambda\phi_1^* + \chi_2\lambda\phi_2^* - \lambda c^* = 0 \tag{3-68}$$

$$-\nabla\left(\vec{u}d^*\right) + \nabla\cdot\left(\frac{\nu_T}{Sc_T}\nabla d^*\right) - \lambda d^* = 0 \tag{3-69}$$

$$-\rho C_p\nabla\left(\vec{u}T^*\right) - \nabla\cdot\left(\alpha\nabla T^*\right) = 0 \tag{3-70}$$

Primal equation from (3-56) to (3-59) and adjoint equation from (3-66) to (3-70) can be expressed in matrix form as (3-71) and (3-72), respectively.

ULSAN NATIONAL INSTITUTE OF SCIENCE AND TECHNOLOGY

$$\begin{pmatrix} -\nabla\cdot D_1\nabla+\Sigma_{a1}+\Sigma_{s21} & -\Sigma_{s12} & -\chi_1\lambda & 0 & 0 \\ -\Sigma_{s21} & -\nabla\cdot D_2\nabla+\Sigma_{a2}+\Sigma_{s12} & -\chi_2\lambda & 0 & 0 \\ 0 & 0 & \nabla\vec{u}+\nabla\cdot\frac{\nu_T}{Sc_T}\nabla+\lambda & 0 & 0 \\ \beta_{h0}E_{f1}\Sigma_{f1} & \beta_{h0}E_{f2}\Sigma_{f2} & 0 & -\nabla\vec{u}-\nabla\cdot\frac{\nu_T}{Sc_T}\nabla-\lambda_d & 0 \\ -(1-\beta_{h0})E_{f1}\Sigma_{f1} & -(1-\beta_{h0})E_{f2}\Sigma_{f2} & 0 & 0 & \rho C_p\nabla\vec{u}-\nabla\cdot\alpha\nabla \end{pmatrix} \begin{pmatrix} \phi_1 \\ \phi_2 \\ c \\ d \\ T \end{pmatrix}$$

$$= \frac{1}{k_{eff}} \begin{pmatrix} \chi_1(1-\beta_0)\nu_1\Sigma_{f1} & \chi_1(1-\beta_0)\nu_2\Sigma_{f2} & 0 & 0 & 0 \\ \chi_2(1-\beta_0)\nu_1\Sigma_{f1} & \chi_2(1-\beta_0)\nu_2\Sigma_{f2} & 0 & 0 & 0 \\ \beta_0\nu_1\Sigma_{f1} & \beta_0\nu_2\Sigma_{f2} & 0 & 0 & 0 \\ 0 & 0 & 0 & 0 & 0 \\ 0 & 0 & 0 & 0 & 0 \end{pmatrix} \begin{pmatrix} \phi_1 \\ \phi_2 \\ c \\ d \\ T \end{pmatrix} \tag{3-71}$$

$$\begin{pmatrix} -\nabla\cdot D_1\nabla+\Sigma_{a1}+\Sigma_{s21} & -\Sigma_{s21} & 0 & \beta_{h0}E_{f1}\Sigma_{f1} & -(1-\beta_{h0})E_{f1}\Sigma_{f1} \\ -\Sigma_{s12} & -\nabla\cdot D_2\nabla+\Sigma_{a2}+\Sigma_{s12} & 0 & \beta_{h0}E_{f2}\Sigma_{f2} & -(1-\beta_{h0})E_{f2}\Sigma_{f2} \\ -\chi_1\lambda & -\chi_2\lambda & -\nabla\vec{u}+\nabla\cdot\frac{\nu_T}{Sc_T}\nabla+\lambda & 0 & 0 \\ 0 & 0 & 0 & \nabla\vec{u}-\nabla\cdot\frac{\nu_T}{Sc_T}\nabla-\lambda_d & 0 \\ 0 & 0 & 0 & 0 & -\rho C_p\nabla\vec{u}-\nabla\cdot\alpha\nabla \end{pmatrix} \begin{pmatrix} \phi_1^* \\ \phi_2^* \\ c^* \\ d^* \\ T^* \end{pmatrix}$$

$$= \frac{1}{k_{eff}} \begin{pmatrix} \chi_1(1-\beta_0)\nu_1\Sigma_{f1} & \chi_2(1-\beta_0)\nu_1\Sigma_{f1} & \beta_0\nu_1\Sigma_{f1} & 0 & 0 \\ \chi_1(1-\beta_0)\nu_2\Sigma_{f2} & \chi_2(1-\beta_0)\nu_2\Sigma_{f2} & \beta_0\nu_2\Sigma_{f2} & 0 & 0 \\ 0 & 0 & 0 & 0 & 0 \\ 0 & 0 & 0 & 0 & 0 \\ 0 & 0 & 0 & 0 & 0 \end{pmatrix} \begin{pmatrix} \phi_1^* \\ \phi_2^* \\ c^* \\ d^* \\ T^* \end{pmatrix} \tag{3-72}$$

ULSAN NATIONAL INSTITUTE OF
SCIENCE AND TECHNOLOGY

In this section, CNRS benchmark simulation is conducted in a two-dimensional lid driven cavity condition. Top region is set as fixed velocity of U_x=0.5 m/s and constant temperature of 900 K, and other regions are set as adiabatic and no slip conditions for velocity and temperature boundary condition. For the neutronics part, zero neutron flux condition and zero gradient conditions for delayed neutron precursors and decay heat precursors are set for all boundary regions. Since it is steady state calculation, the effective multiplication factor k_{eff} is updated by the power iteration method as an eigenvalue problem, and neutron flux is normalized properly by corresponding target power of the 5 MW_{th}. In principle, eigenvalues of the primal equation and adjoint equation should be same, when the adjoint equation is well defined. Corresponding boundary conditions of the adjoint solutions are derived by the definition of the adjoint formulation following Lagrange's identity with primal solution. Boundary conditions of primal and adjoint variables are summarized in Table 3-6 and Table 3-7, respectively. Domain of two-dimensional square cavity consists of 10000 hexahedral elements with 10 mm uniform size each. Solving all equations including primal and adjoint equations, gradient and Laplacian terms are discretized to Gauss linear scheme and divergence terms to Gauss upwind scheme.

ULSAN NATIONAL INSTITUTE OF SCIENCE AND TECHNOLOGY

Table 3-6 Summary of the boundary condition of 2D lid driven cavity: primal field

Variables	Right / left wall	bottom	top	Front/back
ϕ_1	fixedValue uniform 0	fixedValue uniform 0	fixedValue uniform 0	Empty
ϕ_2	fixedValue uniform 0	fixedValue uniform 0	fixedValue uniform 0	
U	noSlip	noSlip	fixedValue U_x=0.5 m/s	
T	zeroGradient	zeroGradient	fixedValue T=900 K	
p_rgh	fixedFluxPressure gradient 0	fixedFluxPressure gradient 0	fixedFluxPressure gradient 0	
c	zeroGradient	zeroGradient	zeroGradient	
d	zeroGradient	zeroGradient	zeroGradient	

Table 3-7 Summary of the boundary condition of 2D lid driven cavity: adjoint field

Variables	Right / left wall	bottom	top	Front/back
ϕ_1^*	fixedValue uniform 0	fixedValue uniform 0	fixedValue uniform 0	Empty
ϕ_2^*	fixedValue uniform 0	fixedValue uniform 0	fixedValue uniform 0	
T*	zeroGradient	zeroGradient	fixedValue T^*=0	
c*	zeroGradient	zeroGradient	zeroGradient	
d*	zeroGradient	zeroGradient	zeroGradient	

ULSAN NATIONAL INSTITUTE OF SCIENCE AND TECHNOLOGY

Primal and adjoint solution for the 2D square cavity case study is shown in Figure 3-4 and Figure 3-5. Comparing the effective multiplication factor, its value is 0.97876 and deviation between eigenvalues of primal and adjoint solution is less than 10 pcm, which indicates that adjoint system is well defined in this system. In general, adjoint solution can be utilized to approximate the perturbed state only with the unperturbed solution to investigate the effects of the small changes in the reactor core composition or geometry on the multiplication factor k_{eff} [34]. By the relationship between primal and adjoint solution, the physical meaning of the adjoint solution in this case relies on the source terms of the adjoint solution in (3-72).

For instance, the adjoint solution of the ϕ_1 is calculated by considering how much amount of the second group of the neutron flux scattered from first to second group and neutron energy generation from the unit energy of the salt. Therefore, it can be interpreted as the importance of the fuel salt on the contribution of the neutron flux distribution. Likewise, the adjoin solution of the delayed neutron precursor c* can be obtained from the adjoint solution of the ϕ_1 and ϕ_2 weighted by the probability of the neutron in certain energy group from fission and velocity field.

Figure 3-6 shows the adjoint sensitivity solution for the 2D lid driven case of the neutron flux group 1 and 2, delayed neutron precursor, decay heat precursor and temperature respectively. Considering the meaning of the adjoint neutron flux that it indicates the importance of the neutron described in previous section, the adjoint sensitivity solution of each group of neutron flux follows the profile of the primal solution. For the delayed neutron precursor, it includes the importance in both neutron flux and the velocity field inside cavity. The adjoint delayed neutron precursor has the distribution just before the primal solution's distribution can be made; for instance, it looks like the distribution of the delayed neutron precursor before Δt such that the location of high importance follows the velocity field. In addition, decay heat precursor and temperature only include the effect of the velocity field on the overall system, such that their magnitudes are relatively small, and their distributions are mainly governed by the velocity field. Therefore, the adjoint sensitivity solution give insights on the importance of the delayed neutron precursor including the flow effect on the neutron flux distribution.

ULSAN NATIONAL INSTITUTE OF
SCIENCE AND TECHNOLOGY

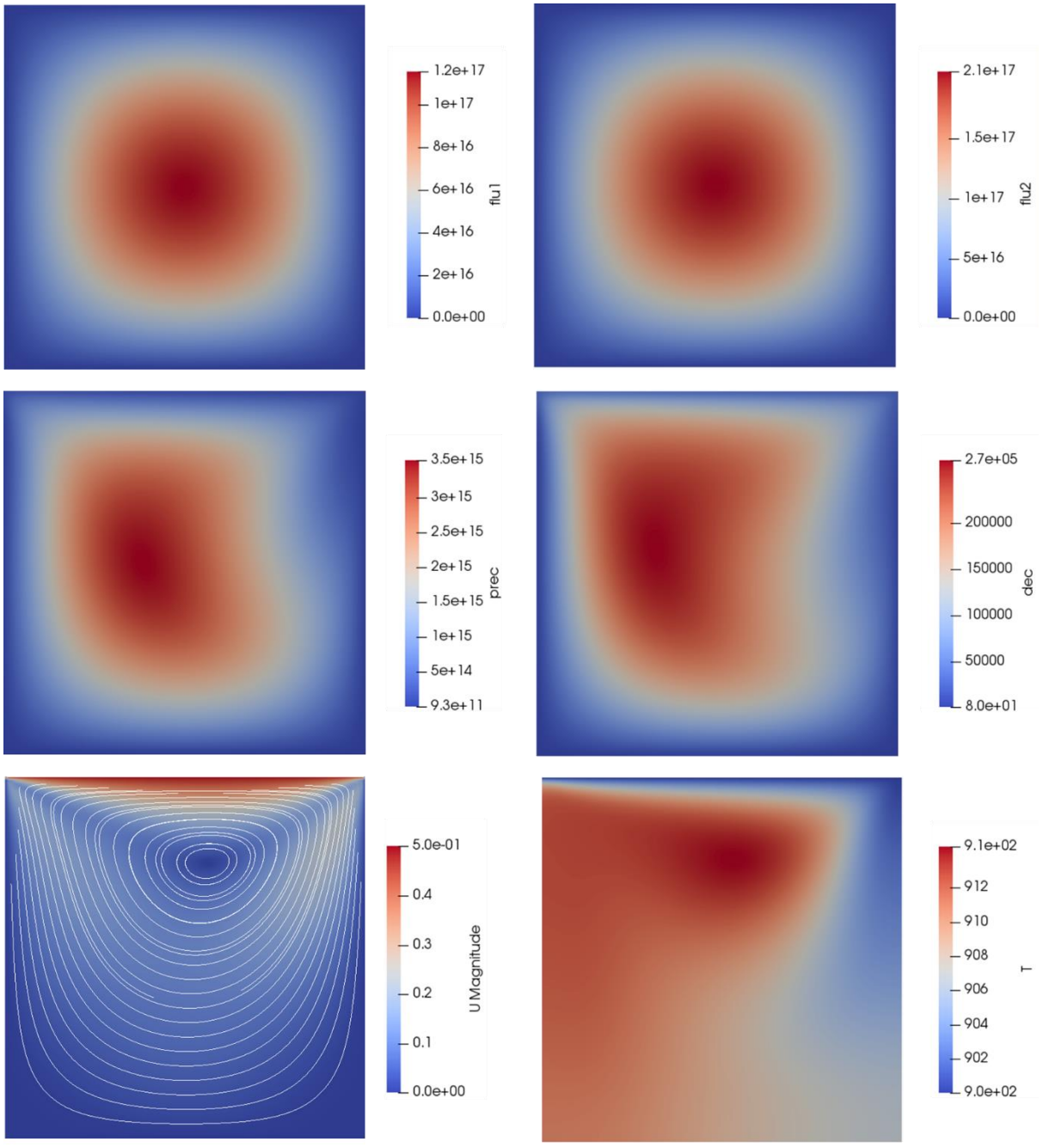

Figure 3-4 Primal solution of 2D lid driven cavity case

ULSAN NATIONAL INSTITUTE OF
SCIENCE AND TECHNOLOGY

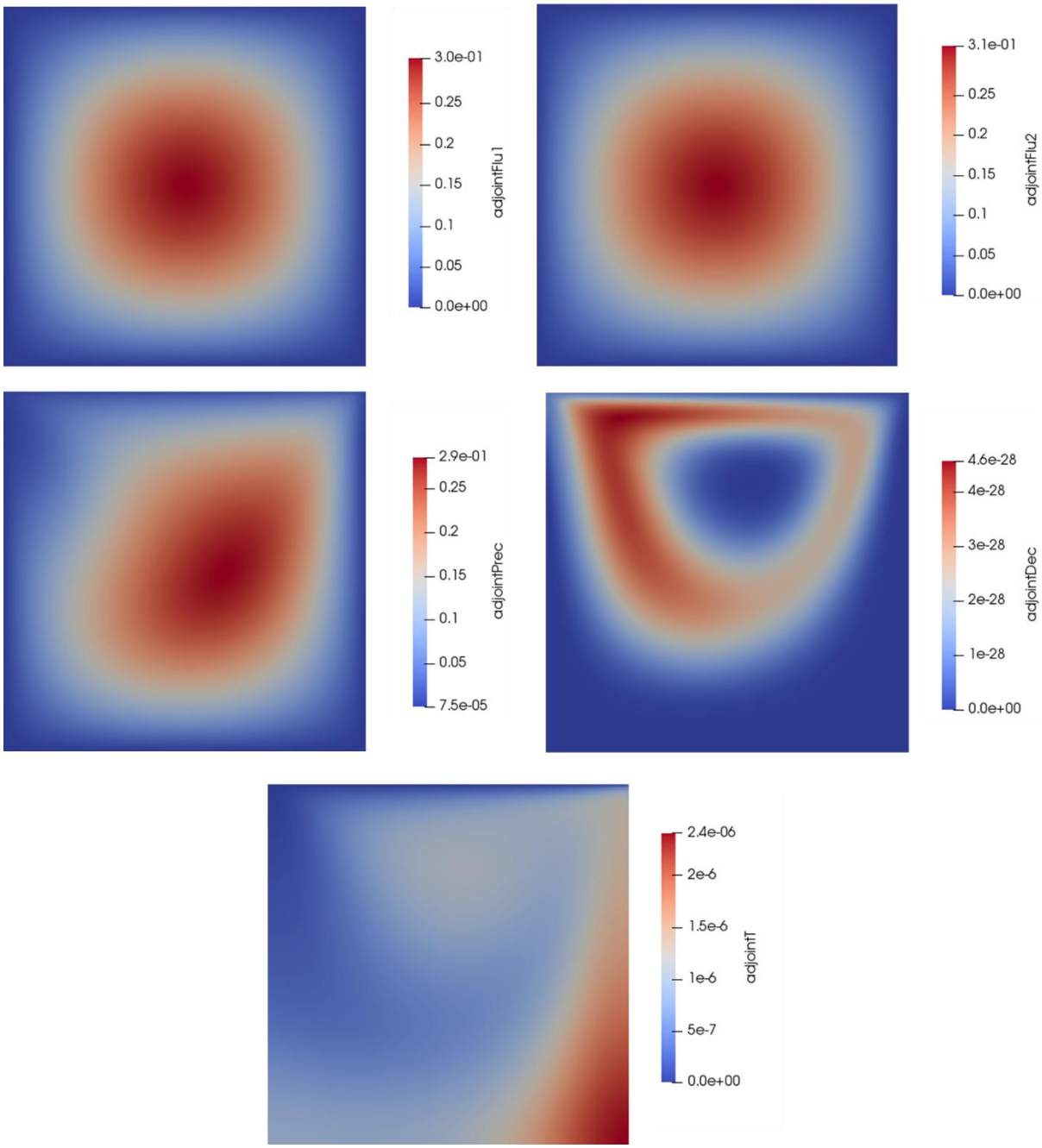

Figure 3-5 Adjoint solution of 2D lid driven cavity case

ULSAN NATIONAL INSTITUTE OF SCIENCE AND TECHNOLOGY

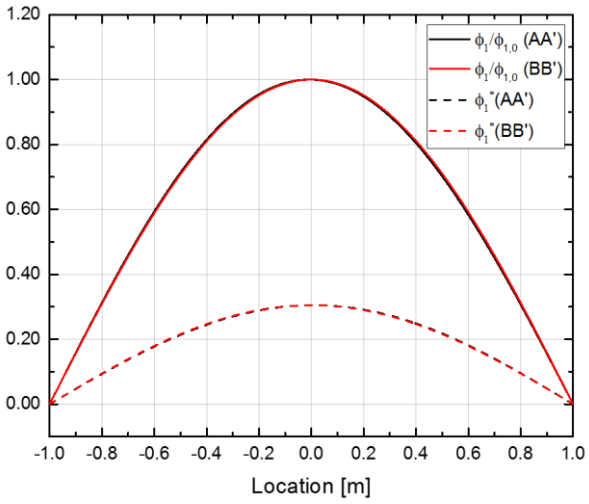

a) ϕ_1 and ϕ_1^*

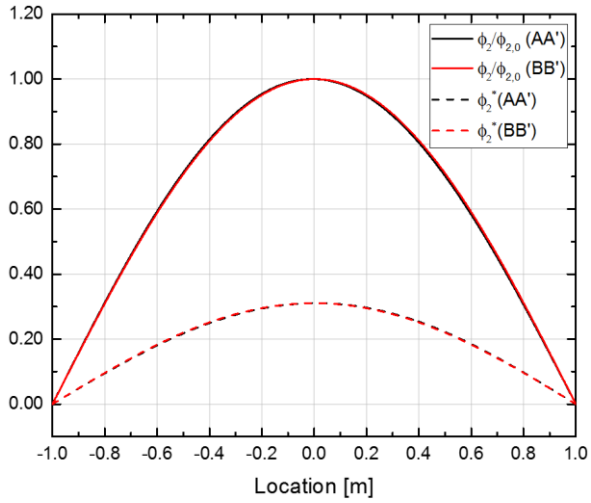

b) ϕ_2 and ϕ_2^*

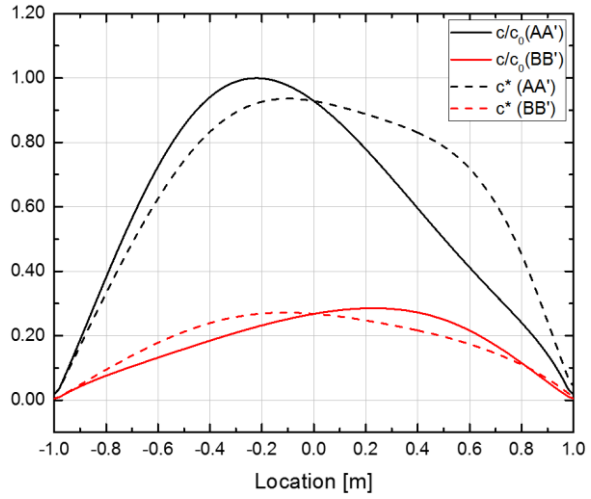

c) c and c*

Figure 3-6 Primal and adjoint solution on line AA' and BB'

ULSAN NATIONAL INSTITUTE OF SCIENCE AND TECHNOLOGY

Based on the primal and adjoint solution, adjoint sensitivity solution can be obtained for given definition of system response types. To verify and validate the implementation of adjoint sensitivity solver in *msrAdjointFoam*, system response P defined as (3-73) is chosen as a reference case and compared the sensitivity of system response P to all input/model parameters by recalculating and using adjoint method.

$$P = \sum_i \left(1, \varphi_i\right) = \phi_1 + \phi_2 + c + d + T \tag{3-73}$$

$$\frac{dP}{d\alpha} = \frac{\partial \phi_1}{\partial \alpha} + \frac{\partial \phi_2}{\partial \alpha} + \frac{\partial c}{\partial \alpha} + \frac{\partial d}{\partial \alpha} + \frac{\partial T}{\partial \alpha} = X_1 + X_2 + Y + W + Z \tag{3-74}$$

$$\frac{dP}{d\alpha} = \sum_i \left(1, \mathrm{x}_i\right) = \sum_i \left(C_i, \mathrm{x}_i^*\right) = C_{X1} X_1^* + C_{X2} X_2^* + C_Y Y^* + C_W W^* + C_Z Z^* \tag{3-75}$$

Adjoint sensitivity fields for certain system response are obtained by taking suitable boundary conditions for them, such that the it can have a duality in mathematical background with the direct sensitivity field. For general Dirichlet and Neumann boundary conditions of the general scalar convection and diffusion equation as (3-76) , the adjoint boundary condition for φ^* can be expressed for the scalar quantity φ and arbitrary boundary matrix B and C [39].

$$Lu \equiv \nabla \cdot \left(\varphi \vec{w}\right) - \nabla^2 \varphi = f \tag{3-76}$$

$$B\varphi \equiv \varphi \quad \text{or} \quad C\varphi \equiv \frac{\partial \varphi}{\partial n} \quad \text{(Dirichlet b.c.)} \tag{3-77}$$

$$B^*\varphi^* \equiv -\varphi^* \quad \text{or} \quad C^*\varphi^* \equiv -w \cdot \vec{n} - \frac{\partial \varphi^*}{\partial n} \quad \text{(adjoint Dirichlet b.c.)} \tag{3-78}$$

$$B\varphi \equiv \frac{\partial \varphi}{\partial n} \quad \text{or} \quad C\varphi \equiv \varphi \quad \text{(Neumann b.c.)} \tag{3-79}$$

$$B^*\varphi^* \equiv w \cdot \vec{n} + \frac{\partial \varphi}{\partial n} \quad \text{or} \quad C^*\varphi^* \equiv \varphi^* \quad \text{(adjoint Neumann b.c.)} \tag{3-80}$$

Considering the definition of the system response P, the boundary conditions of adjoint sensitivity field for this case can be derived. Table 3-8 shows the boundary conditions of the adjoint sensitivity field for the system response P. From Figure 3-7, the distribution of the adjoint sensitivity field for each state variable is obtained for given condition and the type of system response. From the test case results, the *msrAdjointFoam* solver can solve the primal, adjoint, and adjoint sensitivity field properly including Navier-Stokes equations as a combination of the CFD, neutronics, and adjoint solver.

ULSAN NATIONAL INSTITUTE OF SCIENCE AND TECHNOLOGY

Table 3-8 Summary of the boundary condition of 2D lid driven cavity: adjoint sensitivity field for P

Variables	Right / left wall	bottom	top	Front/back
X_1^*	fixedValue uniform 0	fixedValue uniform 0	fixedValue uniform 0	Empty
X_2^*	fixedValue uniform 0	fixedValue uniform 0	fixedValue uniform 0	
*Z**	zeroGradient	zeroGradient	fixedValue $Z^*=0$	
*Y**	zeroGradient	zeroGradient	zeroGradient	
*W**	zeroGradient	zeroGradient	zeroGradient	

ULSAN NATIONAL INSTITUTE OF
SCIENCE AND TECHNOLOGY

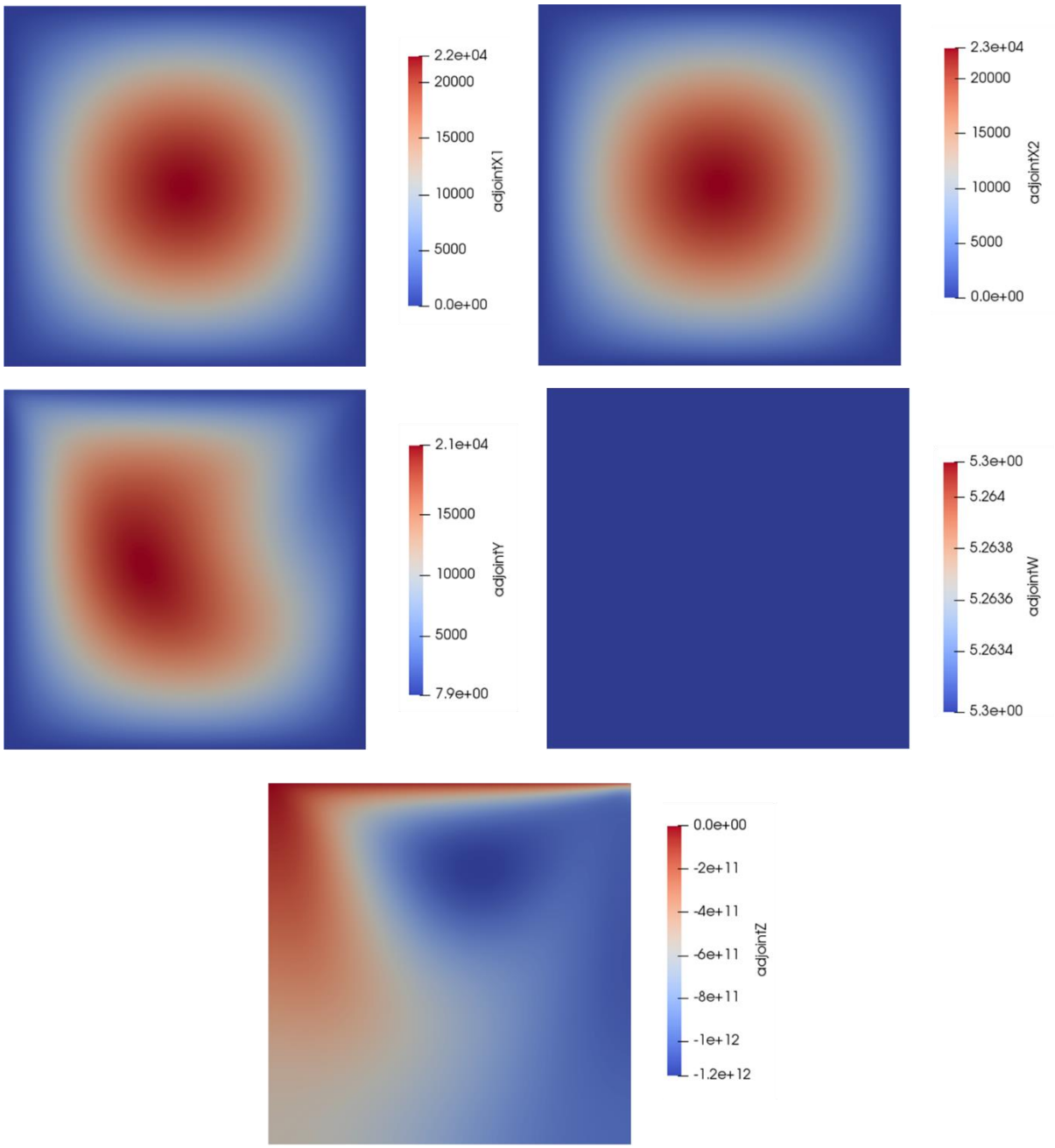

Figure 3-7 Adjoint sensitivity solution of 2D lid driven cavity case for system response P

ULSAN NATIONAL INSTITUTE OF SCIENCE AND TECHNOLOGY

3.2.2.2 MSFR in steady state

Using *msrAdjointFoam* solver, Multiphysics modeling approach on the MSFR by the SAMOFAR project is investigated in terms of the model sensitivity using adjoint sensitivity analysis method. To evaluate the parameter sensitivity on the Multiphysics system analysis results, two-dimensional simplified rectangular loop condition is set as a representative of the 1 sector among 16 sectors of MSFR primary loop. Figure 3-8 shows the configurations of fuel salt loop and design specifications of the MSFR normal operation condition.

In this simulation, only fuel salt of primary loop is in interests and top and bottom reflector and radial fertile blanket is considered as albedo boundary conditions on the neutron flux field defined as (3-81) to distinguish the core and other parts, instead solving those regions directly. Albedo boundary conditions and corresponding albedo coefficients for the given MSFR conditions are provided by Nuclear Reactor Groups of Politecnico di Milano (refer [33], [40]).

$$\alpha = \frac{J_x^-}{J_x^+} = \frac{\frac{1}{4}\phi + \frac{1}{2}D\nabla\phi}{\frac{1}{4}\phi - \frac{1}{2}D\nabla\phi} \tag{3-81}$$

$\vec{n}\cdot\left(D\nabla\phi\right)_S = -\gamma\phi_S$, where S indicates a certain point (3-82)

Since it is steady state simulation, neutron flux and delayed neutron precursor are normalized in each iteration according to the target power, and effective multiplication factor is updated by power iteration method. Heat exchanger part is modeled as uniform volumetric heat removal by applying uniform heat transfer coefficient and reference temperature, T_{cold}. Pump is modeled as a constant momentum source at the given region. Based on the definition of adjoint formulation, corresponding boundary condition of adjoint field is derived from those of primal field. Table 3-9 and Table 3-10 show the boundary conditions of primal and adjoint field for 2D simplified MSFR loop simulations.

ULSAN NATIONAL INSTITUTE OF
SCIENCE AND TECHNOLOGY

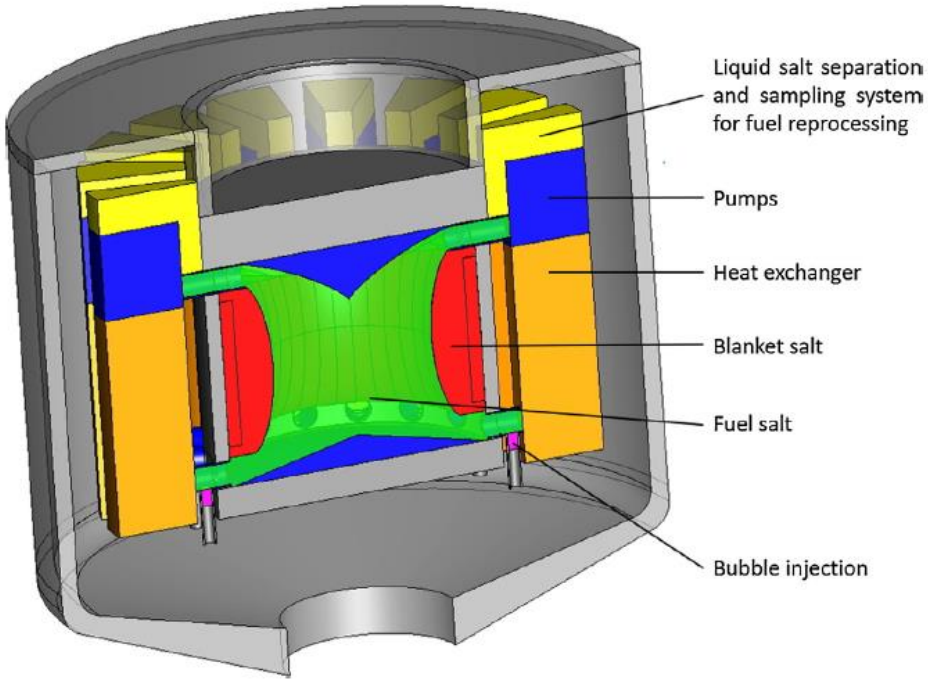

Figure 3-8 Schematic view of the MSFR fuel circuit [41]

ULSAN NATIONAL INSTITUTE OF SCIENCE AND TECHNOLOGY

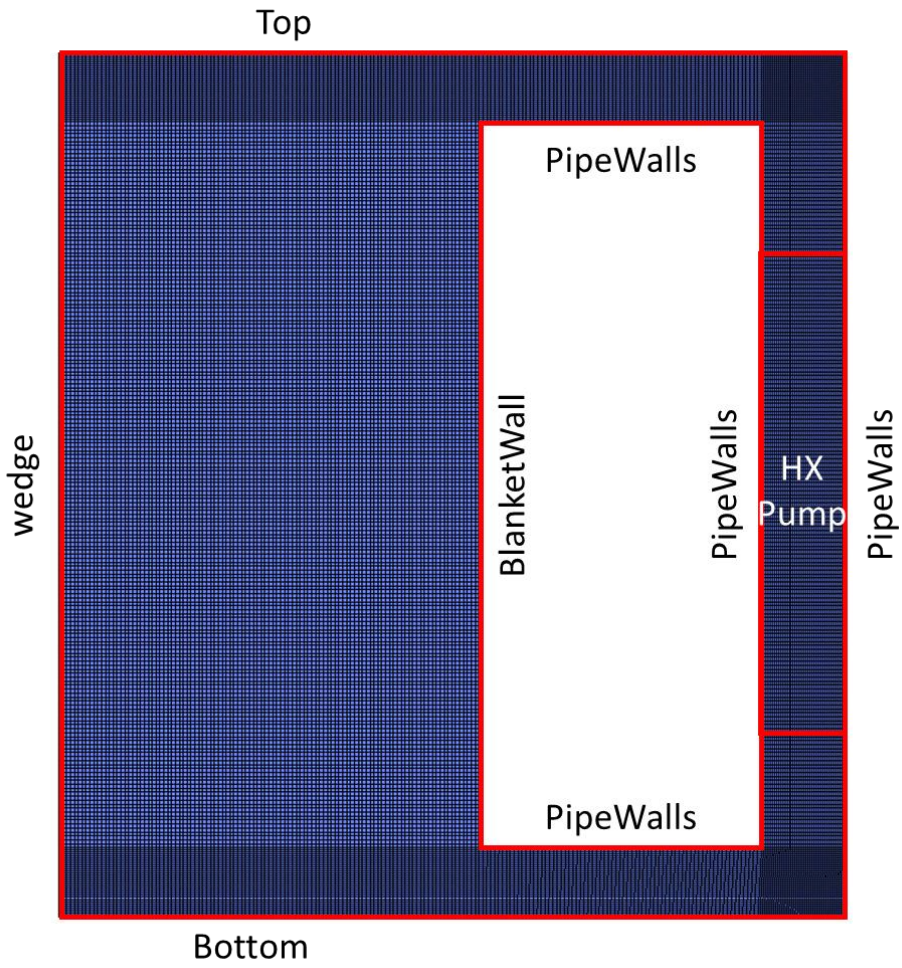

Figure 3-9 Grid configurations of 2D simplified MSFR primary loop simulation

ULSAN NATIONAL INSTITUTE OF SCIENCE AND TECHNOLOGY

Table 3-9 Boundary conditions of primal fields of 2D simplified MSFR loop

Variables	pipeWalls	BlanketWall	Top/bottom	Front/back
ϕ	albedoBC (γ=0.1)	albedoBC (γ=0.066)	albedoBC (γ=0.058)	Wedge
U	noSlip	noSlip	noSlip	
T	zeroGradient	zeroGradient	zeroGradient	
p_rgh	fixedFluxPressure gradient 0	fixedFluxPressure gradient 0	fixedFluxPressure gradient 0	
c_i	zeroGradient	zeroGradient	zeroGradient	
d_i	zeroGradient	zeroGradient	zeroGradient	

Table 3-10 Boundary conditions of adjoint fields of 2D simplified MSFR loop

Variables	pipeWalls	BlanketWall	Top/bottom	Front/back
ϕ^*	albedoBC (modified)	albedoBC (modified)	albedoBC (modified)	Wedge
T^*	zeroGradient	zeroGradient	zeroGradient	
c_i^*	zeroGradient	zeroGradient	zeroGradient	
d_i*	zeroGradient	zeroGradient	zeroGradient	

ULSAN NATIONAL INSTITUTE OF
SCIENCE AND TECHNOLOGY

At first, primal solution of the system is calculated with *msrAdjointFoam* solver. Figure 3-10 shows the steady state behavior of temperature, velocity, prompt heat source and decay heat source. Figure 3-11 to Figure 3-14 shows the primal and adjoint solutions of neutron flux, temperature, delayed neutron precursor group 1 to 8, and decay heat precursor group 1 to 3. Since the simulation domain consists of the rectangular loop having a corner at each part, several recirculation zones of the velocity field are formed near the wall, top and bottom center of the core, and the hot leg and cold leg entrance corner. Especially for the largest recirculation zone near core wall, temperature is the highest due to the less heat removal from the fuel salt flow compared to the relatively large power generation over there. Due to the fact, the strong negative feedback due to the expansion of the fuel salt as well as the Doppler effect modeled by the temperature dependencies of the nuclear data is inserted and then the distribution of the prompt heat generation rate follows the temperature profile. The delayed neutron precursors and the decay heat precursors are accumulated at the near wall region of the core and the top and bottom part at the core center region due to the velocity field distribution, balanced with the decayed and produced from the neutron flux distribution.

These features indicate the necessity of the Multiphysics approach for the liquid fuel molten salt reactor, especially for the thermal-hydraulic characteristics. When it comes to analyze the system behavior, the maximum temperature and the power distribution of the fuel salt is highly dependent on the velocity field and it really determines whether this design of the system is safe or not. In other words, the safety of the reactor design might be misinterpreted according to the Multiphysics modeling for the liquid fuel salt. Therefore, integrated analysis including primal solution as well as its sensitivity at the certain condition is required not only with the system analysis but also with the sensitivity analysis with *msrAdjointFoam* solver.

ULSAN NATIONAL INSTITUTE OF
SCIENCE AND TECHNOLOGY

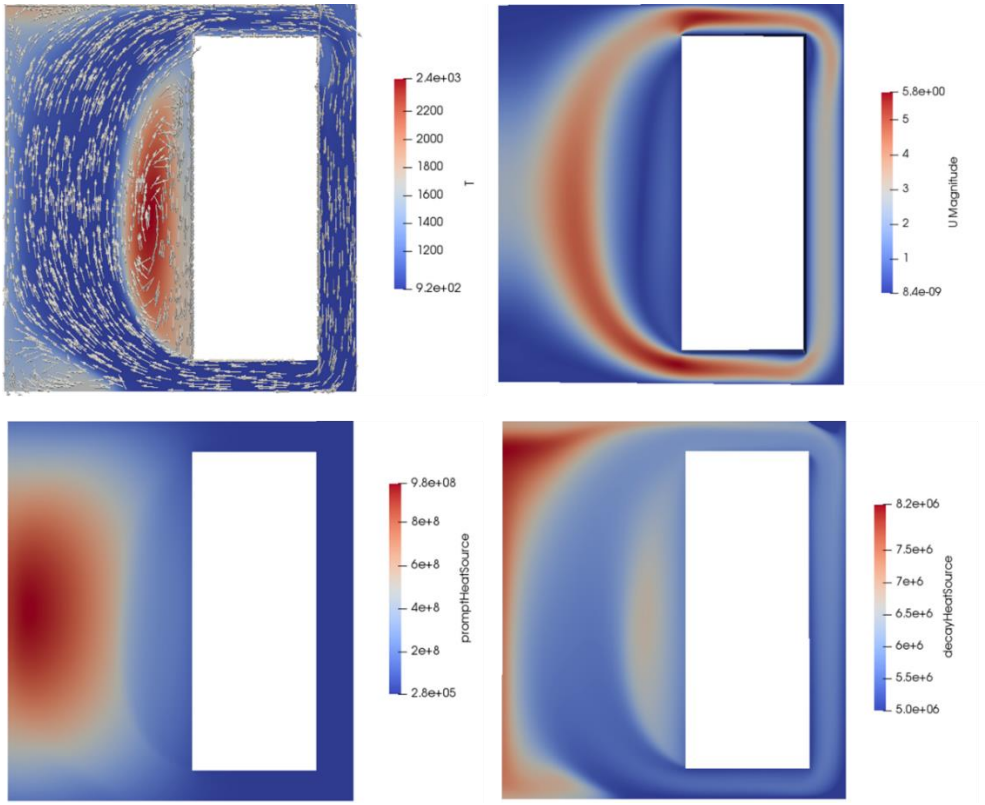

Figure 3-10 Distribution of temperature, velocity, prompt heat source and decay heat source

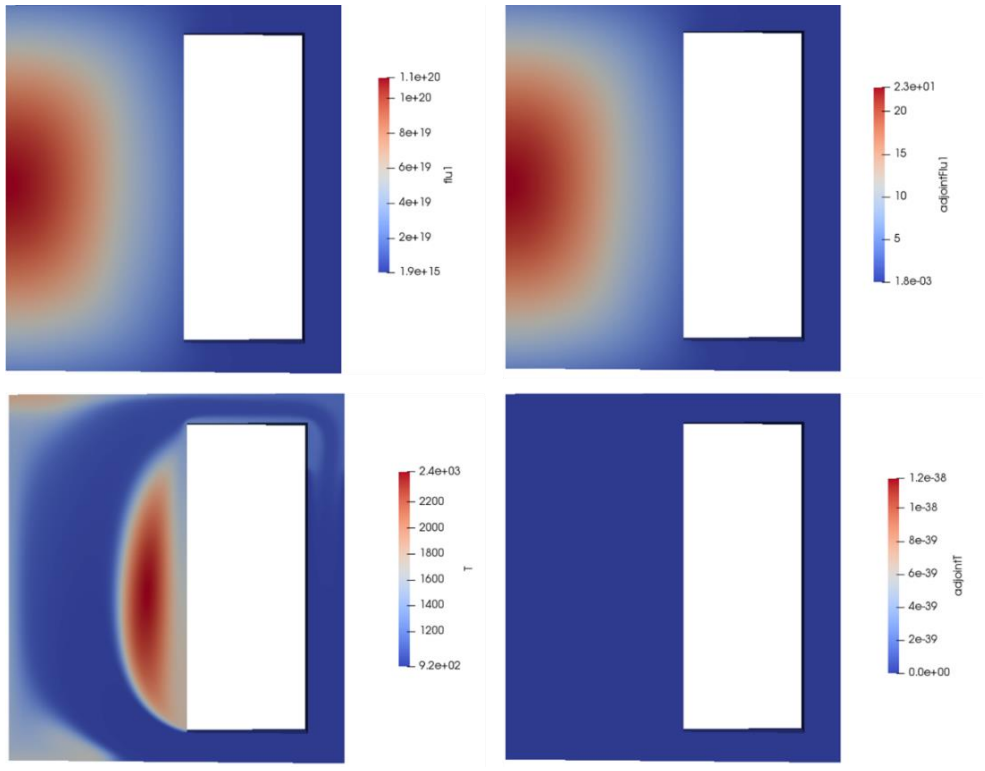

Figure 3-11 Primal and adjoint field of neutron flux and temperature field

ULSAN NATIONAL INSTITUTE OF
SCIENCE AND TECHNOLOGY

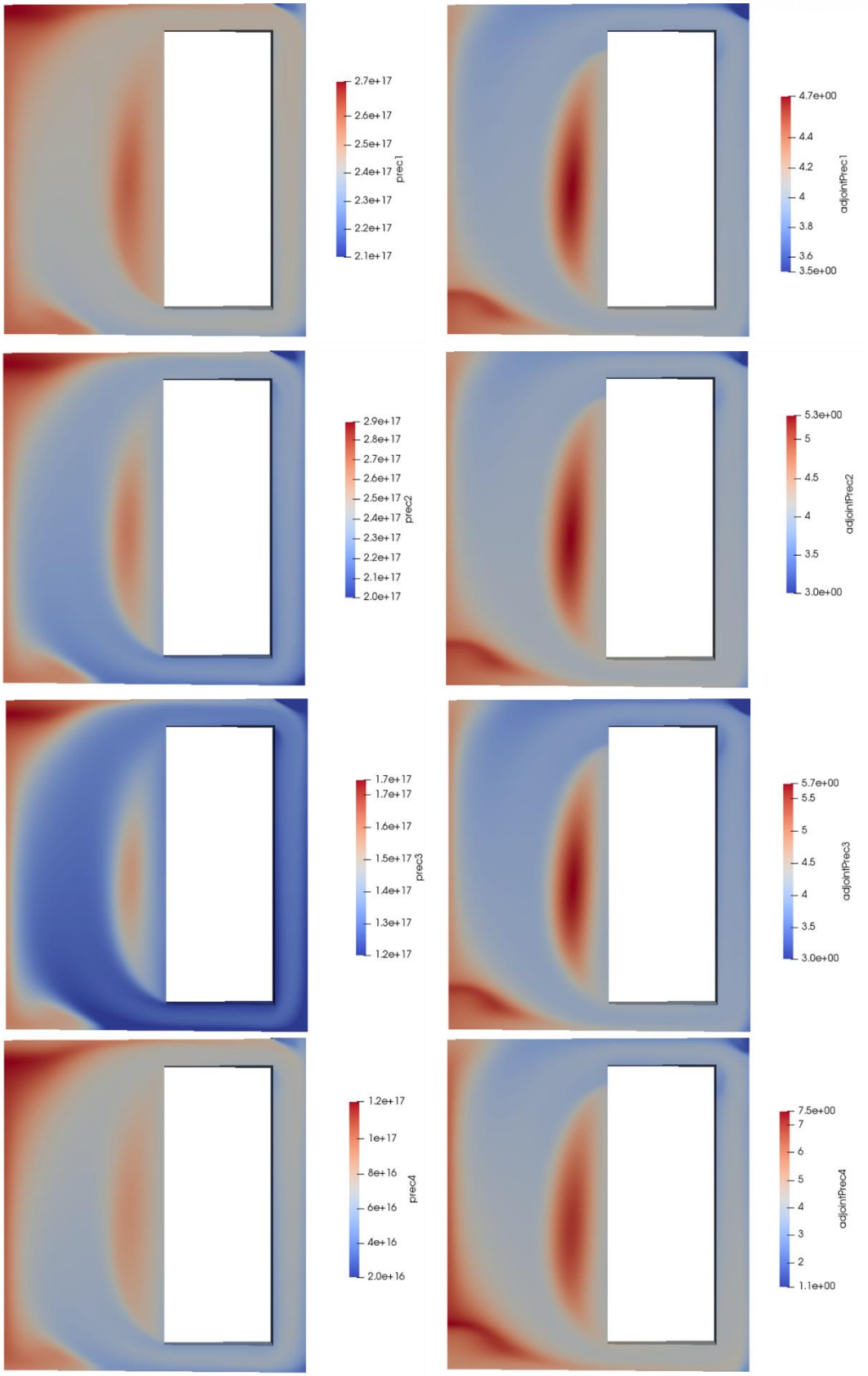

Figure 3-12 Primal and adjoint field of delayed neutron precursors group 1 to 4

ULSAN NATIONAL INSTITUTE OF
SCIENCE AND TECHNOLOGY

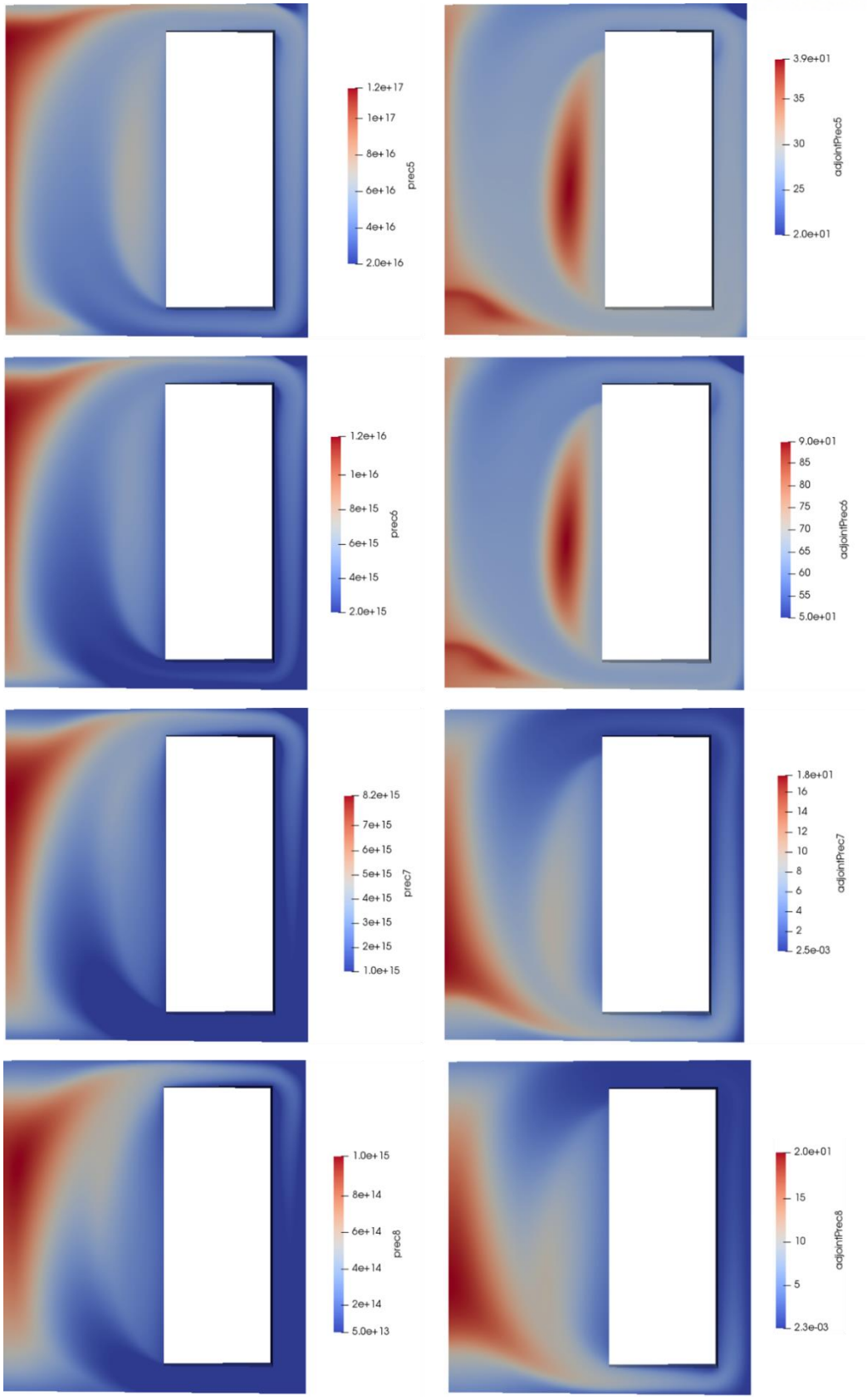

Figure 3-13 Primal and adjoint field of delayed neutron precursor group 5 to 8

ULSAN NATIONAL INSTITUTE OF
SCIENCE AND TECHNOLOGY

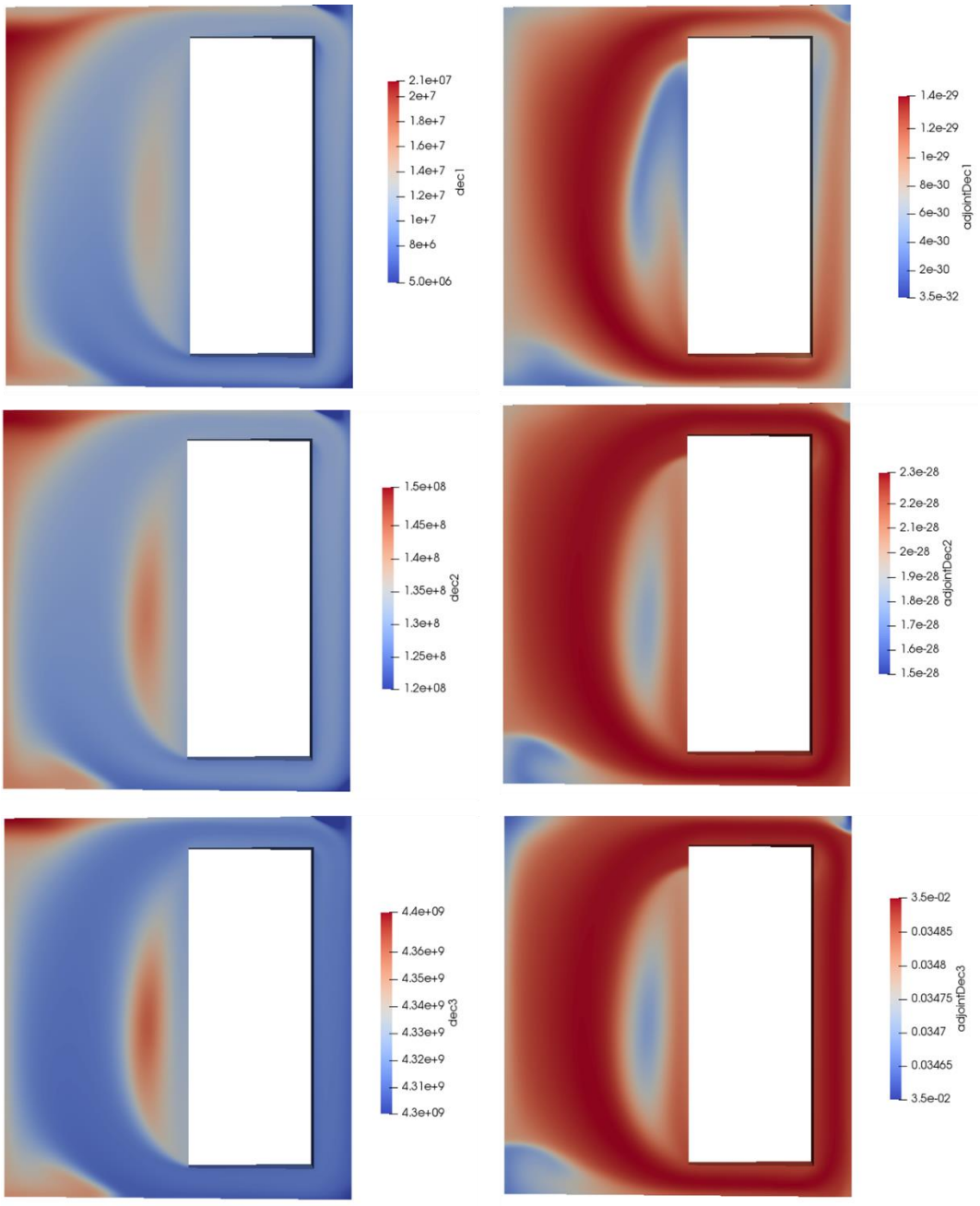

Figure 3-14 Primal and adjoint field of decay heat precursor group 1 to 3

ULSAN NATIONAL INSTITUTE OF SCIENCE AND TECHNOLOGY

Among the various types of the system response, the overall distribution of the neutron flux is selected as a representative system response at this time. Sensitivity of neutron flux from the parameter changes is estimated by setting proper weighting functions of P in general form of system response $R = \sum (P_i, \varphi_i)$ as follows.

$$R = (1, \phi) \text{ and } \frac{dR}{d\alpha} = (1, X) \tag{3-83}$$

According to the general expressions of adjoint boundary conditions in (3-78) and (3-80), proper boundary conditions for the adjoint sensitivity field is derived for this system response. Among them, the albedo boundary condition for the neutron flux field expressed in (3-82) is the mixed boundary condition. However, it adopts the constant value of diffusion coefficient and γ indicated in Table 3-9. Corresponding direct sensitivity field for the neutron flux is set as the zero gradient boundary condition reflecting albedo boundary condition by differentiating it with respect to the certain parameter. Therefore, the adjoint sensitivity field for the neutron flux can be expressed in the zero gradient boundary condition. The boundary conditions for the adjoint sensitivity field in this simulation, summarized in Table 3-11.

Figure 3-15 and Figure 3-16 show the distribution of the adjoint sensitivity field for each variable, X indicated in (3-83) for the system response of $R = (1, \phi)$. Each adjoint sensitivity field indicates the local importance of the system variable on the system response regardless of the parameter. Since the system response is defined as the neutron flux field, the adjoint sensitivity field of the neutron flux follows the distribution of the neutron flux of the primal solution.

ULSAN NATIONAL INSTITUTE OF SCIENCE AND TECHNOLOGY

Table 3-11 Boundary conditions of adjoint sensitivity fields of 2D simplified MSFR loop

Variables	pipeWalls	BlanketWall	Top/bottom	Front/back
X^*	zeroGradient	zeroGradient	zeroGradient	Wedge
Z^*	zeroGradient	zeroGradient	zeroGradient	
Y_i^*	zeroGradient	zeroGradient	zeroGradient	
W_i^*	zeroGradient	zeroGradient	zeroGradient	

ULSAN NATIONAL INSTITUTE OF
SCIENCE AND TECHNOLOGY

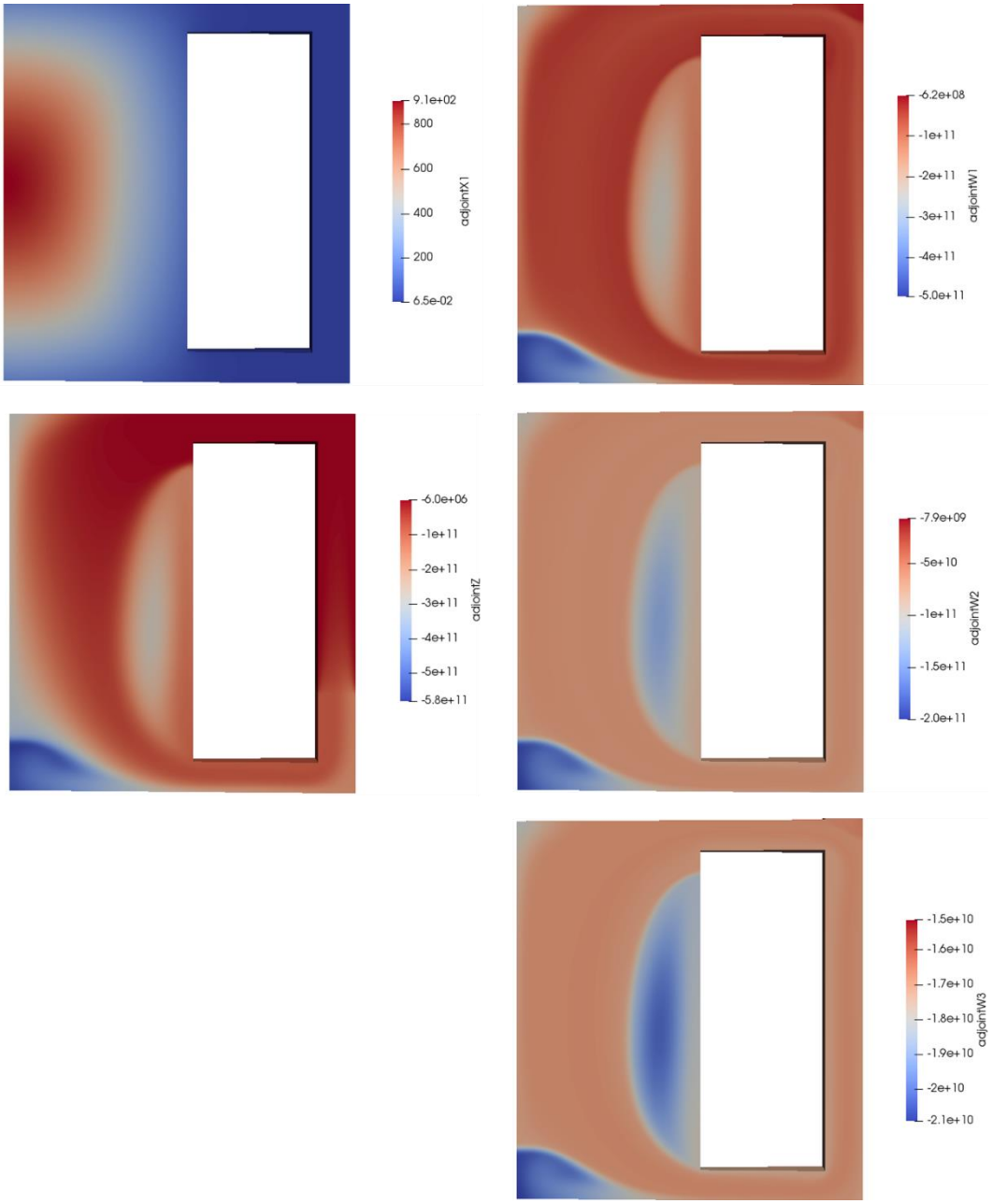

Figure 3-15 Adjoint sensitivity field of neutron flux(X_1), temperature (Z), and decay heat precursor (W_i) when R=(1,ϕ)

ULSAN NATIONAL INSTITUTE OF SCIENCE AND TECHNOLOGY

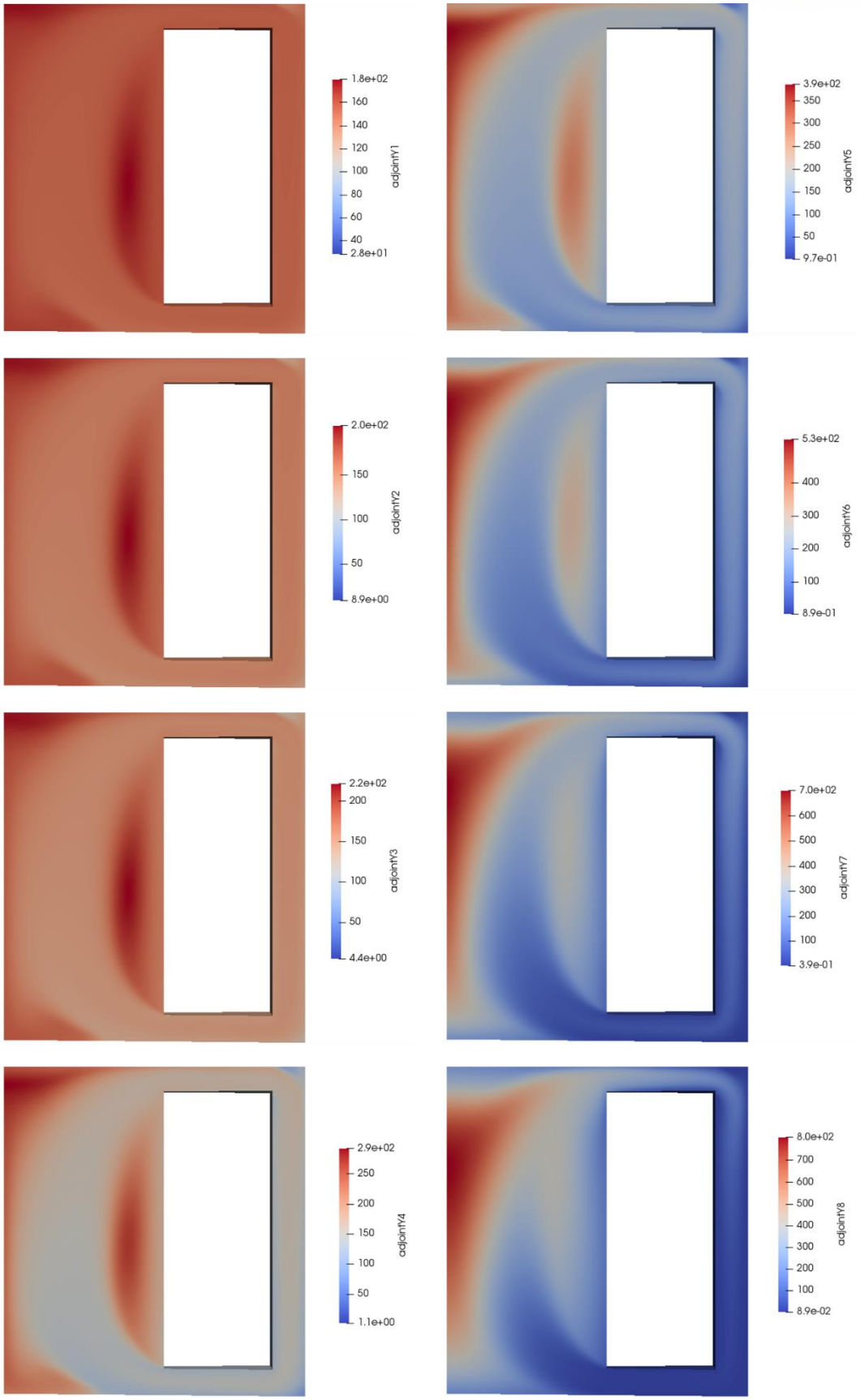

Figure 3-16 Adjoint sensitivity field of delayed neutron precursor (Y_i) when R=(1,ϕ)

ULSAN NATIONAL INSTITUTE OF SCIENCE AND TECHNOLOGY

Figure 3-17 shows the sensitivity field of the $R=(1,\phi)$ obtained from adjoint sensitivity field for the selective parameters such as cold fluid temperature of the heat exchanger (T_{cold}), fission energy generation term ($E_f\Sigma_{f\ ref}$), reference density (ρ_{ref}), temperature coefficient of the diffusion coefficient (α_D), the fraction of the 2nd group of the delayed neutron precursors (β_2), and the fraction of the 1st group of the decay heat precursors (β_{h1}), respectively. From the distribution of the dR/da field obtained from the adjoint sensitivity solution and source function C which is determined by the type of the parameter of interest, the position of highly sensitivity on the neutron flux distribution is clearly recognized. In detail, the sensitivity of the neutron flux to the cold temperature of the heat exchanger is high at the center of the core and the heat exchanger outlet region. It can be interpreted that the magnitude of the neutron flux is shifted when the small perturbation of the cold temperature of the heat exchanger. For the fission energy generation term, the bottom and the center part of the core is dependent on the neutron flux. It shows the complicated structure in the dR/da field from the combined effects of the decay heat precursors and temperature field. For the temperature coefficient of the diffusion coefficient, it affects strongly only at the core center part, and have relatively large influences on the near wall region of the core, due to the neutron flux distribution and temperature feedback on the reactivity.

Figure 3-18 summarized the magnitude of the sensitivity of R=(1,ϕ) to the all input/model parameter using *msrAdjointFoam* solver in MSFR primary loop condition. Among the all parameter, the most important parameter to determine the neutron flux distribution is the reference value of the fission energy term (SP1ref) and the temperature coefficient of the fission energy term (SP1_alphaT). It is obvious that the fission energy generation term is the parameter which represents the tightly coupled behavior between neutronics and thermal hydraulics. From Figure 3-18, it is clearly seen that which parameter is important or highly sensitive to the analysis results.

In this section, the distribution of the sensitivity field to the only several selective parameters are included due to the limited space but any sensitivity field for any system response type to any parameter of interest for the any system can be accessed with *msrAdjointFoam* solver by user's interests. Applying this solver, design work can be done reflecting the real phenomena in real condition such that

ULSAN NATIONAL INSTITUTE OF SCIENCE AND TECHNOLOGY

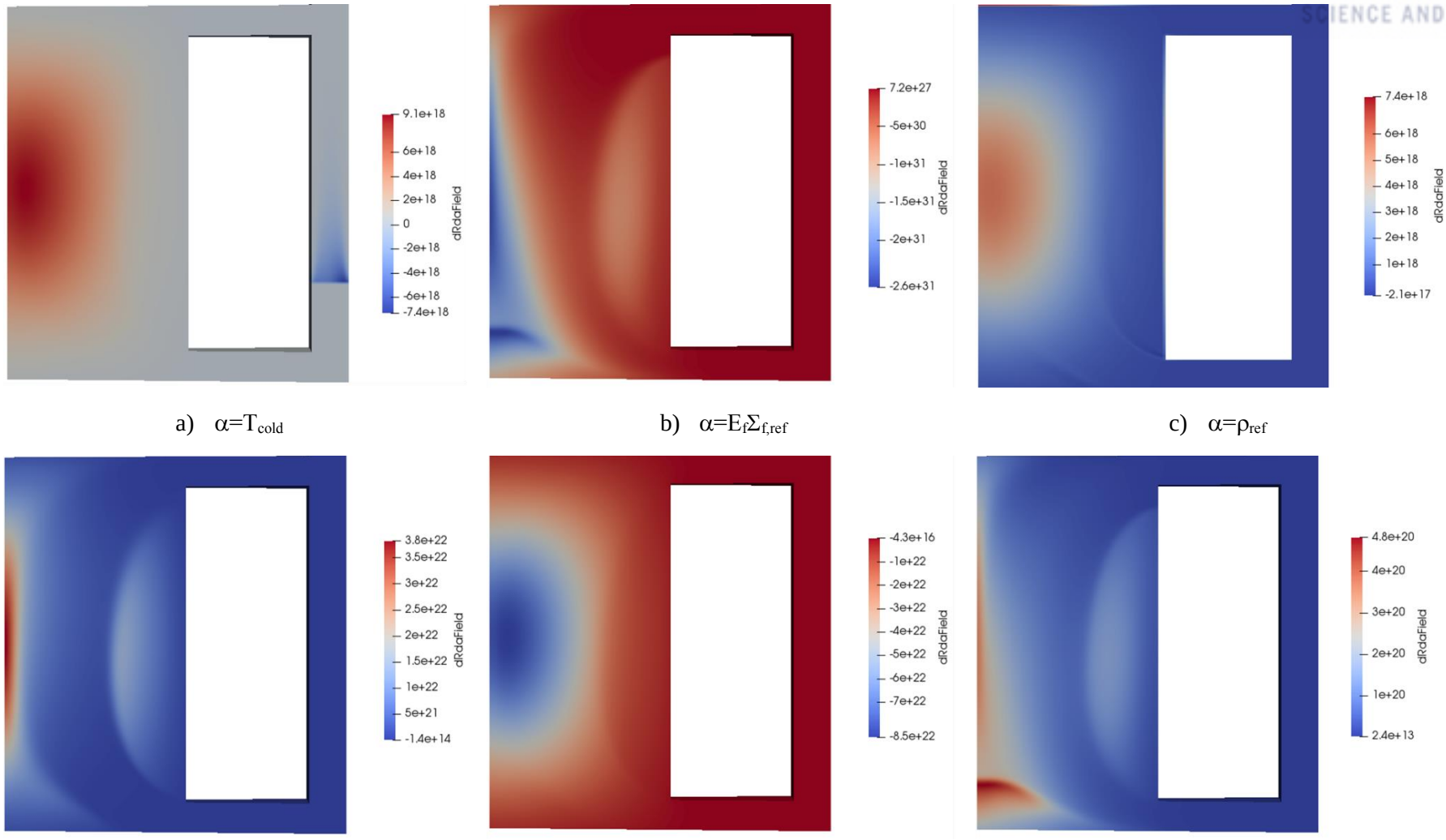

a) $\alpha=T_{cold}$ b) $\alpha=E_f\Sigma_{f,ref}$ c) $\alpha=\rho_{ref}$

d) $\alpha=\alpha_D$ e) $\alpha=\beta_2$ f) $\alpha=\beta_{h,1}$

Figure 3-17 Sensitivity of neutron flux field for 2D simplified circulating liquid fuel loop

ULSAN NATIONAL INSTITUTE OF SCIENCE AND TECHNOLOGY

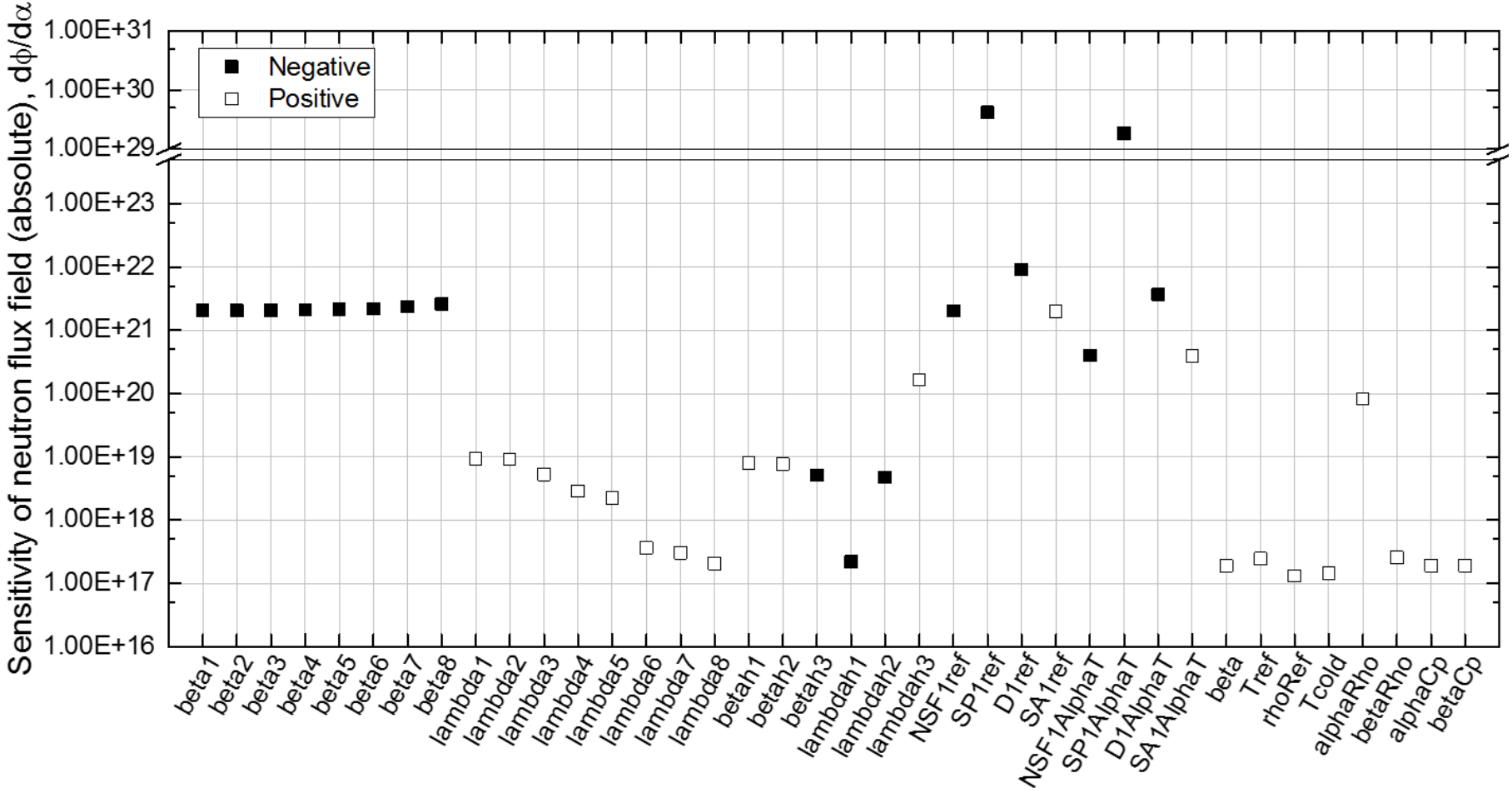

Figure 3-18 Sensitivity of neutron flux field to all parameters in 2D simplified loop condition

ULSAN NATIONAL INSTITUTE OF
SCIENCE AND TECHNOLOGY

From the sensitivity analysis results using adjoint method, changes of the state variables with small perturbation of input or model parameter can be predicted without repeating calculations. For instance, when the system response R is set as $R=(1,\phi)$, adjoint sensitivity field can represent the changes of distribution of neutron flux. Figure 3-19 shows the prediction of neutron flux field when small perturbation of parameter α; such as fission cross section, fraction of decay heat precursor group 1, fraction of delayed neutron precursor, and cold temperature of heat exchanger as follows.

In summary, with *msrAdjointFoam* solver, not only system analysis by solving Multiphysics system including neutronics, thermal-hydraulics, and precursor transport, but also sensitivity field of system response to all input/model parameters based on the adjoint formulation is performed successfully for the primary loop of liquid fueled molten salt reactor. Adjoint sensitivity field can be utilized to predict the changes of major state variables, and further design optimization process can be made to achieve the design target.

ULSAN NATIONAL INSTITUTE OF SCIENCE AND TECHNOLOGY

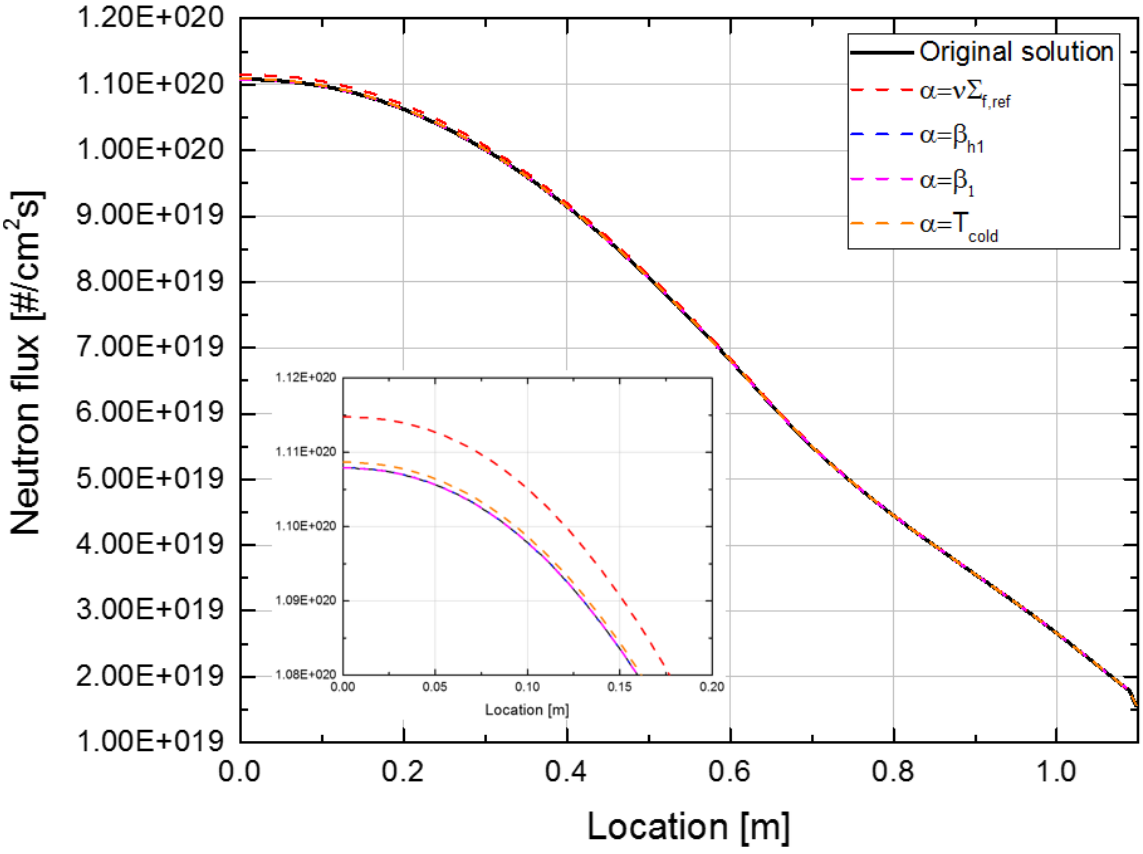

Figure 3-19 Prediction of neutron flux field perturbation based on the adjoint sensitivity solution

ULSAN NATIONAL INSTITUTE OF SCIENCE AND TECHNOLOGY

3.3 Application to New Concept of MSR: Nanofluidic Molten Salt Reactor

3.3.1 Decay Heat Removal System of MSR

The design of liquid fueled molten salt reactor, especially for the decay heat removal system (DHRS) requires a coolant having moderate heat transfer capability for the safe cooling of the fuel salt after drainage. MSBR considered the forced convective cooling channels of U tubes penetrating drain tank [42]. At that time, fluoride salt type coolant was chosen for the DHRS but due to the low level of heat removal, 40 channels are designed to achieve the target heat removal capability. For MSFR, the water cooling well for emergency drain tank cooling system is proposed [43]. For TMSR-LF, two passive systems using sodium heat pipes [44] and water-steam bayonet tubes [45] are proposed. Similar as reactor vessel cooling system for conventional nuclear reactor, AHTR [46] and FUJI [47] adopt the air-cooled natural convective system. Figure 3-20 shows the various designs of the DHRS of the existing MSR designs.

Obviously, design criteria of decay heat cooling system for the drain tank is from high temperature condition, inert reaction with fuel salt or environment, structural integrity of the system, and excellent heat transfer performance of coolant. Although subcritical state of fuel salt in drain tank, decay heat should be removed properly. At this point, selection of the proper coolant for decay heat cooling system takes an important role on the performance and the safety of the system. Table 3-12 summarizes the comparison of the coolant for DHRS of the drain tank. As discussed, same type of the molten salt is one of the most promising coolants for the drain tank assuring reliable performance. It is worthy that why ORNL selected the molten salt as a coolant. First, ORNL considered the candidates of the coolant for decay heat removal of drain tank of MSBR [4] at that moment, and they concluded to use a water-steam bayonet tube heat exchanger with many numbers of the tubes penetrating the drain tank due to its high heat transfer performance based on the phase change. However, double wall type tube adopted to prevent the thermal shock on structures deteriorate its heat transfer efficiency. They also considered the FLiBe salt and liquid metal, however, salt is not good due to the bad heat transfer characteristic as well as liquid metal that requires high cost to confine coolant in system not to leak to fuel salt as well as environment, in spite of its excellent heat transfer characteristic.

Until now, selection of the coolant for drain tank cooling system is focused on the performance viewpoint, however, fuel salt in drain tank should be cooled without any external electricity for safety. In this case, molten salt which is same as base salt of fuel salt seems to be the best option, however, it has poor heat transfer capability, as ORNL recognized. In this context, enhancement of the thermal properties of molten salt will achieve safe and reliable heat removal system by adopting nanofluid technologies.

ULSAN NATIONAL INSTITUTE OF SCIENCE AND TECHNOLOGY

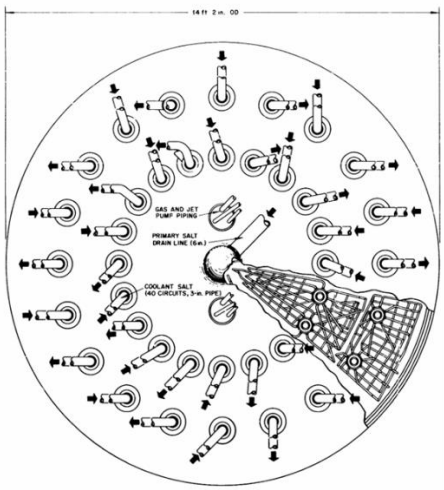

a) DHRS of MSBR (ORNL) [42]

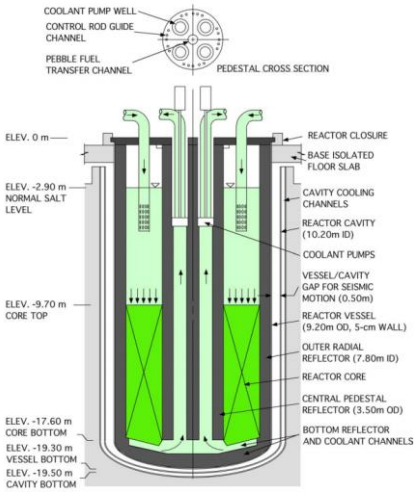

b) AHTR vessel cooling system [46]

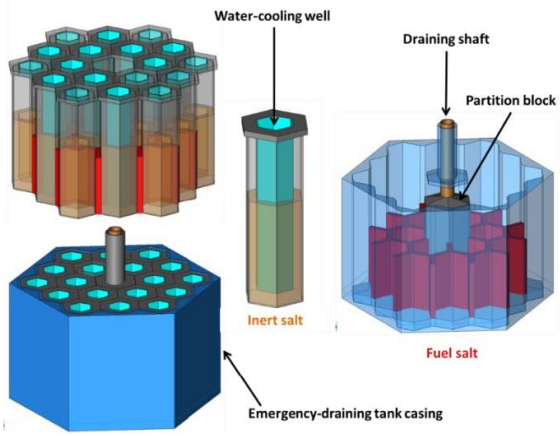

c) DHRS for emergency drain tank of MSFR [43]

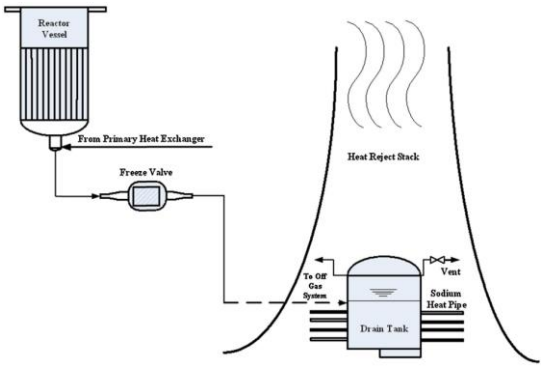

d) Passive DHRS using sodium heat pipe for TMSR-LF [44]

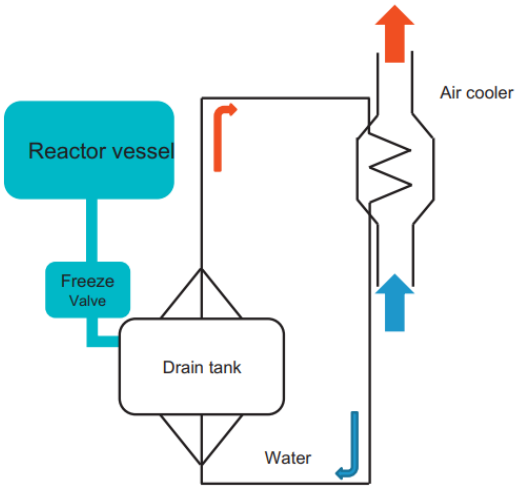

e) Passive cooling system for FUJI-233Um [47]

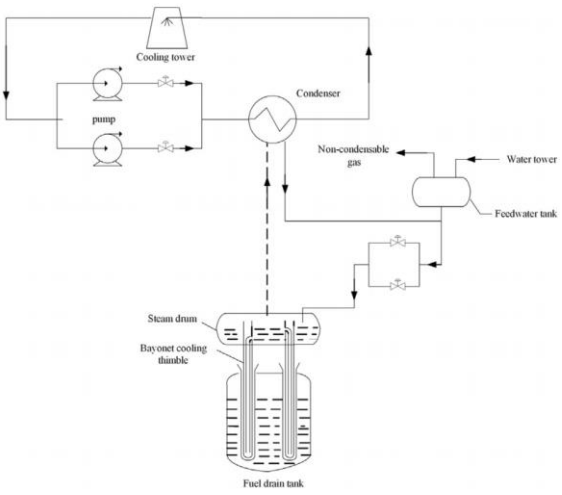

f) Passive DHRS using water-steam bayonet tube for TMSR-LF [45]

Figure 3-20 Decay heat removal systems of existing MSR designs

ULSAN NATIONAL INSTITUTE OF SCIENCE AND TECHNOLOGY

Table 3-12 Comparison of DHRS coolant for drain tank (courtesy from ORNL-4541)

Coolant	Desirable features	Undesirable features
Water-steam (phase change)	• Least danger of freezing • Lowest cost • Used in MSRE drain tank • Relatively easy to get natural circulation	• Requires double barrier tubes to prevent thermal shock on tubes • Relatively large numbers of tubes required
Liquid metals (NaK or Na)	• Excellent heat transfer capability and natural circulation	• Hard to retention in closed system (good if N_2 but worst if air)
$NaBF_4$-NaF	• Reduced thermal shock on drain tank • Relatively low viscosity	• High melting point
^7LiF-BeF_2 (FLiBe)	• No processing of fuel salt is required even in leakage • Least thermal shock on drain system • Experiences in MSRE • No volume changes on freezing	• High melting point • Very expensive
KNO_3-$NaNO_2$-$NaNO_3$	• Inexpensive • Low melting point	• Doubtful stability at high temperature and in radiation field • Salt processing on leakage might be required.

ULSAN NATIONAL INSTITUTE OF SCIENCE AND TECHNOLOGY

3.3.2 The Concept of Nanofluidic MSR and Its Design Philosophy

The nanofluid approach is not a new, but the advanced one from the initial concept of adding small solid particles into base fluid to increase thermal properties of the heat transfer fluid conventionally with aims of the development of fabrication techniques on the nano-sized particles. From much smaller particles than those of other millimeter or micro-sized particles, they can solve the problem of channel clogging and poor suspension stability [48]. Choi firstly proposed the utilization of the nanosized particles to the heat transfer fluids for the enhancement of the thermal conductivity of base fluids [49]. Although it starts the concept of homogeneously dispersed condition of nanoparticles, however, transport and distribution of nanoparticle suspended in fluid cannot be negligible.

To configure the convective heat transfer enhancement with nanofluid, Buongiorno suggested the dispersion model considering both updating thermophysical properties with nanoparticle as well as the effect of the nanoparticle and base fluid relative velocity as a perturbation of energy equation [50]. Nanoparticle concentration C, momentum conservation equation and energy conservation equations of nanofluid with velocity field V are described as follows. Subscripts B stands Brownian motion, and T means thermophoretic diffusion.

$$\rho_f\left[\frac{\partial \mathbf{V}}{\partial t}+(\mathbf{V}\cdot\nabla)\mathbf{V}\right]=-\nabla p+\mu\nabla^2\mathbf{V}+\left[(\rho_p-\rho_f)(C-C_c)-(1-C_c)\rho_f\beta(T-T_c)\right]\mathbf{g} \tag{3-84}$$

$$\frac{\partial T}{\partial t}+(\mathbf{V}\cdot\nabla)T=\alpha\nabla^2T+\frac{(\rho C_p)_p}{(\rho C_p)_f}\left[D_B\nabla C\cdot\nabla T+(D_T/T_c)\nabla T\cdot\nabla T\right] \tag{3-85}$$

$$\frac{\partial C}{\partial t}+(\mathbf{V}\cdot\nabla)C=\nabla\cdot\left(D_B\nabla C+(D_T/T_c)\nabla T\right) \tag{3-86}$$

Nanofluid properties according to the concentration of nanoparticle and their properties is summarized in (3-87) to (3-90) [51].

ULSAN NATIONAL INSTITUTE OF SCIENCE AND TECHNOLOGY

$$\rho_{nf} = (1-\varphi)\rho_{bf} + \varphi\rho_{np} \tag{3-87}$$

$$C_{p,nf} = \frac{(1-\varphi)\rho_{bf}C_{p,bf} + \varphi\rho_{np}C_{p,np}}{\rho_{nf}} \tag{3-88}$$

$$\mu_{nf} = \mu_{bf}\left[\frac{1}{(1-\varphi)^{2.5}}\right] \text{ (Brickman, 1952)} \tag{3-89}$$

$$k_{nf} = k_{bf}\frac{k_{np} + 2k_{bf} + 2\varphi(k_{bf} - k_{np})}{k_{np} + 2k_{bf} - \varphi(k_{bf} - k_{np})} \text{ (Maxwell, 1873)} \tag{3-90}$$

Molten salt and its related heat transfer systems such as solar energy storage system also adopts the nanofluid technique to improve the system efficiency due to low thermal conductivity and specific heat capacity of stable molten salt in high temperature condition [30-31]. By taking advantages of the homogeneously suspended nano-sized particles in molten salt, current molten salt reactor can enhance its safety functions in terms of passive heat removal. In this case, molten salt nanofluid can be the concept of the advanced coolant for the liquid fueled molten salt reactor; fuel salt itself with nanoparticle dispersed, just coolant for decay heat removal system of the drain tank or the mixture of nanoparticles when fuel salt drained into dump tank. Figure 3-21 shows the preconceptual design of nanofluidic molten salt reactor. Especially for the drain tank, dual type decay heat removal system is proposed; forced convective cooling channel penetrating drain tank as conventionally, and passive decay heat removal system (PDRS) pool, natural circulating driven closed loop system. To avoid the thermal shock of the drain tank vessel and possible accident from leakage of coolant, same type molten salt with fuel salt is the current candidate of the coolant for both systems. In this section, the latter option is considered and preliminary investigation on the passive decay heat removal performance by introducing nanoparticles on the fuel salt in dump tank.

ULSAN NATIONAL INSTITUTE OF SCIENCE AND TECHNOLOGY

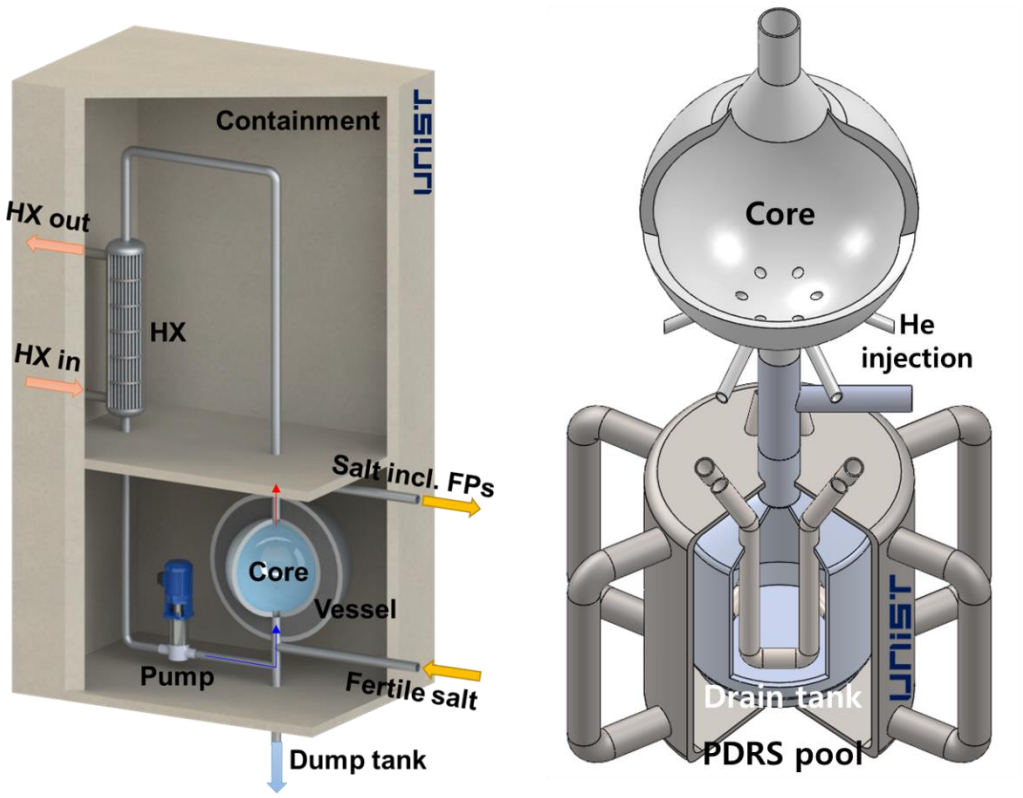

Figure 3-21 Pre-conceptual design of Nanofluidic molten salt reactor (UNIST)

ULSAN NATIONAL INSTITUTE OF SCIENCE AND TECHNOLOGY

3.3.3 Implementation of Nanofluid to Solver: nanoMsrAdjointFoam

Implementing nanofluid physics into *msrAdjointFoam* described in section 3.2, called *nanoMsrAdjointFoam* also can conduct both system analysis and model sensitivity as well. In *nanoMsrAdjointFoam*, volume fraction of nanoparticle and corresponding fluid properties are implemented as follows. Viscous heating of nanoparticles in energy conservation equation (3-64) and buoyancy effect from the particle in momentum conservation equation (3-84) are neglected, since the volumetric heat generation and temperature difference of the fuel salt condition are comparatively larger than those of the conventional nanofluid itself.

$$\frac{\partial C}{\partial t}+\left(\vec{u}\cdot\nabla\right)C=\nabla\cdot\left(D_B\nabla C+\left(\frac{D_T}{T}\right)\nabla T\right) \tag{3-91}$$

$$\rho_{nf}=\left(1-\varphi\right)\rho_{bf}+\varphi\rho_{np} \tag{3-92}$$

$$C_{p,nf}=\frac{\left(1-\varphi\right)\rho_{bf}C_{p,bf}+\varphi\rho_{np}C_{p,np}}{\rho_{nf}} \tag{3-93}$$

$$\mu_{nf}=\mu_{bf}\left[\frac{1}{\left(1-\varphi\right)^{2.5}}\right] \tag{3-94}$$

$$k_{nf}=k_{bf}\frac{k_{np}+2k_{bf}+2\varphi\left(k_{bf}-k_{np}\right)}{k_{np}+2k_{bf}-\varphi\left(k_{bf}-k_{np}\right)} \tag{3-95}$$

Including nanofluid physics in the system equations of molten salt reactor and its related systems, corresponding adjoint system and adjoint sensitivity system in steady state can be derived in same manner as described above. From the thermophoresis effect on the nanoparticle distribution, changes of corresponding adjoint and adjoint sensitivity field are made only in temperature and temperature sensitivity field. Corresponding adjoint, direct sensitivity, and adjoint sensitivity system of nanoparticle concentration is derived as (3-96), (3-97), and (3-98) respectively, where $N=\frac{dC}{d\alpha}$.

ULSAN NATIONAL INSTITUTE OF SCIENCE AND TECHNOLOGY

$$-\nabla\cdot\left(\vec{u}C^*\right)-\nabla\cdot\left(D_B\nabla C^*\right)=0 \tag{3-96}$$

$$\nabla\cdot\left(\vec{u}N\right)-\nabla\cdot\left(D_B\nabla N+\frac{D_T}{T}\nabla Z\right)+K_N\cdot Z=C_N \tag{3-97}$$

, where $C_N=\nabla\cdot\left(\frac{dD_B}{d\alpha}\nabla C\right)+\nabla\cdot\left(\frac{dD_T}{d\alpha}\frac{1}{T}\nabla T\right)$, $K_N=\nabla\cdot\left(\frac{D_T}{T^2}\nabla T\right)$

$$-\nabla\cdot\left(\vec{u}N^*\right)-\nabla\cdot\left(D_B\nabla N^*\right)=P_N \tag{3-98}$$

Corresponding adjoint, direct sensitivity, and adjoint sensitivity system of temperature field is derived as (3-99), (3-100), and (3-101) respectively.

$$-\rho C_p\nabla\cdot\left(\vec{u}T^*\right)-\nabla\cdot\left(\frac{D_T}{T}\nabla N^*\right)=0 \tag{3-99}$$

$$\rho C_p u\cdot\nabla Z+K_Z Z-\left(1-\beta_{h0}\right)E_{f1}\Sigma_{f1}X_1-\left(1-\beta_{h0}\right)E_{f2}\Sigma_{f2}X_2-\lambda_d W=C_Z \tag{3-100}$$

$$\begin{aligned}-\nabla\cdot\left(\vec{u}Z^*\right)+\nabla\cdot\left(\alpha\nabla Z^*\right)+K_Z Z^*+K_{X1}X_1^*+K_{X2}X_2^*+K_Y Y^*+K_W W^*\\ -\nabla\cdot\left(K_{X11}X_1^*\right)-\nabla\cdot\left(K_{X12}X_2^*\right)-\nabla\cdot\left(\frac{D_T}{T}\nabla N^*\right)-\nabla\cdot\left(K_N N^*\right)=P_Z\end{aligned} \tag{3-101}$$

Finally, overall system equations are derived for *nanoMsrAdjointForm* including nanofluid physics. Flowchart of *nanoMsrAdjointFoam* is summarized in Figure 3-22. To verify and validate *nanoMsrAdjointFoam* solver, benchmark simulations are performed for the predicting heat transfer characteristic of nanofluid in natural convection condition for the heated/cooled side wall in square cavity. Choi et al. conducted a numerical simulation on the water-CuO nanofluid natural convection in square enclosure with non-homogeneous dispersion model for nanofluid model and successfully validated with comparing experimental results [54]. Comparing temperature and velocity field distribution in square cavity for the same condition, *nanoMsrAdjointFoam* solver can predict the nanofluid heat transfer having well agreed results with benchmark case of Choi et al.'s work in natural convection condition with Buongiorno's dispersion model. This benchmark is conducted for the water based nanofluid case, which is well-known phenomena with extensive works already done previously. Unfortunately, there is few experimental and numerical studies for the molten salt nanofluid natural convection, this solver can be extended to the future improvement of molten salt nanofluid applications.

ULSAN NATIONAL INSTITUTE OF SCIENCE AND TECHNOLOGY

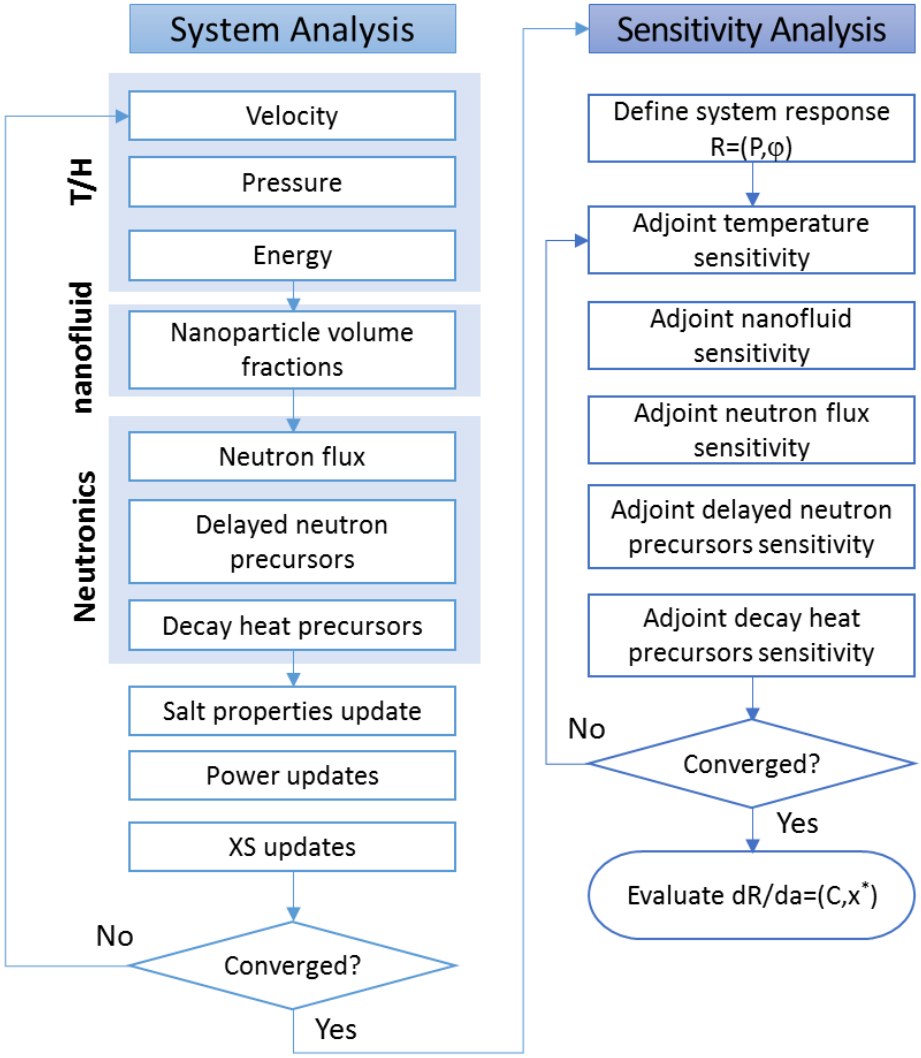

Figure 3-22 Flowchart of *nanoMsrAdjointFoam*

ULSAN NATIONAL INSTITUTE OF
SCIENCE AND TECHNOLOGY

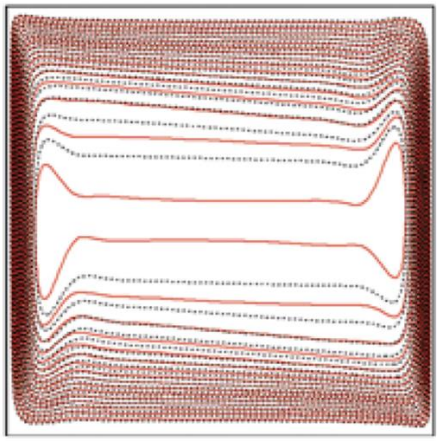

a) Streamline (Choi et al.)

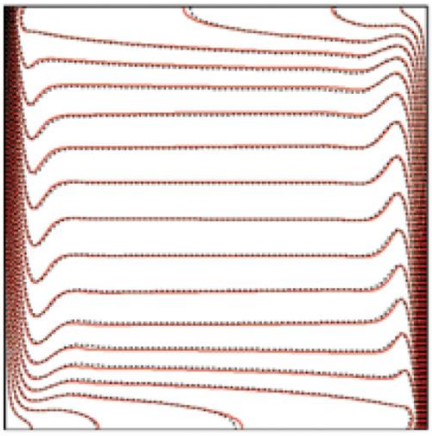

b) Temperature (Choi et al.)

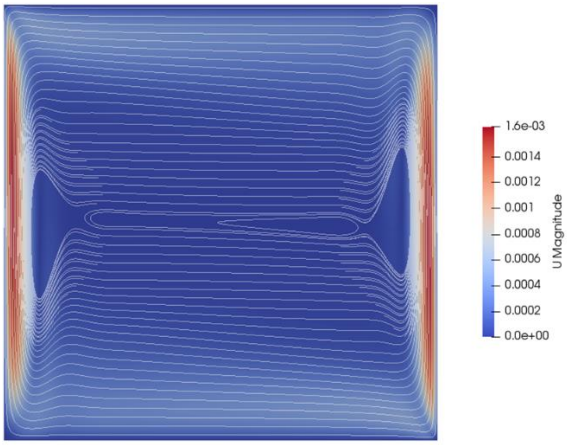

c) Streamline (present study)

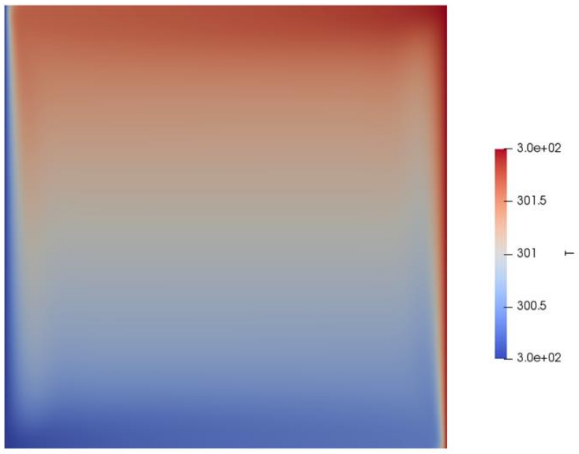

d) Temperature (present study)

Figure 3-23 Comparison of temperature and velocity field under natural convection at Ra=1×10^7 with 1 vol % CuO-water nanofluid (dashed line for nanofluid in (a) and (b))

ULSAN NATIONAL INSTITUTE OF
SCIENCE AND TECHNOLOGY

Considering drain tank filled with fuel salt, natural convection flow is formed from the temperature differences between walls and decay heat generating fuel salt inside. Except the active cooling system such as forced convection cooling channel penetrating drain tank, heat removal performance by natural convection of fuel salt in drain tank need to be evaluated for the design of safety system to have redundancy of decay heat removal function of MSR.

As a preliminary test for the case of molten salt nanofluid, a square cavity filled with fuel salt and 1 vol % of Al_2O_3 particles is simulated in natural convection condition at first. Figure 3-24 shows the distribution of the neutron flux, temperature, velocity, nanoparticle concentration, delayed neutron and decay heat precursors and power generation density in case of the side walls-cooled square cavity filled with fuel salt having 5 MW heat generation with 1 vol % of Al_2O_3 nanoparticle. Due to the natural circulation flow structure; upward flow at center and downward flow at near the side wall region, and two large dominant recirculation flow for the both half of cavity, and transportation of delayed neutron and decay heat precursors along flow structure gives the power distribution is little bit distorted to the top part. For the distribution of nanoparticle, it gets more dominant influences on the velocity field than thermophoresis or Brownian diffusion. It indicates that controlling velocity field by design optimization process would have significance on the performance. For instance, enhancement of heat transfer at the adjacent wall region with concentrating nanoparticles over there takes a important role with increasing thermal conductivity.

ULSAN NATIONAL INSTITUTE OF SCIENCE AND TECHNOLOGY

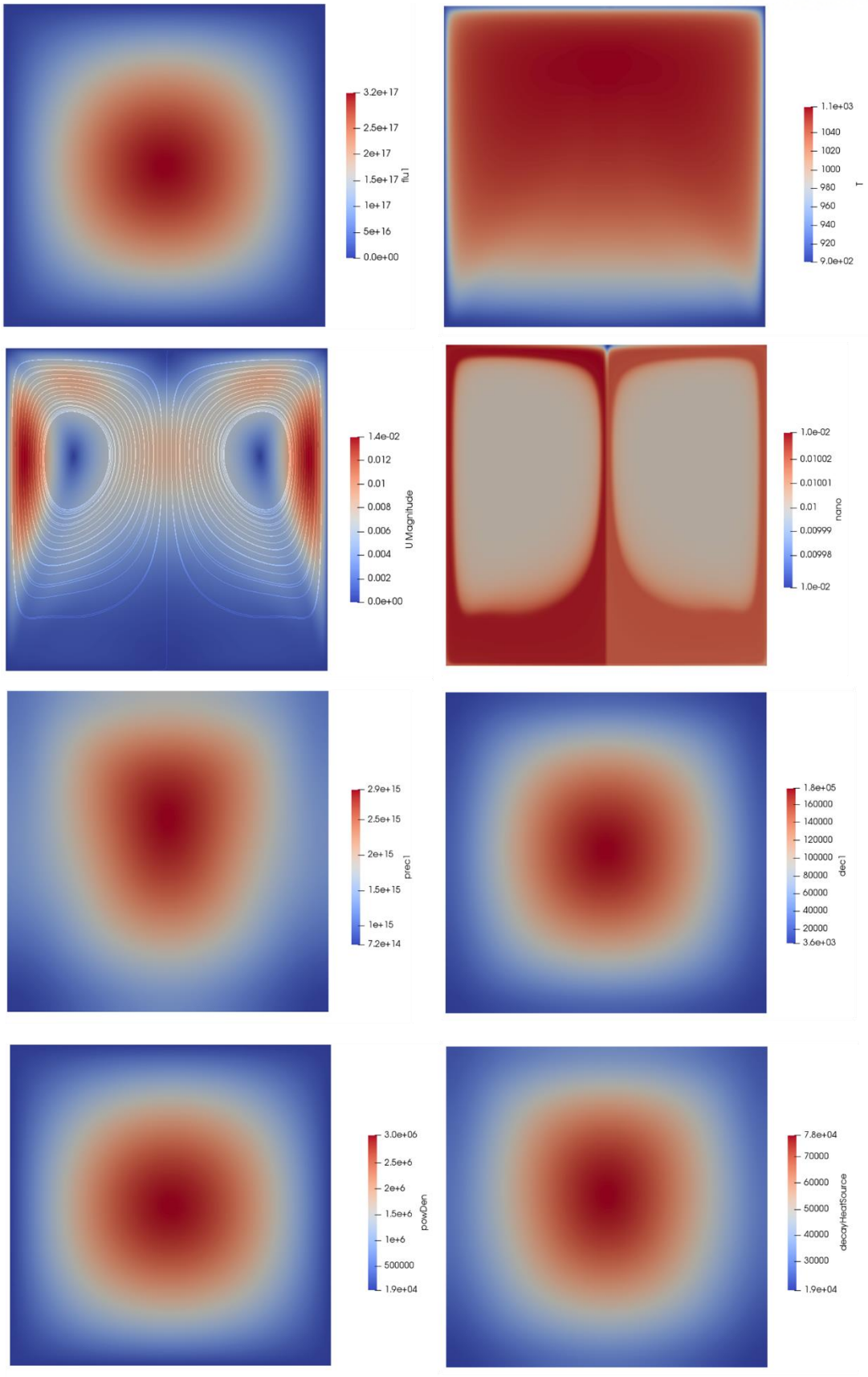

Figure 3-24 Test simulation of square cavity drain tank filled with fuel salt of 5 MW_{th} heat generation with 1 vol % Al_2O_3 nanoparticle

ULSAN NATIONAL INSTITUTE OF SCIENCE AND TECHNOLOGY

3.3.4 Assessment of Decay Heat Removal Capability of Nanofluidic MSR

As mentioned, the concept of the nanofluidic MSR adopts the any type of the molten salt nanofluid as an advanced coolant. The most feasible option for nanofluidic MSR at this moment is the combination of the liquid fuel which is prepared by the eutectic formation of the fuel material with molten salt as conventional way for the primary loop and the coolant of the molten salt nanofluid for the decay heat removal system. Due to the bad thermal properties and high operation temperature of the general molten salt system, consideration of the nanoparticles to enhance the thermal properties can be a reasonable option not to consider the additional protection or other treatments for operating related system. In this section, heat transfer system for the drain tank filled with fuel salt drained from the core with dispersed nanoparticles are considered as a preconceptual design of the passive decay heat removal system and its performance is investigated using extended solver of integrated Multiphysics solver.

To assess the passive decay heat removal performance on the natural circulation flow of fuel salt, *nanoMsrAdjointFoam* solver is used. Natural circulation loop consists of the drain tank, hot leg, cold leg and heat exchanger part. In this case, heat exchange part is modeled by introducing uniform volumetric heat removal term in energy conservation equation in given position. With thermal center height difference, buoyancy on the fuel salt drives the natural circulation flow inside loop. Target system of the drain tank is MSBR drain tank with fuel salt volume of 48.705 m^3 and steady state decay heat generation of 18 MW_{th}. Combined with active decay heat cooling system such as cooling channels of forced convection penetrating drain tank, 5 MW is the target heat removal rate for this system. To improve the performance, nanoparticles with several volume percent mixed is considered by better thermal performance of molten salt. Figure 3-25 shows the simulation domain of drain tank natural circulation loop. Table 3-13 shows the specifications of the PDHRS drain tank loop and simulation conditions.

ULSAN NATIONAL INSTITUTE OF
SCIENCE AND TECHNOLOGY

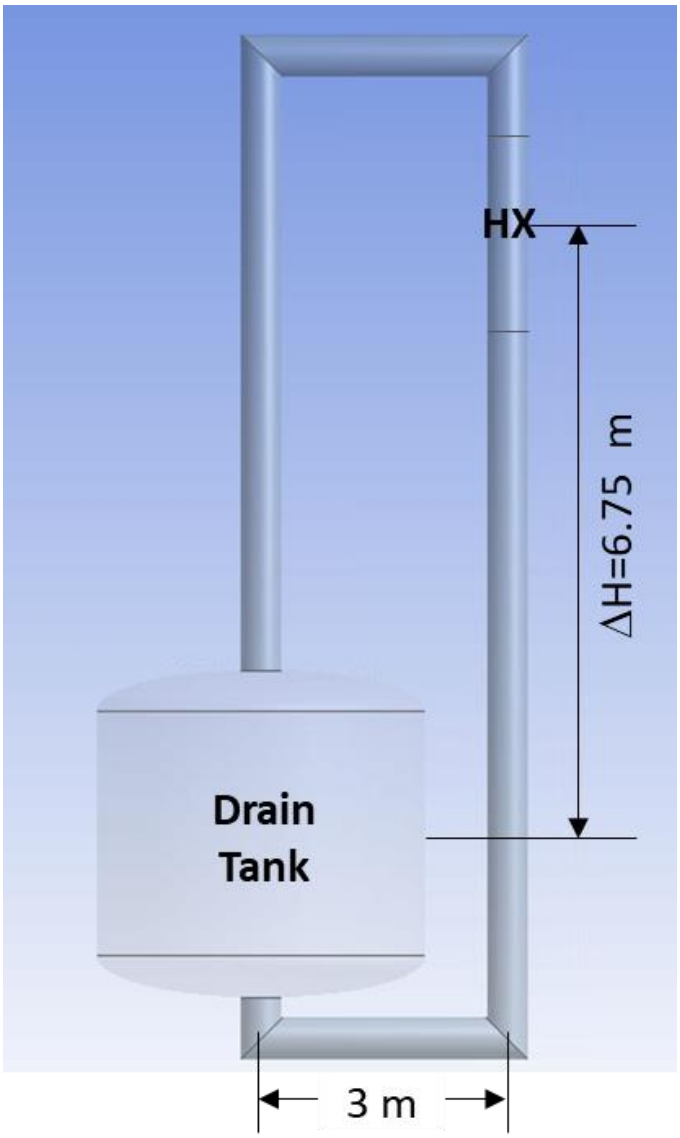

Figure 3-25 Natural circulation loop as a decay heat removal system of drain tank

ULSAN NATIONAL INSTITUTE OF SCIENCE AND TECHNOLOGY

Table 3-13 Specifications of preconceptual design of DHRS for drain tank

Parameter	Value
Fuel salt	$LiF\text{-}BeF_4\text{-}^{235}UF_4$
Target heat removal capacity	5 MW
Loop total volume	51.190 m^3
Drain tank volume	46.081 m^3
Tube diameter	0.6 m
Thermal center height difference	6.75 m
Nanoparticles	Alumina (Al_2O_3, 25 nm) 2 vol % (ρ=3970 kg/m^3, C_p=765 J/kg K, k=40 W/mK)
Heat exchanger	Uniform volumetric heat removal

ULSAN NATIONAL INSTITUTE OF SCIENCE AND TECHNOLOGY

Figure 3-26 and Figure 3-27 show the primal solution of velocity, temperature and flux and delayed neutron precursor and corresponding adjoint solution in the decay heat removal system of drain tank in steady state with heat generation of 5 MW_{th}. Most of the heat is generated in drain tank, and due to the temperature differences between heat exchanger and drain tank, natural circulation flow is formed. Due to this flow pattern, delayed neutron and decay heat precursor is accumulated at the bottom side of the drain tank, and it influences overall neutron flux distribution. Corresponding adjoint solution of neutron flux and delayed neutron precursor, which indicates the importance of the neutron flux is also dependent on the overall flow field inside loop as well.

Based on the primal and adjoint solution, adjoint sensitivity field is obtained for the system responses to predict the neutron flux and temperature field Figure 3-28 shows the adjoint sensitivity field of the system response R=(1,T) the $\alpha=\nu\Sigma_{f,ref}$, $E_f\Sigma_{f,ref}$ and α_ρ, which indicates the local sensitivity on the temperature field. Since most of fission reaction occurs n drain tank, temperature sensitivity on the $\nu\Sigma_{f,ref}$ is the highest value at drain tank according to the distribution of the neutron flux. For the parameter of reference value of fission energy generation term, it has high sensitivity of temperature at the heat exchanger as well as drain tank. Especially for the coefficient of the density, α_ρ, the highest sensitivity is at the inlet and outlet of the drain tank circulation loop. Since the driving force of the natural circulation flow is the density changes from the temperature, which follows the trend having high sensitivity at the highest and lowest temperature region. For the sensitivity on the temperature to all input and model parameters are summarized in Figure 3-29.

ULSAN NATIONAL INSTITUTE OF
SCIENCE AND TECHNOLOGY

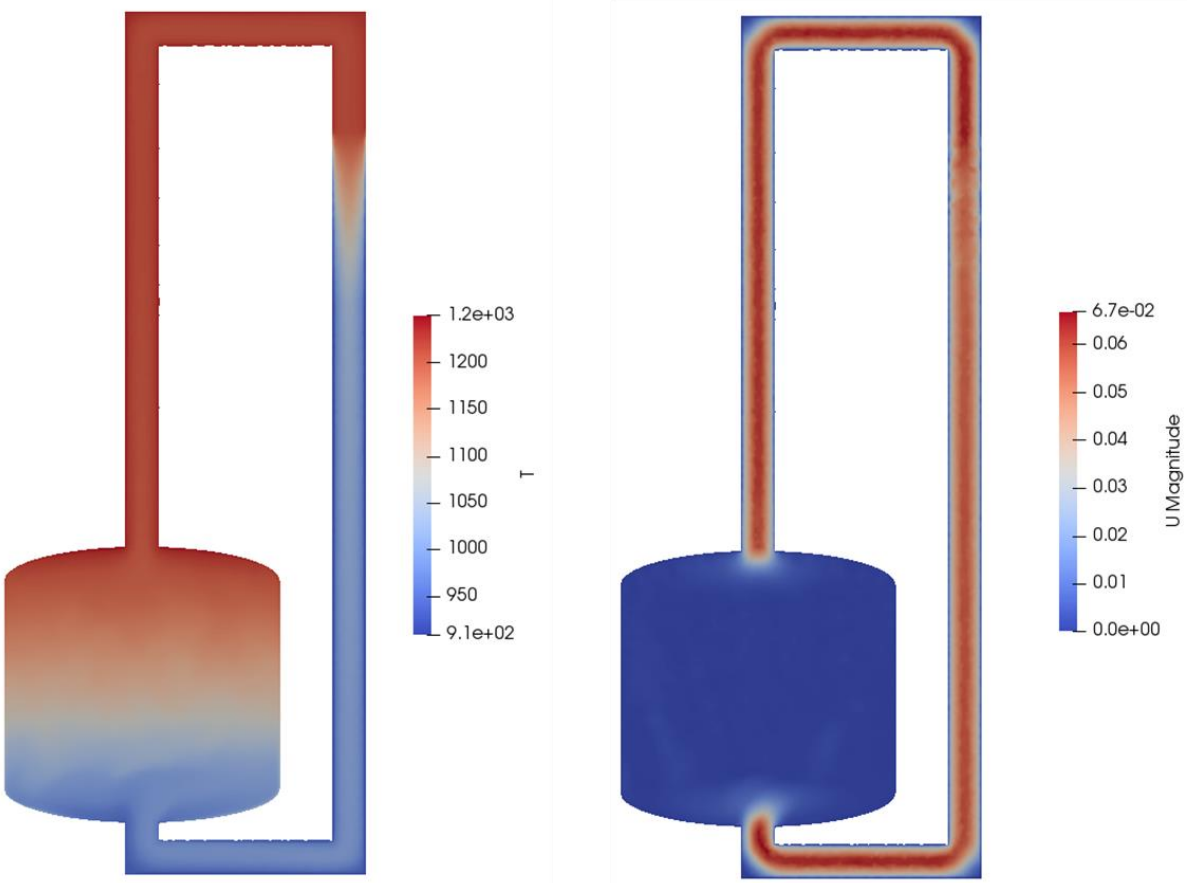

Figure 3-26 Temperature and velocity field of drain tank natural circulation loop (w/o nanoparticles)

ULSAN NATIONAL INSTITUTE OF
SCIENCE AND TECHNOLOGY

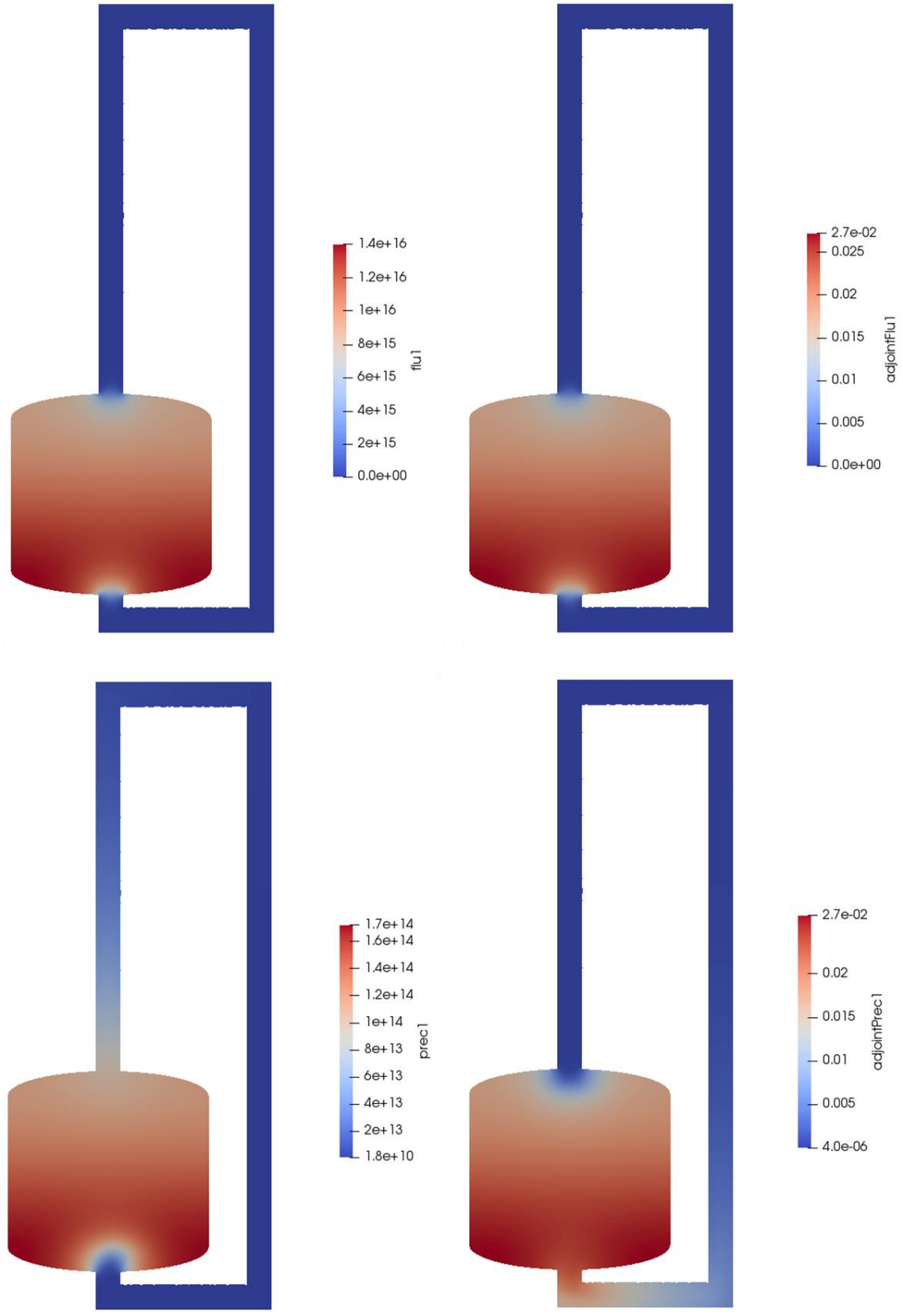

Figure 3-27 Primal and adjoint solution of neutron flux and delayed neutron precursor group 1 (w/o nanoparticles)

ULSAN NATIONAL INSTITUTE OF SCIENCE AND TECHNOLOGY

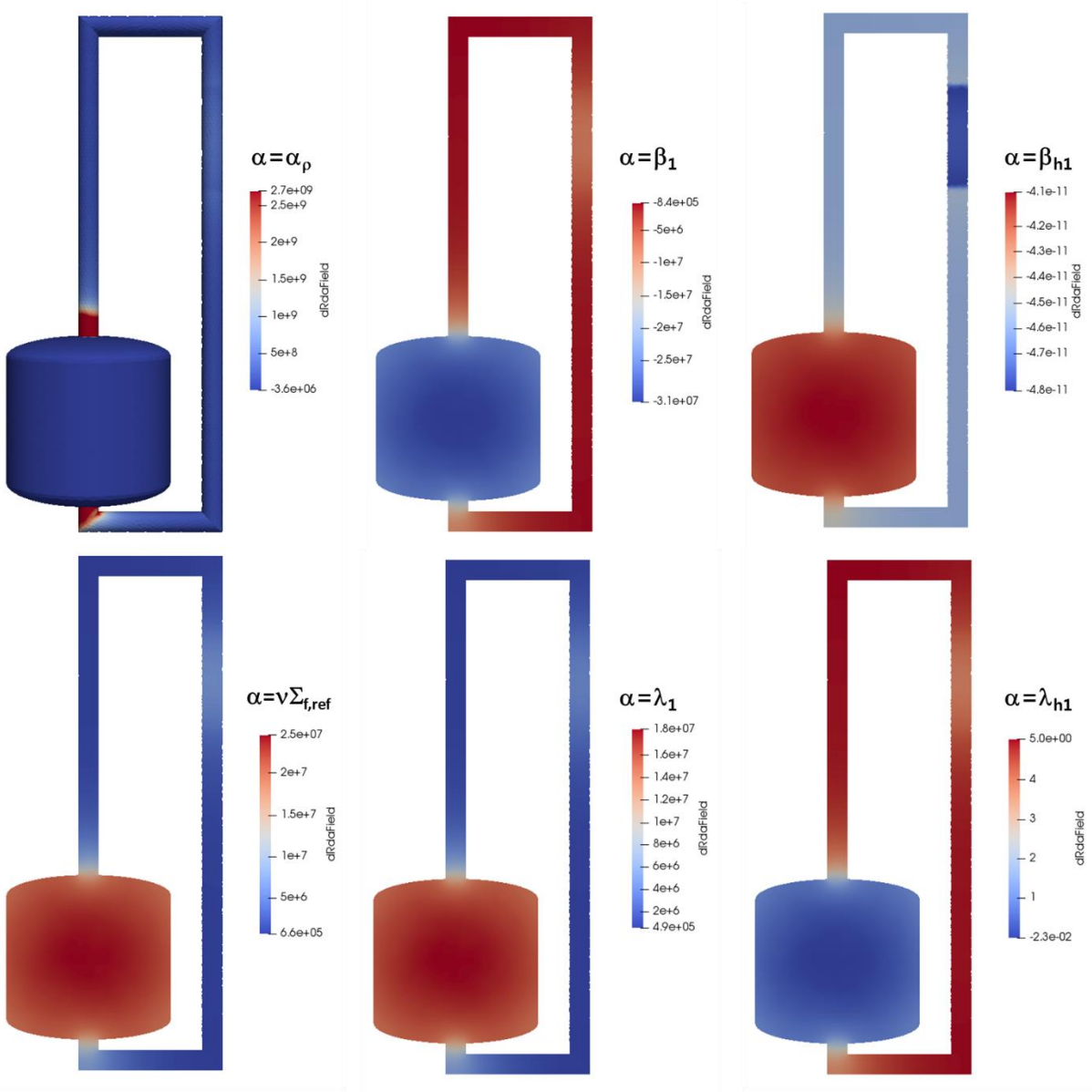

Figure 3-28 Adjoint sensitivity field of decay heat removal system (w/o nanoparticles)

ULSAN NATIONAL INSTITUTE OF SCIENCE AND TECHNOLOGY

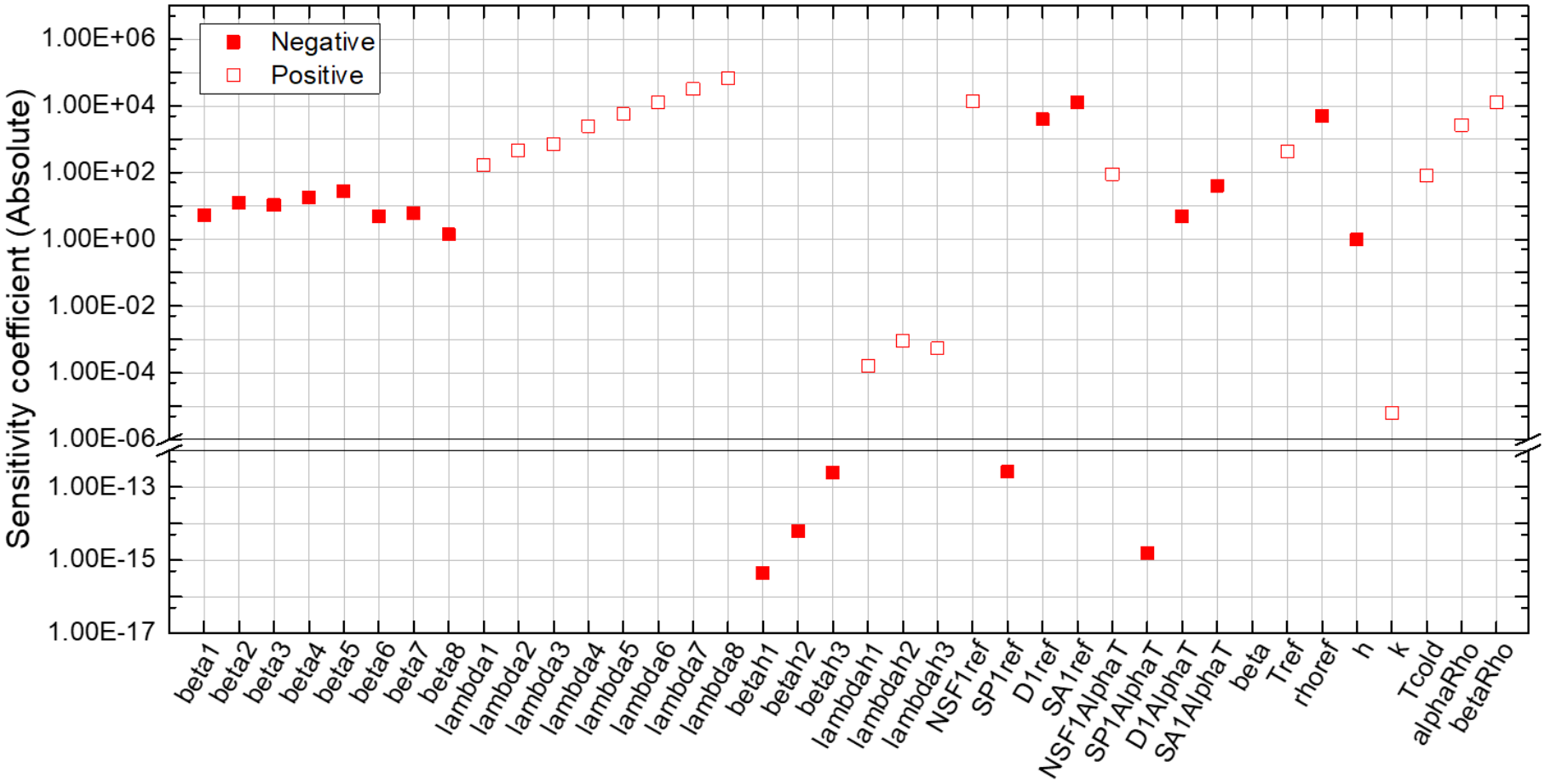

Figure 3-29 Sensitivity coefficient of drain tank natural circulation loop: R=(1,T)

ULSAN NATIONAL INSTITUTE OF SCIENCE AND TECHNOLOGY

From Figure 3-29, important variables on the temperature field among design parameters of the passive decay heat removal system with pure fuel salt are two categories; one is the kinetic constants of the precursors and the other is the thermal properties of the fuel salt. Since kinetic constants of the precursors are dependent on the fuel salt composition, performance of the decay heat removal cannot be changed in terms of design. However, other important parameters; thermal properties of fuel salt can be optimized to achieve better performance of decay heat removal system by adding small volume percent of nanoparticles to fuel salt.

By using *nanoMsrAdjointFoam* solver, natural circulation flow in drain tank loop with fuel salt added 1 vol % of Al_2O_3 nanoparticle is simulated. Figure 3-30 shows the primal and adjoint solution of the decay heat removal system of drain tank with 1 vol % of nanoparticles in fuel salt. Not much difference but reduction of overall temperature ranges in drain tank loop with better thermal properties of fuel salt is achieved. Especially for the nanoparticle distribution, nanoparticles are deposited at the bottom of the drain tank and the lower part of the channel. In terms of the heat transfer behavior on the underlying coupled physics for fuel salt with nanofluid, flow field determined by temperature field can be changed by addition of nanoparticles from enhanced thermal properties. However, deposition of nanoparticles near wall and channel provides additional resistance on the flow field, and ultimately, it affects the overall system behavior. Figure 3-32 shows the comparison of temperature distribution of fuel salt in drain tank according to the fraction of adding nanoparticles. It shows that 5 vol % addition of nanoparticles is not the best performance in decay heat removal with reduced temperature range. In this case, design optimization process can be performed by separating variables to configure each influence on the system, and it can be achieved by adjoint sensitivity method in efficient and comprehensive way.

ULSAN NATIONAL INSTITUTE OF
SCIENCE AND TECHNOLOGY

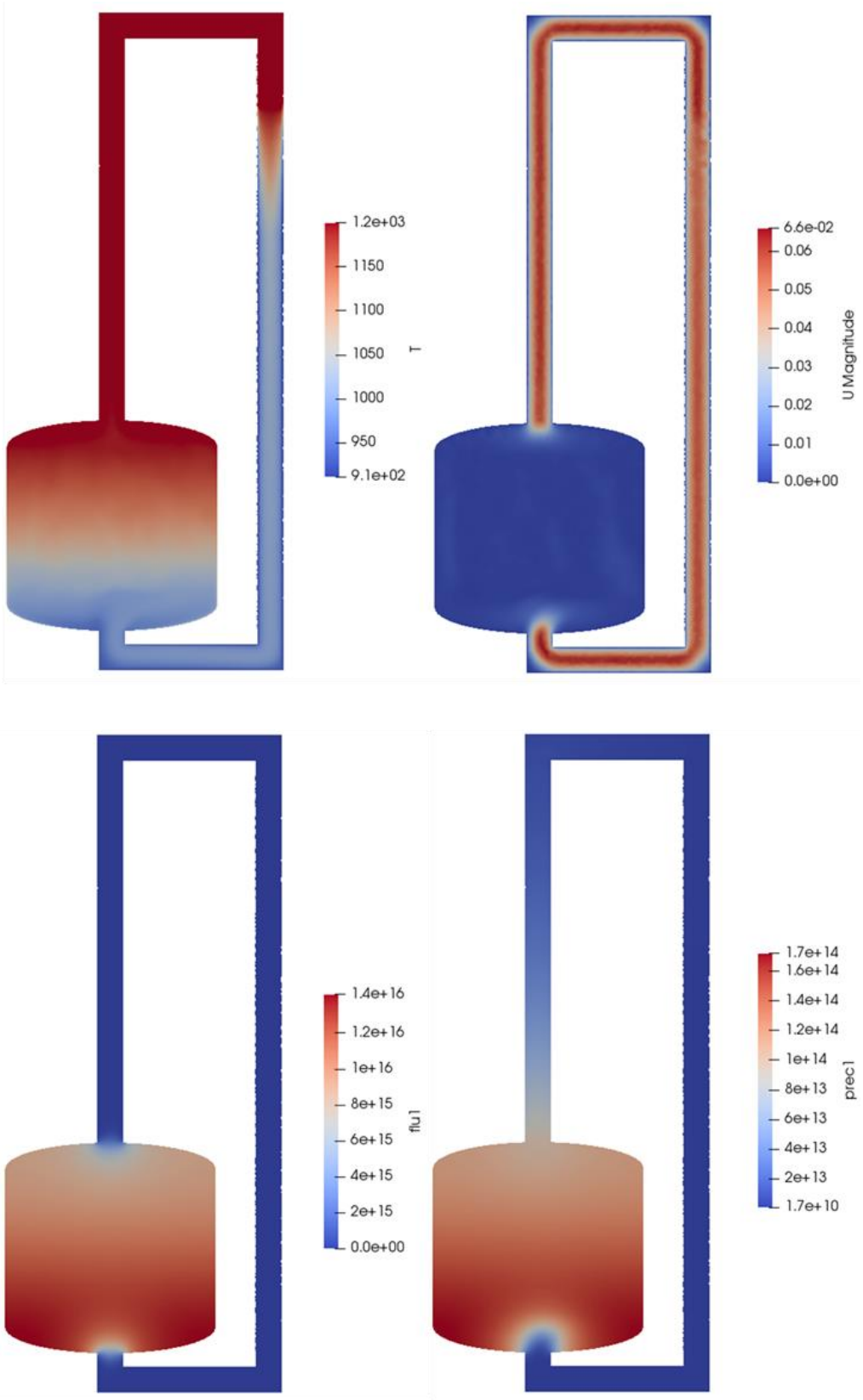

Figure 3-30 Primal and adjoint solution of neutron flux and delayed neutron precursor group 1 (w/ 1 vol % nanoparticles)

ULSAN NATIONAL INSTITUTE OF
SCIENCE AND TECHNOLOGY

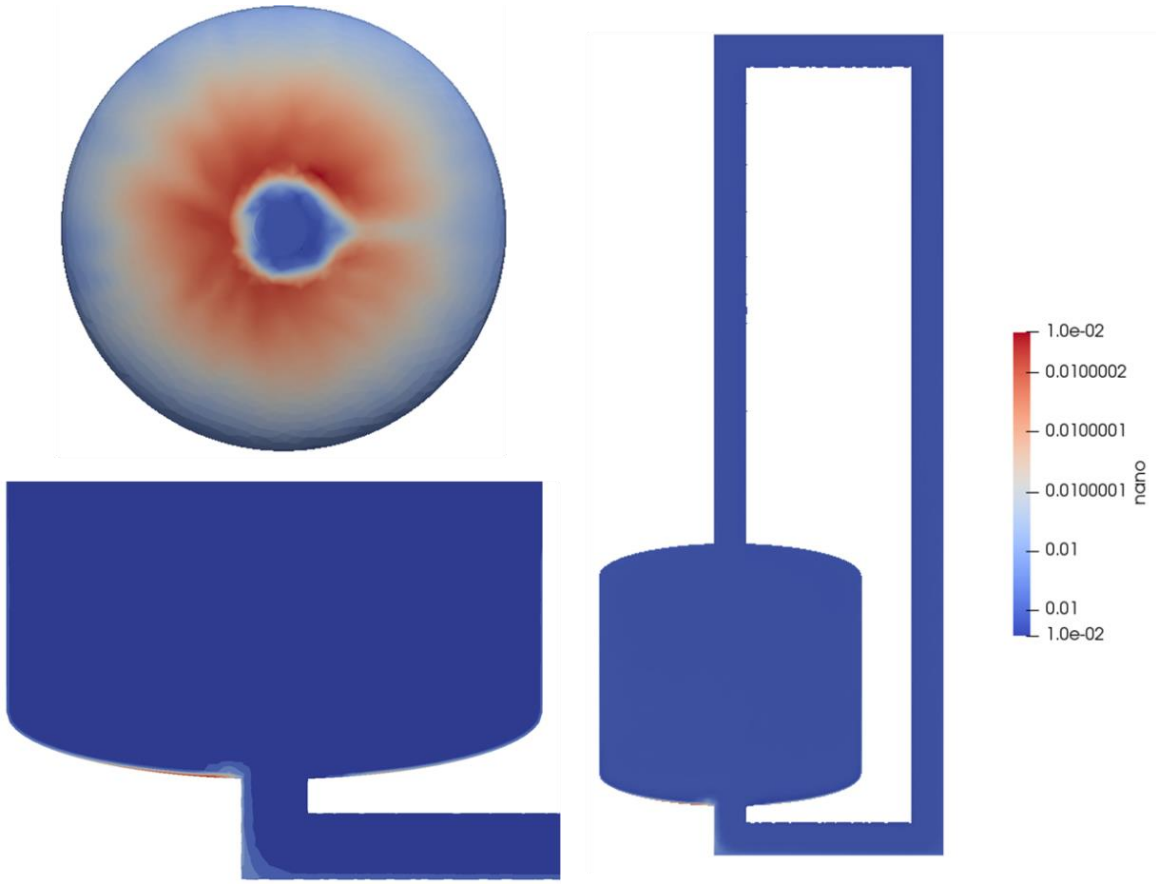

Figure 3-31 Distribution of nanoparticle inside loop (1 vol % nanoparticles)

ULSAN NATIONAL INSTITUTE OF
SCIENCE AND TECHNOLOGY

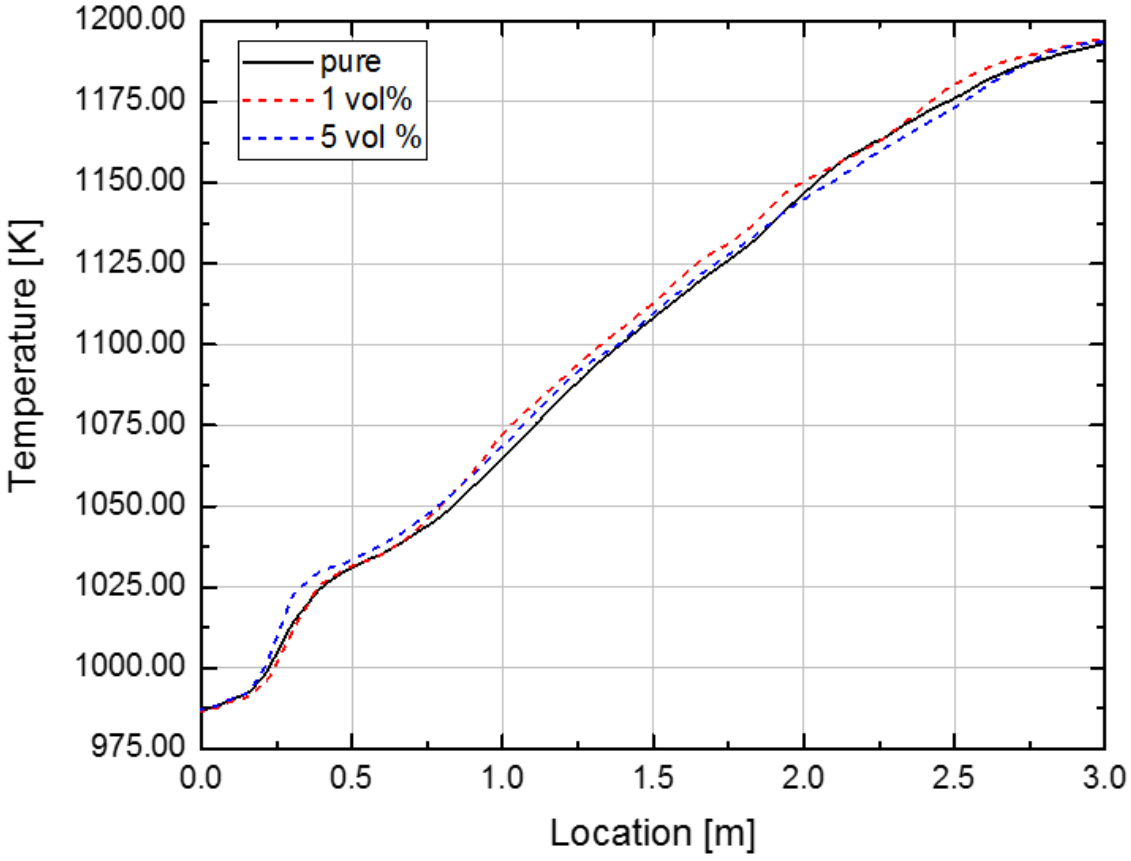

Figure 3-32 Comparison of temperature distribution of drain tank in axial direction

ULSAN NATIONAL INSTITUTE OF
SCIENCE AND TECHNOLOGY

CHAPTER 4 CONCLUSIONS AND RECOMMENDATIONS

4.1 Conclusions

4.1.1 Adjoint-based Sensitivity Analysis Method on the Multiphysics Approach

Adjoint based sensitivity analysis method is developed for the circulating liquid fuel system in steady state, which has two tightly coupled physics, i.e., neutronics and thermal-hydraulics. A set of sensitivity equation for this system is transformed into an adjoint system by the definition of adjoint operators. Then, sensitivity of system response to any parameter, defined as a sum of functionals for each variable in steady state is evaluated with corresponding adjoint solutions including all coupled effects between two physics without any assumptions. Since the derived adjoint solutions derived are independent from the parameter itself, sensitivity of system response to any parameter using adjoint method can significantly reduce computational efforts compared to recalculation. Adjoint-based sensitivity analysis method developed in this paper is expected to have a wide applicability for any Multiphysics system with saving lots of computational resources. Using adjoint based method, the changes in importance of parameter according to modeling options, the variations of sensitivity from the perturbation of parameter value, and sensitivity of various types of system responses are analyzed by means of a simplified model of the MSFR. From 1D steady state simulation results, adjoint-based sensitivity method can predict the sensitivity of any type of system responses for any parameter, in any modeling cases compared with recalculation and direct method. It is obvious that the adjoint based method can save lots of time and computational costs with large number of parameters and types of system response.

4.1.2 Development of Integrated Multiphysics Tool for Liquid fueled MSR

Based on the developed system analysis and sensitivity analysis method with adjoint method, integrated multi-physics tool for the molten salt reactor anlaysis is developed with aims of open source Multiphysics toolkit, OpenFOAM called *msrAdjointFoam*. With the adjoint-based method, the sensitivity analysis to the large number of parameters including model, properties, correlations or design value of systems for the various types of system response under interests can be conducted with good accuracy and efficiency. In addition, the influences from relationships between dependent variables and parameters can be predicted in the sensitivity analysis with adjoint-based method, as well. According to the modeling options; i.e. considering or not the dependence of nuclear data and thermophysical properties on temperature, have a significant impact on the importance of parameters

ULSAN NATIONAL INSTITUTE OF
SCIENCE AND TECHNOLOGY

on the system response. It means proper modeling is required to evaluate the sensitivity of the complex multiphysics system. Extending the design and sensitivity analysis method based on the adjoint formulation on the Multiphysics approach, application of the molten salt nanofluid is considered to enhance the performance of the passive decay heat removal system for the drain tank by natural circulation flow. Natural circulation flow with nanoparticle is the representative case of the coupled physics. In this case, separation of variables to configure each influence on the system performance is expected to help the design optimization with aims of the adjoint sensitivity method.

ULSAN NATIONAL INSTITUTE OF SCIENCE AND TECHNOLOGY

4.2 Recommendations

This work focused on the analysis and its sensitivity of Multiphysics model of the circulating liquid fuel system physically based on the adjoint sensitivity analysis procedure for the first time, and properly implemented to the *msrAdjointFoam* based on the open source Multiphysics toolkit, OpenFOAM [55]. This section discusses the future extensions and application area of the methodology on the Multiphysics approach built for the liquid fueled MSR.

First, it should be noted that the sensitivity of the system response is considered in first order, expressed in the first derivatives of the system variables on the response. For the higher order system response of interests, methodology built on the Multiphysics approach can be combined with 2nd order adjoint sensitivity analysis method developed by prof. Cacuci [56] and extended to the coupled physics system. Second, all adjoint sensitivity solutions described in CHAPTER 3 is obtained with freeze velocity field, which is calculated in primal field solver. Due to the high non-linearity of Navier-Stokes equation, adjoint and adjoint sensitivity field of momentum conservation equation is not easily obtained in conservative form, and it is not fully demonstrated yet for the single physics only. The state of the art of the adjoint technique is on the design optimization tool of aerodynamics field based on the CFD approach [39], [57]–[59]. In addition, turbulence effects on the flow of the high Prandtl number fluid such as molten salt is not also considered in this work. Since flow field governs overall system behavior on the circulating liquid fuel system, it should be carefully considered; which turbulence model, wall function, or turbulent Prandtl number (also turbulent Schmidt number) would be suitable on fuel salt system. Luzzi et al. performed the effect of the turbulence models on the analysis of circulating liquid fuel system comparing with analytical solution and commercial CFD code FLUENT, and COMSOL simulation results [60]. Combining non-conservative form of Navier-Stokes equations; i.e. incompressible Navier-Stokes equation, *msrAdjointFoam* can be extended to the design optimization tool for molten salt reactor or molten salt related systems based on the sensitivity analysis in deterministic way. Moreover, turbulence model can be also implemented based on the proper adjoint techniques for the adjoint system equations. Not only for the liquid fueled MSR, spent fuel reprocessing also requires the liquid fuel technologies for the design and operation of relative systems with comprehensive understanding of underlying physics.

In terms of molten salt nanofluid, its non-homogeneous behavior and influence on the heat transfer is still open for future research. There is few available result that investigated the influences of the distribution of nanoparticle on the heat transfer experimentally measured except Khalili et al.'s work [61], and they found that influence of the adjacent region of wall on the effect of dispersion of nanoparticle will be studied more. Bahiraei pointed out there might be another factors for particle migration additionally from balance of the Brownian motion, convection, thermophoresis, gravity

ULSAN NATIONAL INSTITUTE OF
SCIENCE AND TECHNOLOGY

effects [62]. However, nanofluid physics does not mean the transport of nanoparticle only. Considering tiny solid particles of fission products generated in fuel salt during operation would be treated as nanoparticles. Therefore, nanofluid physics implemented to this solver can give much useful information on the transport and distribution of those tiny fission products, and it can possibly be extended combining with transition and conversion of those species to predict their influences on the neutron economy as well. This work only focused on the design and its model sensitivity on the molten salt reactor and its related systems based on the available Multiphysics models including neutronics, thermal-hydraulics, species transport and finally nanofluid physics. They might be implemented with more realistic models and then, it can be utilized for the meaningful design work not only on the molten salt reactor, but also other nuclear power plant systems.

ULSAN NATIONAL INSTITUTE OF SCIENCE AND TECHNOLOGY

References

[1] "Generation IV International Forum." [Online]. Available: https://www.gen-4.org/gif/jcms/c_9260/public. [Accessed: 09-Nov-2018].

[2] M. E. Bunker, "Early Reactors --- From {Fermi}'s Water Boiler to Novel Power Prototypes," *Los Alamos Sci.*, vol. 7, pp. 124–131, 1983.

[3] A. M. Weinberg, *Fluid Fuel Reactors*, First prin. Massachusetts, USA: Addison-Wesley publishing company, Inc., 1958.

[4] R. C. Robertson, "MSRE Design and operations report : Part I - Description of reactor design," 1965.

[5] E. S. B. R. C. Robertson, O. L. Smith, R. B. Briggs, "Two-fluid molten salt breeder reactor design study," Oak Ridge, Tennessee, 1970.

[6] "Two-Fluid MSBR Core Designs." [Online]. Available: http://energyfromthorium.com/history/msbr-design-two-fluid-core/. [Accessed: 09-Nov-2018].

[7] IAEA ARIS, "Status Report – MSR-FUJI," 2016.

[8] T. J. Dolan, *Molten Salt Reactors and Thorium Energy*. Woodhead Publishing, 2017.

[9] Electric Power Research Institute, "Program on Technology Innovation: Technology Assessment of a Molten Salt Reactor Design: The Liquid-Fluoride Thorium Reator (LFTR)," Palo Alto, California, USA, 2015.

[10] Seaborg Technologies, "Seaborg Wasteburner Molten Salt Reactor," 2015.

[11] "MCFR TerraPower." [Online]. Available: http://terrapower.com/technologies/mcfr. [Accessed: 29-Oct-2018].

[12] M. Brovchenko *et al.*, "Preliminary safety calculations to improve the design of Molten Salt Fast Reactor," in *Proceedings of PHYSOR 2012 (Advances in Reactor Physics Linking Research, Industry, and Education)*, 2012.

[13] E. E. Lewis, *Fundamentals of nuclear reactor physics*. Elsevier, 2008.

[14] A. Cammi, V. Di Marcello, L. Luzzi, V. Memoli, and M. E. Ricotti, "A multi-physics modelling approach to the dynamics of Molten Salt Reactors," *Ann. Nucl. Energy*, vol. 38, no. 6, pp. 1356–1372, 2011.

[15] D. G. Cacuci, "Predictive modeling of coupled multi-physics systems: I. Theory," *Ann. Nucl. Energy*, vol. 70, pp. 266–278, 2014.

[16] D. J. Diamond, "Phenomena Important in Molten Salt Reactor Simulations," no. January, 2018.

[17] M. Allibert *et al.*, *Molten salt fast reactors*. Elsevier Science, 2016.

[18] D. G. Cacuci, *Sensitivity & Uncertainty Analysis, Volume I: Theory*. New York, USA: Champan& Hall/CRC, 2003.

[19] M. Ionescu-Bujor and D. G. Cacuci, "A comparative review of Sensitivity and uncertainty analysis of large-scale systems. I: Deterministic methods," *Nucl. Sci. Eng.*, vol. 147, pp. 189–203, 2004.

[20] G. I. Marchuk, *Adjoint Equations and Analysis of Complex Systems*. SPRINGER-

ULSAN NATIONAL INSTITUTE OF SCIENCE AND TECHNOLOGY

SCIENCE+BUSINESS MEDIA, B.V., 1995.

[21] International Atomic Energy Agency, “Progress in Methodologies for the Assessment of Passive Safety System Reliability in Advanced Reactors,” Vienna, Austria, 1996.

[22] L. Gilli, D. Lathouwers, J. L. Kloosterman, and T. H. J. J. van der Hagen, “Application of Sensitivity Analysis To a Simplified Coupled Neutronic Thermal-Hydraulics Transient in a Fast Reactor Using Adjoint Techniques,” in *Proceedings of International Conference on Mathematics and Computational Methods Applied to Nuclear Science and Engineering (M&C 2011)*, 2011.

[23] Z. Perkó, D. Lathouwers, J. L. Kloosterman, and T. Van Der Hagen, “Adjoint-Based Sensitivity Analysis of Coupled Criticality Problems,” *Nucl. Sci. Eng.*, vol. 173, no. 2, pp. 118–138, 2013.

[24] G. Rodigari, “Application of the Adjoint Sensitivity Analysis to the Delayed Neutron Parameters in a Molten Salt Reactor,” Technische Universiteit Delft, 2008.

[25] D. G. Cacuci, “Sensitivity theory for nonlinear systems. I. Nonlinear functional analysis approach,” *J. Math. Phys.*, vol. 22, no. 12, pp. 2794–2802, 1981.

[26] L. Nguyen-Tuan, T. Lahmer, M. Datcheva, and T. Schanz, “Global and local sensitivity analyses for coupled thermo–hydro–mechanical problems,” *Int. J. Numer. Anal. Methods Geomech.*, vol. 41, no. 5, pp. 707–720, 2017.

[27] E. M. Oblow, “Sensitivity Theory for Reactor Thermal-Hydraulics Problems,” *Nucl. Sci. Eng.*, vol. 68, no. December, pp. 322–337, 1978.

[28] M. Aufiero *et al.*, “Development of an OpenFOAM model for the Molten Salt Fast Reactor transient analysis,” *Chem. Eng. Sci.*, vol. 111, pp. 390–401, 2014.

[29] M. Aufiero *et al.*, “Calculating the effective delayed neutron fraction in the Molten Salt Fast Reactor: Analytical, deterministic and Monte Carlo approaches,” *Ann. Nucl. Energy*, vol. 65, pp. 78–90, 2014.

[30] S. Wang, A. Rineiski, and W. Maschek, “Molten salt related extensions of the SIMMER-III code and its application for a burner reactor,” *Nucl. Eng. Des.*, vol. 236, no. 14–16, pp. 1580–1588, 2006.

[31] A. Lindsay, G. Ridley, A. Rykhlevskii, and K. Huff, “Introduction to Moltres: An application for simulation of Molten Salt Reactors,” *Ann. Nucl. Energy*, vol. 114, pp. 530–540, 2018.

[32] C. Fiorina, I. Clifford, M. Aufiero, and K. Mikityuk, “GeN-Foam: A novel OpenFOAM® based multi-physics solver for 2D/3D transient analysis of nuclear reactors,” *Nucl. Eng. Des.*, vol. 294, pp. 24–37, 2015.

[33] E. Cervi, S. Lorenzi, A. Cammi, and L. Luzzi, “Development of a multiphysics model for the study of fuel compressibility effects in the Molten Salt Fast Reactor,” *Chem. Eng. Sci.*, vol. 193, pp. 379–393, 2019.

[34] J. J. Duderstadt and W. R. Martin, *Transport Theory*. New York, USA: Wiley, 1942.

[35] H. Jasak, “Error Analysis and Estimation for the Finite Volume Method with Applications to Fluid Flows,” 1996.

[36] T. Holzmann, *Mathematics, Numerics, Derivations and OpenFOAM®*. Holtzmann CFD, URL www.holzmann-cfd.de, 2016.

[37] M. Aufiero *et al.*, “Development of an OpenFOAM model for the Molten Salt Fast Reactor transient analysis,” *Chem. Eng. Sci.*, vol. 111, no. July 2015, pp. 390–401, 2014.

ULSAN NATIONAL INSTITUTE OF SCIENCE AND TECHNOLOGY

[38] M. Aufiero and P. Rubiolo, “Testing and Verification of Multiphysics Tools for Fast-Spectrum MSRs: The CNRS Benchmark,” in *Transactions of the American Nuclear Society*, 2018, vol. 118, pp. 837–840.

[39] M. Giles, N. Pierce, M. Giles, and N. Pierce, “Adjoint equations in CFD - Duality, boundary conditions and solution behaviour,” *13th Comput. Fluid Dyn. Conf.*, 1997.

[40] M. Aufiero, “Development of Advanced Simulation Tools for Circulating-fuel Nuclear Reactors,” Politecnico di Milano, 2014.

[41] D. Gérardin, M. Allibert, D. Heuer, A. Laureau, and C. Seuvre, “Design Evolutions of the Molten Salt Fast Reactor,” pp. 1–10.

[42] Oak Ridge National Laboratory, “Conceptual Design Study of a Single-Fluid Molten-Salt Breeder Reactor,” ORNL-4541, pp. 1–207, 1971.

[43] M. Brovchenko *et al.*, “Design-Related Studies for the Preliminary Safety Assessment of the Molten Salt Fast Reactor,” *Nucl. Sci. Eng.*, vol. 175, no. 3, pp. 329–339, 2013.

[44] C. Wang, D. Zhang, S. Qiu, W. Tian, Y. Wu, and G. Su, “Study on the characteristics of the sodium heat pipe in passive residual heat removal system of molten salt reactor,” *Nucl. Eng. Des.*, vol. 265, pp. 691–700, 2013.

[45] L. Sun, L. Sun, C. Yan, D. Fa, and N. Wang, “Conceptual design and analysis of a passive residual heat removal system for a 10 MW molten salt reactor experiment,” *Prog. Nucl. Energy*, vol. 70, pp. 149–158, 2014.

[46] C. W. Forsberg, P. F. Peterson, and P. S. Pickard, “Molten-Salt-Cooled Advanced High-Temperature Reactor for Production of Hydrogen and Electricity,” *Nucl. Technol.*, vol. 144, no. 3, pp. 289–302, 2003.

[47] T. Ishiguro, W. F. G. Van Rooijen, Y. Shimazu, and H. Mochizuki, “Design of a passive residual heat removal system for the FUJI-233Um molten salt reactor system,” *Ann. Nucl. Energy*, vol. 64, pp. 398–407, 2014.

[48] A. A. Minea, *Advances in New Heat Transfer Fluids: From Numerical to Experimental Techniques*. Boca Raton, FL: CRC Press, 2017.

[49] S. U. S. Choi and J. A. Eastman, “Enhancing thermal conductivity of fluids with nanoparticles,” *ASME Int. Mech. Eng. Congr. Expo.*, vol. 66, no. November, pp. 99–105, 1995.

[50] J. Buongiorno, “Convective Transport in Nanofluids,” *J. Heat Transfer*, vol. 128, no. 3, p. 240, 2006.

[51] D. Dey, P. Kumar, and S. Samantaray, “A review of nanofluid preparation, stability, and thermo-physical properties,” *Heat Transf. - Asian Res.*, vol. 46, no. 8, pp. 1413–1442, 2017.

[52] B. Muñoz-Sánchez, J. Nieto-Maestre, I. Iparraguirre-Torres, A. García-Romero, and J. M. Sala-Lizarraga, “Molten salt-based nanofluids as efficient heat transfer and storage materials at high temperatures. An overview of the literature,” *Renew. Sustain. Energy Rev.*, vol. 82, no. September 2016, pp. 3924–3945, 2018.

[53] B. Jo and D. Banerjee, “Enhanced specific heat capacity of molten salt-based nanomaterials: Effects of nanoparticle dispersion and solvent material,” *Acta Mater.*, vol. 75, pp. 80–91, 2014.

[54] S. K. Choi, S. O. Kim, T. H. Lee, and D. H. Dohee, “Computation of the natural convection of nanofluid in a square cavity with homogeneous and nonhomogeneous models,” *Numer. Heat Transf. Part A Appl.*, vol. 65, no. 4, pp. 287–301, 2014.

[55] Openfoam Foundation, “OpenFOAM | The OpenFOAM Foundation.” [Online]. Available:

ULSAN NATIONAL INSTITUTE OF SCIENCE AND TECHNOLOGY

https://openfoam.org/.

[56] D. G. Cacuci, "Second-order adjoint sensitivity analysis methodology (2nd-ASAM) for computing exactly and efficiently first- and second-order sensitivities in large-scale linear systems: I. Computational methodology," *J. Comput. Phys.*, vol. 284, pp. 687–699, 2015.

[57] C. Othmer, E. De Villiers, and H. Weller, "Implementation of a continuous adjoint for topology optimization of ducted flows," *18th AIAA Comput. Fluid …*, no. June, pp. 1–7, 2007.

[58] W. Liu, R. Duan, C. Chen, C. H. Lin, and Q. Chen, "Inverse design of the thermal environment in an airliner cabin by use of the CFD-based adjoint method," *Energy Build.*, vol. 104, pp. 147–155, 2015.

[59] C. K. Giannakoglou, D. I. Papadimitriou, E. M. Papoutsis-Kiachagias, and C. Othmer, "Adjoint methods in CFD-based optimization - Gradient computation & beyond," *ECCOMAS 2012 - Eur. Congr. Comput. Methods Appl. Sci. Eng. E-b. Full Pap.*, no. Eccomas, pp. 8523–8539, 2012.

[60] L. Luzzi, A. Cammi, V. Di Marcello, and C. Fiorina, "An approach for the modelling and the analysis of the MSR thermo-hydrodynamic behaviour," *Chem. Eng. Sci.*, vol. 65, no. 16, pp. 4873–4883, 2010.

[61] E. Khalili, A. Saboonchi, and M. Saghafian, "Experimental study of nanoparticles distribution in natural convection of Al2O3-water nanofluid in a square cavity," *Int. J. Therm. Sci.*, vol. 112, pp. 82–91, 2017.

[62] M. Bahiraei, "Particle migration in nanofluids: A critical review," *Int. J. Therm. Sci.*, vol. 109, pp. 90–113, 2016.

ULSAN NATIONAL INSTITUTE OF
SCIENCE AND TECHNOLOGY

Acknowledgement

First and foremost, I would like to express my deepest gratitude to my advisor Prof. In Cheol Bang, who encouraged me to grow myself into an independent researcher as a nuclear engineer from his generous support and precious advices. His endless endurance and trust make me to choose the right decision at every moment. It is my obligation to not just say thank you for everything you did for me, but to repay for his generous favor by trying my best and doing challenges in my whole life as a researcher who is able to contribute the society.

I really appreciate my committee members, Prof. Ji Hyun Kim, Prof. Seung Jun Lee of UNIST, Prof. Hisashi Ninokata and Prof. Antonio Cammi of Politecnico di Milano to improve the quality and complete my thesis work. I should acknowledge Prof. Hisashi Ninokata and Prof. Antonio Cammi, especially. During and after period of visiting Milan for research, their generous supports and encouragement make me to concentrate my time to think about the problem in ultimate way and have curiosity about all problems starting from scratch.

I also thank to our lab members, nuclear thermal-hydraulics and reactor safety laboratory of UNIST. Dr. Seung Won Lee and Mr. Sung Man Kim, who always greeted me with kindness, Dr. Seong Dae Park, who always gave me some practical advices and treated dinner whenever I visited Daejeon, Dr. Sarah Kang, who encouraged me all the times and still supports me, Dr. Han Seo, who taught me experiment for the first time and give much of know-how on experiment. Thanks to you, I was able to enjoy this period without any problem and have a great time in lab. Especially, I'd like to say to Dr. Kyung Mo Kim that it was lucky for me to do a project with much of discussions with you. I really learned a lot from experiences sharing with you and it was really supporting me that you always trusted me. I promise that I will not forget your advice. Dr. Seok Bin Seo, who shared time with me in Milano for 6 months and have discussions a lot about research and study. I had a lot of help from various viewpoint of your suggestions while talking with you. I hope I can give you a help to you in future. Sungbo Moon, who always smile me, In Guk Kim, who is brilliant to make something in a short time, Hyo Heo, who shares much of common experiences with me, Minho Lee, who is very smart guy in our lab, and Haneol Park, who share common experiences in Australia, Do Yeong Lim and Ji Yong Kim, who are always enthusiastic for all things. Thank you all, and I was so happy to share the time with you guys.

In addition, I would like to appreciate Dr. Hyung Tae Kim of the heavy water reactor and severe accident safety analysis department of KAERI who advised my internship in 2013 for 2 months in Daejeon, Mr. Young Jun Kim and Mr. Min Cheol Park of KONICOF who supports me to provide opportunities of Nuclear Global Internship in 2014, Dr. George Broaudakis and Dr. Mark Ho of the

ULSAN NATIONAL INSTITUTE OF
SCIENCE AND TECHNOLOGY

centre of nuclear application of ANSTO, Australia who helped me and encouraged me at that time, Dr. Wang Kee In of the light water reactor nuclear fuel safety research department of KAERI who taught the bottom to top of CFD simulations during 8 months as a research student, Eric Cervi and Dr. Stefano Lorenzi of Politecnico di Milano, Italy who had great discussion with me every time, and all students of Nuclear Reactor Groups including Prof. Lelio Luzzi and Prof. Marco Enrico Ricotti who showed great hospitality and helped me a lot. Thanks to everyone, I was able to have great experiences in Korea, Australia, and Italy during my period.

I'd like to appreciate my precious friends to give encouragement to me and their supports, Jiwon Lim, Daae Choi and Hyoyeon Bang, who are my strength and always with me. Seorim Park, Sunyoung Park, who shared time from 1st year of UNIST with me, Suhwan Kim, who always called me first. Besides, Dr. Tae Ho Kim, and Dr. Seung Hyun Kim of UNIMAT lab., Dr. Gwan Yoon Jeong, and Dr. Tae Won Cho of nuclear fuel lab., I also appreciate you guys to help me and had a good time with you. Mr. Jong Soo Lee of NEOSYS, thank you to support to build my experimental apparatus and much of practical advices.

For my family, I should express my gratitude to my father and mother, who supports me without any doubt while I didn't do well, and my sister Yeong Ju Jeong, her husband Sang Heon Han, and her lovely son Gyo Won Han as well. And, Dr. Sooyoung Choi, who always cheer me with all his heart and knows myself even better than me, I sincerely appreciate you with all my heart, and I'm sure that we will be a good partner to each other in our life with full of happiness.

Thanks to you all, I was able to focus on my study and finally complete my Ph. D thesis work for 5 years successfully without any struggles. At the starting point of long race, not the end, I'd like to resume to go through challenges toward a wider world. Again, thank you so much for your supports with all my heart.

ULSAN NATIONAL INSTITUTE OF SCIENCE AND TECHNOLOGY

감사의 글

먼저 학부 과정부터 학위과정 내내 아낌없는 격려와 지도로 원자력공학도로서 독립적인 연구자로 도약할 수 있도록 기회를 주신 지도교수님 방인철 교수님께 깊은 감사의 말씀을 드립니다. 지난 5년간 저는 교수님께 많이 부족한 학생이었을 텐데, 매 순간 저를 일깨워 주시고, 옳은 선택할 수 있도록 기다려 주시고 믿어 주셔서 감사드립니다. 교수님께서 저에게 해 주신 값진 조언과 아낌없는 지원에 비해서 감사하다는 말씀만 드리기엔 너무 부족합니다. 사회에 공헌하는 연구자로써 성장하여 항상 도전하는 자랑스러운 제자가 되어 그 은혜에 보답하도록 노력하겠습니다.

그리고 저희 박사 학위 논문의 질을 향상시킬 수 있도록 심사위원으로서 귀중한 시간 할애해주신 울산과학기술원 김지현 교수님, 이승준 교수님, 이탈리아 Politecnico di Milano 의 Prof. Antonio Cammi와 Prof. Hisashi Ninokata께 감사드립니다. Prof. Cammi 와 Prof. Ninokata 두분 덕분에 짧은 기간이었지만 밀라노에서 값진 경험을 할 수 있었고, 연구자로서 더욱 성장하고 고민할 수 있는 시간을 가질 수 있었습니다. 항상 모든 문제에 호기심을 가지고 Scratch 부터 시작하는 학자 되겠습니다.

긴 시간 동고동락한 우리 열수력 연구실 식구들에게도 감사의 인사 전하고 싶습니다. 대학원 진학 전부터 늘 반갑게 인사해 주셨던 이승원 박사님과 김성만 선배님. 항상 아낌없는 조언 해주시고 대전 출장 때마다 밥도 많이 사주신 박성대 박사님. 저에게 늘 용기를 북돋아 주시고 지금도 저를 너무 아껴 주시는 강사라 박사님. 저의 첫 실험을 도와주시고 많은 노하우를 가르쳐 주신 서한 박사님. 선배님들 덕분에 학위기간동안 다양한 경험할 수 있었고, 연구실 생활 순조롭게 할 수 있었습니다. 진심으로 감사드립니다. 저의 영원한 사수 김경모 박사님, 오빠와 함께 연구하면서 같이 고민하고 의논하며 정말 많이 배울 수 있었습니다. 항상 부족한 저지만 이끌어주고 믿어 주셔서 감사하고, 제가

ULSAN NATIONAL INSTITUTE OF SCIENCE AND TECHNOLOGY

매번 투덜거릴 때마다 해 주시던 조언 잊지 않겠습니다. 늘 제 질문을 유쾌하게 받아 주셨던 서석빈 박사님, 오빠랑 이런 저런 이야기 나누면서 다방면에서 많은 도움을 받았습니다. 저도 오빠에게 그리고 후배들에게 도움이 되도록 노력하겠습니다. 항상 저에게 웃음을 선사해줬던 성보 오빠, 뚝딱뚝딱 뭐든 잘 만드셨던 인국 오빠, 나의 유일한 동기 효, 중간에서 큰 역할 해주고 있는 민호, 호주 후배이자 실험 후배 한얼이, 항상 의지가 넘치는 지용이, 도영이까지. 못난 저이지만 랩 식구들 덕분에 연구실 생활 즐겁고 보람차게 할 수 있었습니다. 이 자리를 빌어 고맙다고 전하고 싶습니다.

그리고 2013년 2달간 인턴기간 지도해주신 한국원자력연구원 중수로·중대사고안전연구부 김형태 박사님, 2014년 원자력글로벌인턴십 호주 파견 연구 지원해주신 KONICOF 김영준 선생님, 박민철 선생님. 호주 원자력과학기술청(ANSTO) Centre of Nuclear Application 부서의 Dr. George Braoudakis, Dr. Mark Ho. 2015년부터 2016년까지 약 8개월 연구생 기간동안 지도해주신 한국원자력연구원 경수로핵연료안전연구부 인왕기 박사님. 2017년부터 2018년 약 6개월간 이탈리아 밀라노 파견연구기간동안 늘 좋은 디스커션 상대가 되어 주었던 Eric Cervi, Dr. Stefano Lorenzi를 포함하여 늘 호의로 대해주던 Politecnico di Milano Nuclear Reactor Group 모든 학생들과 Prof. Lelio Luzzi, Prof. Marco Enrico Ricotti. 모두들 덕분에 국내외에서 소중한 경험하고 한단계 성장할 수 있었습니다.

항상 나의 힘이 되어주고 말없이도 잘 통하는 임지원. 연락은 자주 못하지만 언제나 함께 있는 느낌인 최다애, 멀리서든 가까이서든 용기주는 방효연, 늘 응원해줘서 고맙고 우리 더 자주 보고 더 행복하자. 대학교 1학년때부터 언제나 나의 동지가 되어주었던 나의 룸메이트였던 서림, 선영아. 너희 덕분에 많은 힘을 얻었어. 늘 먼저 전화 준 김수환. 고맙고 취업 축하한다. 한 연구실 식구처럼 같이 생활한 재료랩 태호 오빠랑 승현 오빠, 핵연료랩 관윤 오빠랑 태원이, 실험장치 제작으로 늘 애써 주시던 네오시스 이종수 사장님도 모두 감사드립니다.

ULSAN NATIONAL INSTITUTE OF SCIENCE AND TECHNOLOGY

마지막으로, 연락도 자주 안하고 늘 바쁘다고 투정부리는 작은 딸 물심양면으로 지원해주고 격려해주신 아버지 어머니, 항상 응원해주는 언니, 형부, 똘똘한 교원이까지. 모두 믿고 기다려 주셔서 감사합니다. 늘 발전하는 사람이 되어 가족들에게 큰 도움이 되는 사람이 되겠습니다. 그리고, 대학원 기간 내내 도와주고 나보다 나를 더 잘 아는 최수영 박사, 늘 옆에서 힘이 되어 줘서 고맙고, 앞으로도 즐겁고 행복하게 잘 지내보자.

아무것도 모르던 학생이던 제가 박사학위논문의 마지막 장을 쓸 수 있었던 건, 많은 분들을 만나서 배울 수 있던 기회와 연구에만 집중할 수 있도록 격려해주시고 전폭적인 지지를 주신 모든 분들 덕분이라 생각됩니다. 끝이 아닌 시작점에서, 앞으로 더 넓은 세상에서 끊임없이 도전해보려 합니다. 모든 분들께 다시한번 진심으로 감사드리며 이 글을 마칩니다.